

IMPERIAL COLLEGE LONDON

DEPARTMENT OF MATHEMATICS

MSCI RESEARCH PROJECT

Forecasting Returns for High Frequency Cryptocurrency Websocket Data

June 9, 2024

Author: Isaac Jefferson Lee
Email: isaac.lee20@imperial.ac.uk
CID: 01859216

Supervisor: Dr. Mikko S. Pakkanen

Submitted in partial fulfillment of the requirements for the MSci Mathematics with a Year
Abroad (G104) at Imperial College London

The source code for the models found in this paper can be found at:
<https://github.com/isaacjeffersonlee/BinanceOrderbookForecasting.git>

Abstract

In this paper we explore various machine learning models for predicting high frequency returns for four of the most popular cryptocurrency perpetual futures trading pairs, BTCUSDT, ETHUSDT, MATICUSDT and SOLUSDT. Specifically we train and evaluate models for classifying the direction of the smoothed mid-price change for high frequency prediction horizons. We introduce a novel data set, constructed from a live WebSocket stream from Binance, the worlds largest centralized cryptocurrency exchange. We explore how different data representations affect model performance and how performance varies for different trading pairs and prediction horizons. We use a mixture of traditional machine learning and deep learning models and show that simple and explainable traditional models can rival the performance of far larger and more complex state of the art deep learning models.

Plagiarism statement

The work contained in this thesis is my own work unless otherwise stated.

Signature: Isaac Jefferson Lee

Date: June 9, 2024

Contents

1	Introduction	5
1.1	Centralized Markets & The Orderbook	5
1.2	Related Works	5
1.3	Overview	6
1.4	Contributions	7
2	Orderbook Data	8
2.1	Orderbook Mechanism	8
2.2	The Data	9
2.2.1	Data Source	9
2.2.2	Websocket Data	9
2.3	Orderbook Shape	12
2.4	Orderflow Imbalance	12
2.4.1	Linear Price Impact Model	13
2.4.2	PanelOLS Results	14
2.4.3	Conclusion	15
3	Predictive Modelling	19
3.1	The Modelling Objective	19
3.2	Model Architecture Background	20
3.2.1	Logistic Regression	20
3.2.2	Decision Trees	21
3.2.3	Artificial Neural Networks	23
3.2.4	Convolutional Neural Networks	24
3.2.5	Long Short-Term Memory	25
3.3	Model Architectures	25
3.3.1	Orderbook Features	25
3.3.2	lrLOB & lrOF	26
3.3.3	xgbLOB & xgbOF	27

3.3.4	DeepLOB	28
3.3.5	DeepOF	30
3.4	Methodology	30
3.4.1	Sliding Window Setup	30
3.4.2	Data Normalization	31
3.4.3	Choice of label discretization parameter	31
3.4.4	Model Training	31
3.5	Results	32
3.5.1	Classification Metrics	32
3.5.2	Model Results	33
3.5.3	Feature Importances	43
3.5.4	Modelling Recommendations	46
4	Conclusion	47
4.1	Summary	47
4.2	Conclusions	47
4.3	Future Work	48
A	Extended Classification Results	49
B	Extended PanelOLS Results	53
C	Websocket Data Summary Statistics	58
D	Alternative Data Source	61
D.1	Introduction	61
D.2	On Efficient Parsing	62
D.3	The Parsing Algorithm	63
D.4	Complexity Analysis	63
D.5	Data Issues	63
E	DeepLOB Detailed Model Architecture	67

Chapter 1

Introduction

1.1 Centralized Markets & The Orderbook

Financial markets exist in many forms. Perhaps the most popular is the *centralized* market, where all trading activity is handled by a central *trusted* authority. The advantage of using a centralized market is that prices are kept fair and government/financial authority regulation is much easier to implement. With the advent of *blockchain technology*¹, [1], *Decentralized markets* have risen in popularity. Decentralized markets allow clients to cut out the middle man and directly trade with each other. *Automated market making* algorithms, [2], are used to ensure the decentralized markets have sufficient liquidity for efficient operation. Decentralized exchanges have the advantage of removing any need for trust of a third party, which is an advantage for markets such as the *cryptocurrency*² market, where scams are common and exchanges have a tendency to collapse, [3]. Of course the downside of decentralized exchanges is that they are harder to regulate, [4], and therefore are less attractive to risk averse institutional investment. In this paper we concern ourselves with centralized exchanges in the context of the cryptocurrency market.

Centralized exchanges use a *limit orderbook* to organize all buying and selling activity. The limit orderbook is a datastructure that stores all unfilled buy and sell orders. These orders sit on the orderbook at different levels and are indexed by price. This gives us a snapshot of the current supply and demand. It is well established that for most markets, supply and demand are key drivers of price movement, [5]. It then follows that we should be able to predict the future price movement of a security by using only the information contained in its orderbook. This is the main aim of this paper.

1.2 Related Works

Since the introduction of electronic exchanges, orderbook modelling has been a widely studied active area of research. Early works used parametric models such as [6] who use autoregressive linear models with handcrafted features such as spread and trade imbalance to forecast future mid-price returns at the minute resolution or [7] who introduce Hawkes processes for modelling

¹A blockchain is a distributed ledger/datastructure that stores transactions/contracts in a cryptographically secure and distributed way without the need for trust of a centralized organization.

²Cryptocurrencies are digital currencies which are transacted using blockchain technology.

orderbook events. [8] use tensor regressions for high frequency orderbook mid-price returns forecasting. Due to their parametric nature, these models all inherently make assumptions on the causal relationships that drive mid-price movement. With the explosion in popularity/practicality of deep learning over the past few decades, [9], [10], [11], [12], [13], [14], we have seen several deep learning approaches to the orderbook modelling task. Deep learning has the benefit of having fewer assumptions/restrictions on model architecture and excels at modelling large complex systems with high dimensional and non-linear dynamics, such as an orderbook. [15] was one of the first works to use deep neural networks for mid-price prediction (specifically they used MLPs, [16], [17], with several hidden layers). [18] use a neural Bag-of-Features approach, achieving state of the art performance for high frequency mid-price returns prediction at the time. A breakthrough in the field was made when [19] proposed a specialized deep learning model, coined DeepLOB, for high frequency mid-price returns prediction. The DeepLOB model uses CNNs, [12], for feature extraction and LSTMs, [11], for temporal dependency extraction. They showed that the DeepLOB model significantly outperforms all other state of the art models of the time. The DeepLOB model uses the orderbook data in raw form. It turns out that this is not the best representation for predictive modelling. *Orderflow*, is a stationary orderbook representation, first introduced in [20] in the context of linear price impact modelling. [21] build on the work of [19] and adapt the DeepLOB model to use orderflow input, instead of the raw orderbook representation. This adapted model is named DeepOF and [21] show that it significantly outperforms the DeepLOB model. [22] further build on this work by again modifying the DeepOF model to include extra volume features at deeper levels of the model.

The majority of these papers are trained and evaluated on the LOBSTER, [23], NASDAQ orderbook dataset. This is a dataset that has become the gold standard for orderbook modelling, since it is well researched, documented and easily accessible. In this paper we turn away from traditional finance and look to model cryptocurrency orderbook price movement. The cryptocurrency market is still a very new area of research with far fewer published papers. Of note are [24] who use traditional machine learning models and [25] who use LSTM based models to forecast Bitcoin mid-price movement. It is worth noting that these papers focus on forecasting movement for longer time periods, such as minutes, hours or even days. To our knowledge, there are no published papers on **high frequency** mid-price movement prediction, akin to [19], [21], [22], but for **cryptocurrency data**.

1.3 Overview

In this paper we explore various machine learning models for predicting high frequency returns for four of the main cryptocurrency futures trading pairs, BTCUSDT, ETHUSDT, MATICUSDT and SOLUSDT. We construct a novel data set from a live WebSocket stream from Binance, the worlds largest centralized cryptocurrency exchange. Following [20], we define a stationary transformation of the raw orderbook data called orderflow, and motivate its definition by showing that under a stylized model of the orderbook, orderflow can be used to measure linear price impact of orderbook events. We then define our modelling objective as a three-class classification problem, predicting the direction of the smoothed mid-price returns for several prediction horizons. For this task, we introduce several traditional machine learning and also deep learning models that use either the orderflow representation or the raw orderbook representation. Specifically, from traditional ML we introduce Logistic Regression and XGBoost models. For our deep learning models, we use the deepLOB model from [19] and the deepOF model from [21], which use the raw orderbook/orderflow representations respectively. We train, validate and test our models for each trading pair and multiple prediction horizons on eight windows from 05-02-2024 to 25-02-2024. We present the results on the test set and also evaluate the feature importances for each XGBoost model.

1.4 Contributions

In this paper we present two main contributions.

1. The first major contribution we make is the application of high frequency limit orderbook modelling to cryptocurrency data. Specifically we train and evaluate models for classifying the direction of the smoothed mid-price change for prediction horizons ranging from ≈ 500 milliseconds to ≈ 20 seconds for Binance perpetual futures limit orderbook WebSocket data. In the literature all similar modelling, [19], [21], [22], has been done on traditional equities data, such as the NASDAQ, [23]. To our knowledge, we are the first paper to explore high frequency orderbook forecasting on cryptocurrency data. Our dataset is also unique, since it has been gathered from a live WebSocket, [26], endpoint and to our knowledge, there have been no similar papers published on forecasting live orderbook data. This is exciting, since this live data is openly available and anyone can create a connection and start receiving live updates. This massively lowers the barrier to entry for practical trading applications and is one of the benefits of trading on cryptocurrency exchanges. Also, often times a historical dataset may be used for model evaluation but then, in practice, no live feed is available with sufficient latency and or resolution. Since we are directly using data stored from a live feed, we can guarantee that such a data source will be available for downstream trading strategies.
2. The second contribution we make is the use of XGBoost, [27], for high frequency orderbook modelling. Within the quantitative finance industry, XGBoost is a very popular model and is very widely used. It has the ability to model high dimensional complex non-linear feature relationships with tighter control of overfitting and greater explainability when compared to deep learning methods. For many quantitative finance applications model explainability is extremely important. It is a necessity to be able to understand and explain when and why a model is not performing as expected, especially when one has to answer to angry investors. In this paper we show that XGBoost with orderflow features can rival state of the art deep learning models, [19], [21], [22], for this application.

Chapter 2

Orderbook Data

2.1 Orderbook Mechanism

On centralized exchanges, *the orderbook* is the main data structure used to organize buying and selling activity. There are two main orders a client can submit, *market orders* and *limit orders*. Market orders get instantly matched at the *best available price* and executed. Limit orders specify a desired transaction price to buy/sell for a given volume. If the order cannot be instantly filled by current supply, the limit order will be posted to the limit orderbook, to be filled by future matching orders. Essentially the orderbook keeps track of the current (unfilled) supply and demand. The limit orders that are posted to the orderbook are organized into levels, indexed by price. So all limit orders with the same price (and side) are combined into a single level, and their volumes are aggregated. Note that the orderbook can contain hundreds of thousands of levels but the majority of the activity is focused around the top levels. The *bids* are the buy orders, and the *asks* are the sell orders. Ask levels are sorted by price in ascending order and bid levels are sorted in descending order. The first/top ask level price is the lowest ask price, and the first/top bid level price is the highest bid price. So if a client wishes to buy, the *best available price* is the first/top/lowest ask price and if they wish to sell, their best available price is first/top/highest bid price. See Figure 2.1 for a visual representation of the limit orderbook. When new orders arrive, they will be matched against the orderbook and either posted or filled. If enough orders are matched at a certain price, all the volume for that price level will be consumed and the price will be removed from the orderbook and the next best price will take its place for that level. In this way, the state of the orderbook is constantly changing, as new orders are submitted and price levels are partially or fully filled.

We define the mid-price to be the average of the best bid and ask price. This single value is often used to represent the current price of the asset. We also define the spread to be the difference between the best bid and ask price. Smaller spreads are highly correlated with high trade volume [28].

It is important to note that there are three main levels of granularity when it comes to orderbook representations. Firstly we have L1 data, which is only the best bids and asks, with their corresponding volumes. Then we have L2 data, which is all price levels with their corresponding volumes, with one volume value per price level (i.e. volumes are summed across orders for each price level). Then the most granular is L3 data, which contains all price levels, with multiple volume values for each price level. Specifically the volumes at a given price level are broken down into their individual order values. So if, from time $t - 1$ to time t , 2 orders are



Figure 2.1 A visual representation of the orderbook (specifically for L2 data).

submitted with volumes v_a and v_b , then the $L2$ representation would show $V_t = V_{t-1} + v_a + v_b$, whereas the $L3$ representation would give us $\mathbf{V}_t = [\mathbf{V}_{t-1}; v_a, v_b]$

For a more in-depth exposition of the mechanism of the limit orderbook, we refer the interested reader to [29].

2.2 The Data

In this section we introduce our data source and give some visualizations.

2.2.1 Data Source

Our data has been gathered from Binance directly. Binance is the largest cryptocurrency exchange in terms of daily volume, with a revenue of \$12 billion in 2022 according to [30]. It was founded in 2017 by Changpeng Zhao. Binance was chosen because of its high volume, popularity and decent API availability. Binance also offers perpetual USDT futures which is the main security of focus for this paper.

2.2.2 Websocket Data

Most communication on the internet takes place via a communication protocol known as HTTP, or Hypertext Transfer Protocol, [31]. HTTP works in a single direction. We send a request to a server, then the server sends back a response and then the connection is closed. Of course for real time streaming applications this is too slow and ideally we would like to keep the connection open continuously. Introducing the WebSocket protocol, [26]. WebSocket is a bidirectional communication protocol that can send data from a client to a server or from a server to a client by reusing the established connection channel. The connection is kept open until terminated by either the server or the client. Almost all live streaming applications such as trading,

monitoring, etc. use the WebSocket protocol to continuously receive the live data on a single communication channel.

Binance offers live Websocket data with various endpoints. We use the endpoint:

`wss://fstream.binance.com/ws/{tradingpair}@depth{L}@100ms`

to stream top L best bids and asks every approximately 100ms. We log this data to an SQL database on an AWS server. Due to free-tier limitations we only have about 30GB of storage on the server, which corresponds to approximately a month of data for four trading pairs. This is also about the limit of how much data we can fit into memory at any one time. For these reasons we only work with 20 days of data, from the start to the end of February, 2024. Specifically we have data for 2024-02-05 13:07:53.664 until 2024-02-25 11:18:50.866. This gives us approx. 12 million datapoints for each trading pair. Since we are looking at such high frequencies, this data should be satisfactory. We choose BTCUSDT, ETHUSDT, SOLUSDT and MATICUSDT as our futures trading pairs of interest. We choose these because they are all high enough volume to have good liquidity but also have significant enough difference in traded volume so that their comparative study should be interesting. We store this data as a DataFrame for each trading pair. Each row contains the top 10 bid and ask prices and quantities for a given time. See Table 2.1 for an example DataFrame for MATICUSDT.

Row	timestamp	ask_price_1	...	ask_price_10	bid_price_1	...	bid_price_10	ask_qty_1	...	ask_qty_10	bid_qty_1	...	bid_qty_10
0	1707138494390	0.7877	...	0.7886	0.7876	...	0.7867	9368.0	...	58006.0	15095.0	...	44990.0
1	1707138494515	0.7877	...	0.7886	0.7876	...	0.7867	9367.0	...	58006.0	15095.0	...	84785.0
2	1707138494760	0.7877	...	0.7886	0.7876	...	0.7867	9367.0	...	58006.0	15095.0	...	44990.0
3	1707138494881	0.7877	...	0.7886	0.7876	...	0.7867	9367.0	...	58006.0	15095.0	...	44990.0
4	1707138495248	0.7877	...	0.7886	0.7876	...	0.7867	9356.0	...	58006.0	15099.0	...	44990.0
⋮	⋮	⋮	⋮	⋮	⋮	⋮	⋮	⋮	⋮	⋮	⋮	⋮	⋮
11294483	1708857980137	0.9726	...	0.9735	0.9725	...	0.9716	16199.0	...	64495.0	20555.0	...	37554.0
11294484	1708857980246	0.9726	...	0.9735	0.9725	...	0.9716	16199.0	...	61163.0	19527.0	...	37554.0
11294485	1708857980360	0.9726	...	0.9735	0.9725	...	0.9716	20199.0	...	61163.0	19527.0	...	37554.0
11294486	1708857980494	0.9726	...	0.9735	0.9725	...	0.9716	21610.0	...	61163.0	19577.0	...	37554.0
11294487	1708857980602	0.9726	...	0.9735	0.9725	...	0.9716	22992.0	...	61163.0	18401.0	...	37554.0

Table 2.1 Example data for MATICUSDT.

We note that the websocket data is not regular, but comes **approximately** every 100ms. This means that the time difference/timedelta, Δt ms between updates is not constant and therefore this is technically not a timeseries in the proper sense. For some of our applications we will resample this data into regular intervals. We present summary statistics for the timedeltas for each symbol in table 2.2. We see that most of the timedeltas are larger than the 100ms promised by the endpoint, with a mean of 133ms and median 116ms. We also see a maximum timedelta of around 1 minute and a minimum timedelta of 3ms. Whilst this is less than ideal for an experimental setup, we leave these outliers in, since they represent the real world inconsistencies that one would find when using such a data source.

	BTCUSDT Δt ms	ETHUSDT Δt ms	MATICUSDT Δt ms	SOLUSDT Δt ms
count	12891080	13612890	11294487	13334051
median	116	114	122	115
mean	133	126	152	129
std	50	41	82	47
min	3	3	3	3
25%	107	105	108	107
50%	116	114	122	115
75%	142	133	162	135
max	61604	61862	61697	61815

Table 2.2 Summary statistics for the time difference between observations in our dataset in ms, Δt ms, for each trading pair.

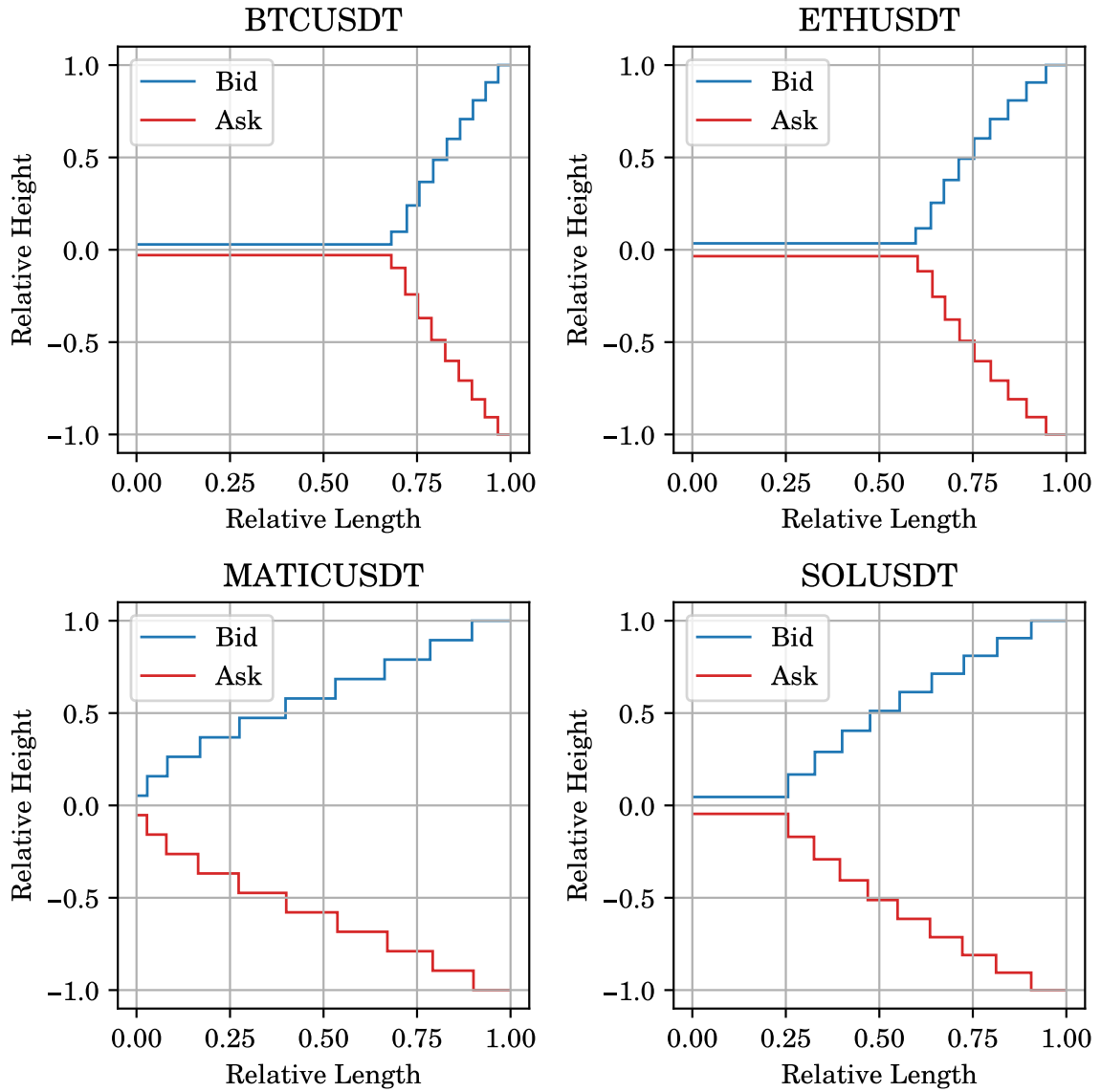


Figure 2.2 Average orderbook shape for each trading pair.

2.3 Orderbook Shape

In this section we aim to give a general overview of the shape of the orderbook for each trading pair in our data. We define the height of a level $\ell \in \{1, 2, \dots, 10\}$ on the x side as $\Delta p_\ell^x = p_\ell^x - p_{\ell-1}^x$, with $x \in \{B, A\}$. Where B, A denote the bid, ask sides respectively. In other words, the price difference between the ℓ^{th} and $\ell - 1^{th}$ bid/ask price level. We note that by definition, $\Delta p_\ell^A < 0, \forall \ell$ and $\Delta p_\ell^B > 0, \forall \ell$. The length of a level ℓ on the x side is denoted by q_ℓ^x and represents the total volume for the ℓ^{th} price level. We also define the mid-price as an average of the best bid and ask price, i.e.

$$p_0 := \frac{1}{2}(p_1^A + p_1^B) \quad (2.1)$$

Following [6], we normalize the level heights by the price difference between the 10th level and the mid-price, i.e. total height. The level length is also normalized by the total length from the first level to the 10th level, i.e.

$$\tilde{q}_\ell^x := \frac{q_\ell^x}{\sum_{j=1}^{10} q_j^x} \quad (2.2)$$

$$\Delta \tilde{p}_\ell^x := \frac{\Delta p_\ell^x}{\sum_{j=1}^{10} \Delta p_j^x} = \frac{\Delta p_\ell^x}{|p_0 - p_{10}^x|} \quad (2.3)$$

We average the bids and asks over all entries and then calculate the normalized lengths and heights. We visualize the results for each trading pair in Figure 2.2. This gives us a good idea of the overall average shape of the orderbooks.

We see that across all trading pairs the average orderbook is mostly symmetric, which is what we would expect. Perhaps more interestingly we see that for BTCUSDT the relative length for the first price level is much larger (higher volume) compared to the other top 10 levels. In fact, we observe that the relative length of the first level seems to be increasing as a function of the trading pairs popularity/volume. If we were to order the trading pairs in terms of trading volume, from lowest to highest we would have MATICUSDT, SOLUSDT, ETHUSDT and BTCUSDT. This ordering is also the ordering of the relative length of the first level. So it seems that the more popular a trading pair is, the more the volume is weighted towards the top of the orderbook. Also another interesting point is that after the first level the relative lengths are almost identical, suggesting e.g. that there is just as much activity in the 10th level compared to the 2nd level of the orderbooks. [6] used a similar methodology to visualize the shape of the orderbook, but for stocks from the Australian Securities Exchange, ASX. The shape of the orderbook found in [6] looks a lot like the MATICUSDT orderbook shape, which agrees with our previously discussed first level length - volume relationship, since the ASX (in 2009) had much less volume compared to BTCUSDT in 2024.

2.4 Orderflow Imbalance

In this section we introduce a key concept in this paper, *orderflow*, which was first introduced in [20], in the context of linear price impact modelling. We take a brief detour here to apply this model to our data, in order to motivate the use of orderflow later on in our predictive modelling.

We start by defining the Orderflow Imbalance, a stationary transformation of the orderbook data first introduced in [20]. Since mid-price movement is governed by supply and demand, we need to identify the different orderbook states and how they relate to supply and demand. We will initially only concern ourselves with the top of the orderbook.

For each of our observations, we have the best bid price and best bid quantity, which we denote by p^B, q^B and the best ask price and best ask quantity p^A, q^A . If we enumerate our observations through time by n , then according to [20], we have the following orderbook events:

- $p_n^B > p_{n-1}^B$ or $q_n^B > q_{n-1}^B$, suggesting an increase in demand.
- $p_n^B < p_{n-1}^B$ or $q_n^B < q_{n-1}^B$, suggesting a decrease in demand.
- $p_n^A < p_{n-1}^A$ or $q_n^A > q_{n-1}^A$, suggesting an increase in supply.
- $p_n^A > p_{n-1}^A$ or $q_n^A < q_{n-1}^A$, suggesting a decrease in supply.

Then [20] defines the quantity e_n to represent the contribution of the n^{th} event as $e_n := e_n^B - e_n^A$ where e_n^B and e_n^A are defined in (2.4).

$$\begin{aligned} e_n^B &:= I_{\{p_n^B \geq p_{n-1}^B\}} q_n^B - I_{\{p_n^B \leq p_{n-1}^B\}} q_{n-1}^B \\ e_n^A &:= I_{\{p_n^A \leq p_{n-1}^A\}} q_n^A - I_{\{p_n^A \geq p_{n-1}^A\}} q_{n-1}^A \end{aligned} \quad (2.4)$$

Then we sum these individual contributions from time $t - h$ to the current time t , to get the Order Flow Imbalance at time t :

$$\text{OFI}_h(t) := \sum_{n: t_n \in [t-h, t]} e_n \quad (2.5)$$

2.4.1 Linear Price Impact Model

In this subsection we introduce the linear price impact model from [20] that motivates the above orderflow definition. Firstly, let us define $\Delta p_\delta(t+h) := (p(t+h) - p(t))/\delta$, i.e. the change in price measured in ticks, where δ is the ticksize for the given trading pair. Note that a tick is defined as the smallest price increment in which the price for a pair is quoted, i.e. the precision. Using the Binance API we retrieve the ticksizes as:

trading pair	δ
BTCUSDT	0.1
ETHUSDT	0.01
SOLUSDT	0.001
MATICUSDT	0.0001

Table 2.3 Trading pairs and their ticksizes, δ .

[20] considers a stylized model of the orderbook where the volume beyond the top level is equal to D and all trading activity only occurs at the top level. Of course this is a big assumption but from our previous exploration we showed this to be largely justified for high volume pairs such as BTCUSDT and ETHUSDT. Under these assumptions, we have three main events on the bid side:

1. Market sell orders remove M^s volume from the bid.
2. Limit buy orders add L^b volume to the bid.
3. Limit buy cancels remove C^b volume from the bid.

We can analogously define quantities for the ask side. Then under the above assumptions:

$$\Delta p = \left[(L^b - C^b - M^s)/2D \right] - \left[(L^s - C^s - M^b)/2D \right] \quad (2.6)$$

This is equivalent, (up to some truncation) to:

$$\Delta p = \frac{\text{OFI}}{2D} + \epsilon \quad (2.7)$$

since $\text{OFI} = L^b - C^b - M^s - L^s + C^s + M^b$.

So under our stylized assumptions, we see that the price change in ticks is directly proportional to the Orderflow Imbalance. Therefore [20] suggest the following relation:

$$\Delta p_\delta(t) = \beta \text{OFI}_h(t) + \epsilon_t \quad (2.8)$$

where β is the *price impact coefficient* and ϵ_t is the noise term. So β measures the instantaneous impact of the n^{th} event on the mid-price. [20] assume the price impact coefficients are constant for half-hour intervals (indexed by i), and estimate them using OLS:

$$\Delta p_\delta(t) = \hat{\beta}_i \text{OFI}_h(t) + \hat{\alpha}_i + \hat{\epsilon}_t \quad (2.9)$$

2.4.2 PanelOLS Results

We split our data into half-hour windows and then perform PanelOLS across windows to estimate the average coefficients. We set $h = 1000ms$ and present the results for BTCUSDT here. (The R^2 values for the other symbols are very similar and can be found in the appendix).

BTCUSDT PanelOLS Results for h = 1000ms

Dep. Variable:	Δp_δ	R-squared:	0.3590
Estimator:	PanelOLS	R-squared (Between):	-0.3865
No. Observations:	12891080	R-squared (Within):	0.3590
Date:	Tue, Mar 26 2024	R-squared (Overall):	0.3585
Time:	16:15:04	Log-likelihood	-6.11e+07
Cov. Estimator:	Clustered		
		F-statistic:	7.218e+06
Entities:	956	P-value	0.0000
Avg Obs:	1.348e+04	Distribution:	F(1,12890123)
Min Obs:	953.00		
Max Obs:	1.676e+04	F-statistic (robust):	4743.2
		P-value	0.0000
Time periods:	16761	Distribution:	F(1,12890123)
Avg Obs:	769.11		
Min Obs:	1.0000		
Max Obs:	956.00		

	Parameter	Std. Err.	T-stat	P-value	Lower CI	Upper CI
	OFI	1.1829	0.0172	68.871	0.0000	1.1492 1.2166

F-test for Poolability: 19.309,
Distribution: F(955,12890123),
Included effects: Entity.

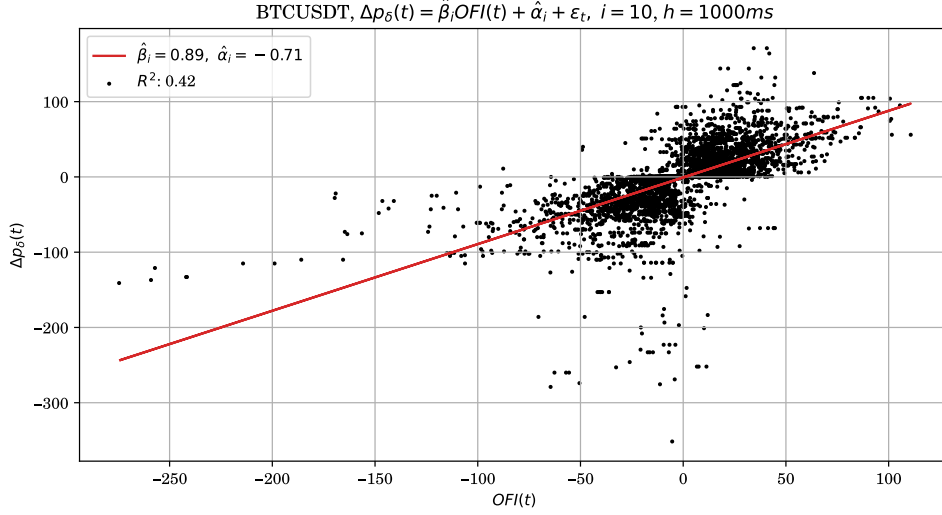


Figure 2.3 OFI contemporaneous regression for an example half-hour window for BTCUSDT.

We observe very similar R^2 values across all trading pairs, around 0.35, confirming the linear relation (2.8). We also visualize the regression for an example half hour window in Figure 2.3.

We repeat the procedure for different values of h and plot the results in Figure 2.4. We see that R^2 increases in h and then plateaus around $h = 20,000ms$.

Instead of averaging across intervals, we can also examine how the price impact coefficients change across intervals. We visualize the results in Figures 2.5 - 2.8. We see that, for our data, for all trading pairs the average price impact coefficient is initially decreasing in time for the first few hours of the day. It then recovers and begins to (roughly) increase again. We also see that the variance of the price impact coefficients are fairly constant across different intervals. The fact that we have trends in price impact coefficients suggests that the impact of a new orderbook event on the mid-price varies throughout the day, with some periods having less impact (assuming the linear price impact model given by (2.8)). The smallest average coefficients seem to occur around 06:00AM and so we suggest placing trades around this time if the goal is to minimize price impact.

2.4.3 Conclusion

Whether this model is too simple to realistically model price impact in a useful way is not something we explore in this paper. The purpose of this section rather, was to introduce orderflow and show that it has relevance for influencing price changes in the orderbook.

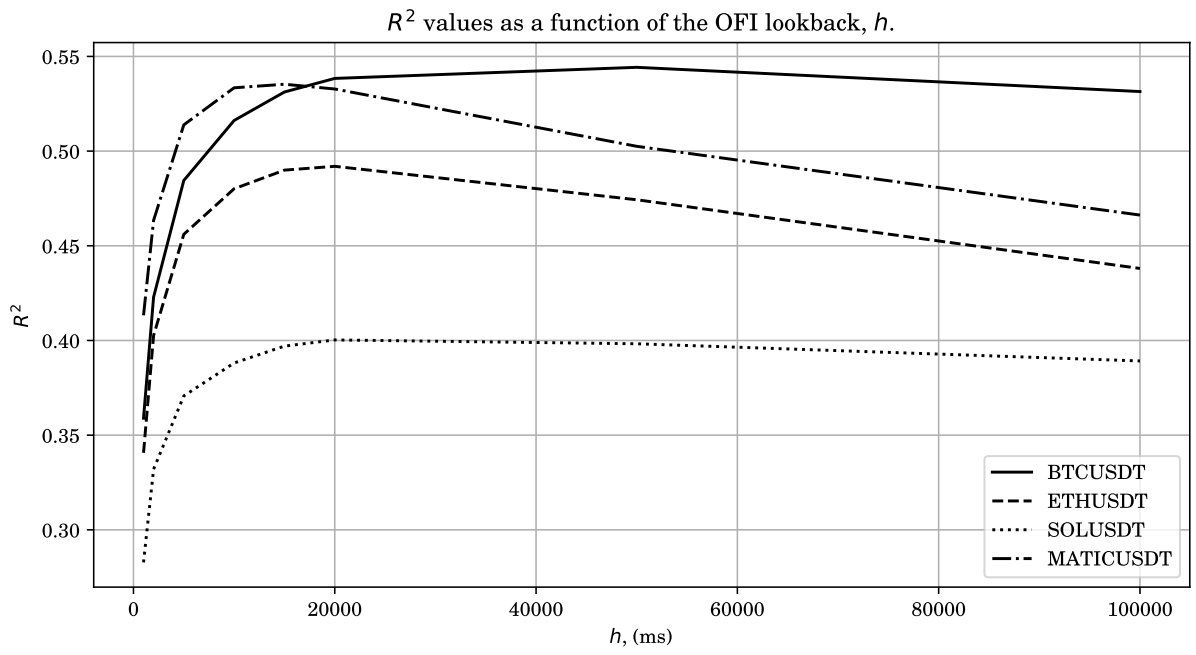


Figure 2.4 Effect on contemporaneous regression $\Delta p_\delta(t) = \hat{\beta}_i \text{OFI}_h(t) + \hat{\alpha}_i + \hat{\epsilon}_t$, R^2 values when varying the lookback period, h , that defines $\text{OFI}_h(t)$.

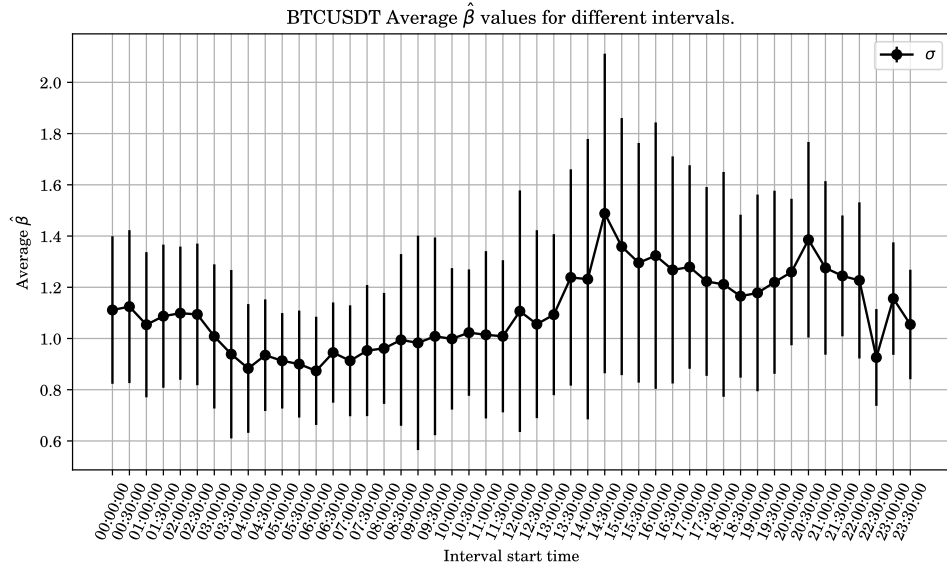


Figure 2.5 BTCUSDT Average price impact coefficients for different half-hour intervals. Note that errorbars represent standard deviations.

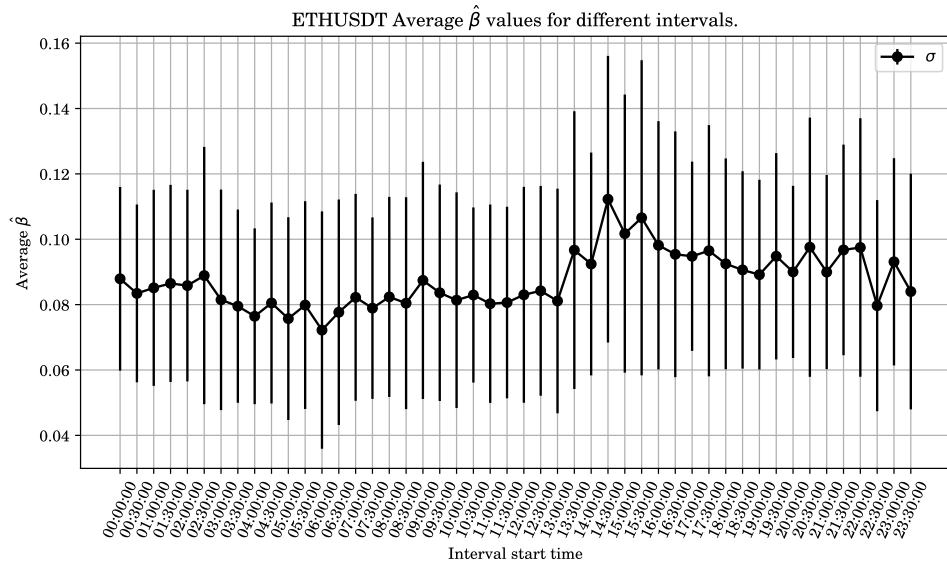


Figure 2.6 ETHUSDT Average price impact coefficients for different half-hour intervals. Note that errorbars represent standard deviations.

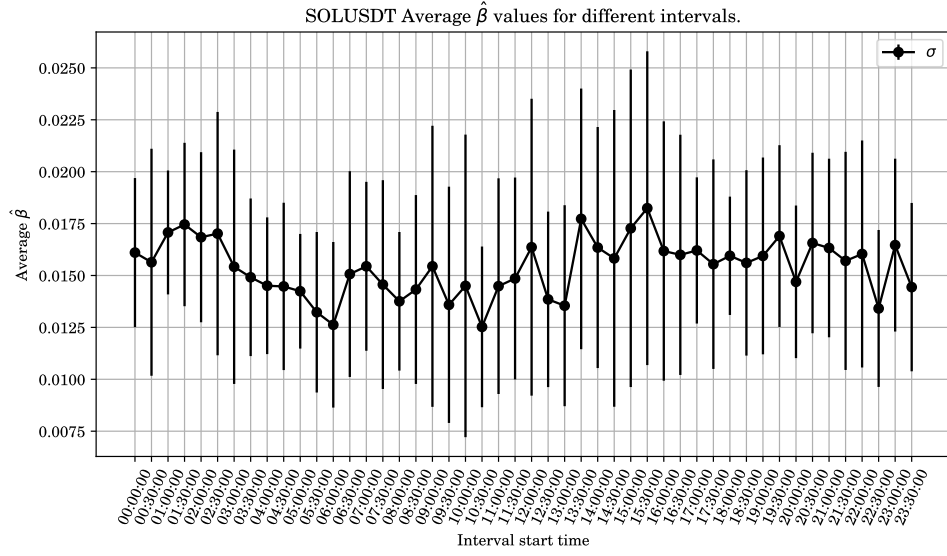


Figure 2.7 SOLUSDT Average price impact coefficients for different half-hour intervals. Note that errorbars represent standard deviations.

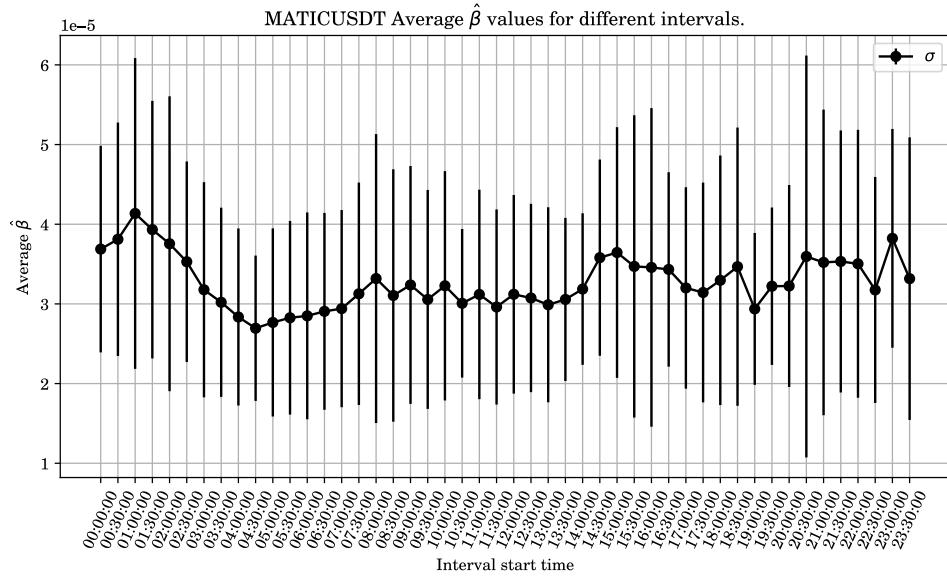


Figure 2.8 MATICUSDT Average price impact coefficients for different half-hour intervals. Note that errorbars represent standard deviations.

Chapter 3

Predictive Modelling

3.1 The Modelling Objective

Our main aim in this chapter is to predict future mid-price¹ movement. There are multiple possible modelling setups when it comes to mid-price movement prediction. [21] frame this as a regression problem, directly predicting future mid-price values at multiple horizons. [19] and [22] predict the sign of the returns, in a multi-class classification setting. They argue that due to the highly stochastic nature of financial data, simply calculating labels based on returns from $p_0(t)$ and $p_0(t + k)$ leads to a label set with a lower signal to noise ratio, so smoothed returns are used.

In this paper we use the multi-class classification setup. Following [19], we adopt the smoothed labelling method first introduced in [32]. Define the quantites:

$$m_-(t) := \frac{1}{k} \sum_{i=0}^k p_0(t - i) \quad (3.1)$$

$$m_+(t) := \frac{1}{k} \sum_{i=1}^k p_0(t + i) \quad (3.2)$$

$$\ell(t) := \frac{m_+(t) - m_-(t)}{m_-(t)} \quad (3.3)$$

So $m_-(t)$ represents the average price for the previous k prices and current price and $m_+(t)$ represents the average price for the next k prices. Then we calculate the smoothed returns $\ell(t)$ as the return of this smoothed price. Then we discretize these returns according to (3.4) in order to give us three distinct class labels for use in classification.

$$y(t) = \begin{cases} +1 & \text{if } \ell(t) \in (\epsilon, \infty) \\ 0 & \text{if } \ell(t) \in [-\epsilon, \epsilon] \\ -1 & \text{if } \ell(t) \in (-\infty, -\epsilon) \end{cases} \quad (3.4)$$

So given the information we have up to and including time t , our aim is to build a model to predict $y(t)$.

¹Recall in (2.1) we defined the mid-price, $p_0(t)$ to be the average of the best bid and ask prices at time t .

See Figure 3.1 for a sample of our mid-price data, colour coded according to class label. We see regions of mid-price downtrend are labelled with -1 (coloured red), regions of mid-price plateau are labelled with 0 (coloured blue) and regions of mid-price uptrend are labelled with +1 (coloured green).

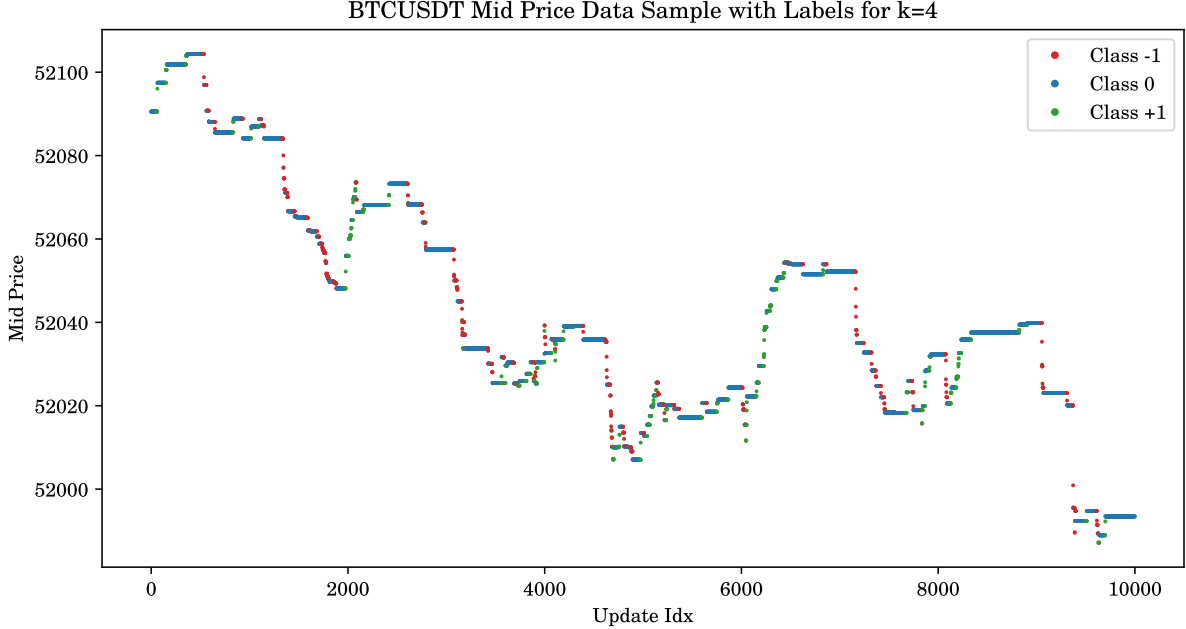


Figure 3.1 An example BTCUSDT mid-price sample, coloured according to class label. Note that the discretization parameter, ϵ is set ≈ 0 and the prediction horizon is $k = 4$ updates.

Note that in some implementations, the prediction horizon is given over some time interval, such as predicting the movement for the next 10 seconds. In this paper, we instead define our prediction horizon in terms of ticks/updates/datapoints. This choice was made as our WebSocket data arrives at irregular times, and for some short intervals there is no available data. We expect the results to be very similar when using a time-based horizon.

3.2 Model Architecture Background

In this section we explain the general theory needed for our classification models.

3.2.1 Logistic Regression

Linear regression is one of the oldest and most robust predictive models used in all areas of science. Its simplicity, explainability and robustness means it is a common choice for a baseline/benchmark model.

Logistic regression, first introduced in [33], is the natural extension of linear regression to the classification setting. The key idea is to model the *log odds* as linear functions of our data.

Suppose we have C classes, indexed by $1, 2, \dots, C$, then we assume the following linear model:

$$\begin{aligned}\log \frac{\mathbb{P}(Y = 1|X = x)}{\mathbb{P}(Y = C|X = x)} &= \alpha_1 + \beta'_1 x \\ \log \frac{\mathbb{P}(Y = 2|X = x)}{\mathbb{P}(Y = C|X = x)} &= \alpha_2 + \beta'_2 x \\ &\vdots \\ \log \frac{\mathbb{P}(Y = C - 1|X = x)}{\mathbb{P}(Y = C|X = x)} &= \alpha_{C-1} + \beta'_{C-1} x\end{aligned}$$

Note that because the probabilities must sum to 1, we have $C - 1$ degrees of freedom. Also note that the choice of denominator is not important as the model is equivariant under the choice of denominator class.

With some re-arrangement, we get the posterior probabilities:

$$\begin{aligned}\mathbb{P}(Y = c|X = x) &= \frac{\exp(\alpha_c + \beta'_c x)}{1 + \sum_{\ell=1}^{C-1} \exp(\alpha_\ell + \beta'_\ell x)} \\ \mathbb{P}(Y = C|X = x) &= \frac{1}{1 + \sum_{\ell=1}^{C-1} \exp(\alpha_\ell + \beta'_\ell x)}\end{aligned}$$

Where $c \in 1, 2, \dots, C - 1$.

Interestingly we note that the log odds representation is equivalent to a bijective mapping of the linear functions $\alpha_c + \beta'_c x$ onto $[0, 1]$ using the sigmoid function: $1/(1 + \exp(-x))$. Note that the parameters $(\alpha_c, \beta_c)_{c=1}^C$ are fit by maximizing the log-likelihood using gradient descent methods. So given some observation, x_t , our model gives us the posterior probabilities of the observation belonging to each class. In order to make a classification, we can simply choose the class with the highest posterior probability, and assign this class to \hat{y}_t . We refer the interested reader to [34] for a more in-depth exposition of the theory.

3.2.2 Decision Trees

Decision Trees are another very popular class of machine learning models with a large amount of success in a wide range of fields. There are two main types; decision trees for classification and decision trees for regression. The theory for both is very similar and they share the same ideas. We focus on classification here. The main idea is to learn an *optimal* partition of our data using binary trees, with each non-leaf node representing a split of our data on one variable. The model learns which features to split on at each level and which threshold values to use for the splits. More formally, following [34], suppose our data is $X \in \mathbb{R}^{n \times d}$, then we seek to partition our data into M regions, R_1, R_2, \dots, R_M , and then our prediction is given by:

$$\hat{y}(x) = \sum_{m=1}^M c_m 1\{x \in R_m\} \quad (3.5)$$

Where c_m is the most common class in region R_m , i.e.

$$c_m = \arg \max_{c \in \{1, 2, \dots, C\}} |\{y_i : y_i = c \wedge x_i \in R_m\}| \quad (3.6)$$

Consider splitting our data with feature j , and threshold s . We denote the resulting partitions with R_1 and R_2 , defined as:

$$\begin{aligned}R_1(j, s) &:= \{X : X_j \leq s\}, \\ R_2(j, s) &:= \{X : X_j > s\}\end{aligned} \quad (3.7)$$

The *optimal* j and s are chosen to solve:

$$j^*, s^* = \arg \min_{j, s} \mathcal{L}(R_1(j, s), R_2(j, s)) \quad (3.8)$$

Where \mathcal{L} is some loss function measuring how well the partition splits the data.

Since checking all combinations of features and threshold values would be computationally infeasible, the fitting algorithm uses an iterative greedy approach, choosing the optimal splits at each level based on some loss function that measures how well the split partitions the data for the next level. One commonly used loss function is the misclassification error:

$$\mathcal{L}(R_1, R_2) = \min_{c_1} \frac{1}{n_1} \sum_{x_i \in R_1(j, s)} 1(y_i \neq c_1) + \min_{c_2} \frac{1}{n_2} \sum_{x_i \in R_2(j, s)} 1(y_i \neq c_2) \quad (3.9)$$

In practice other loss functions, such as *cross-entropy* or *gini impurity*, are often used. They are also differentiable which is a key property for certain optimization algorithms. We again refer the interested reader to [34] for a more in-depth discussion of these details.

Simple decision trees have high variance, meaning they can easily overfit to training data. For this reason, various *ensemble* methods were devised to reduce overfitting. We introduce one such method, *Boosting*. The basic idea is to iteratively train many *weak learners* and then combine their predictions to produce a single, more robust prediction. Weak learners are simple models which are only slightly better than randomly guessing and have low variance and high bias. In theory, by combining many weak learners, boosting lowers the model bias, whilst keeping variance low. In more detail, in each iteration, we fit a weak classifier (e.g. a single decision tree stump). We then compute the error according to some loss function. Then we use this error to define the weight for the current iteration, then we re-weight our training data, using this weight, so samples where the model performed badly are given more weight in the next iteration. Then our final output model will be a weighted sum of the predictions of the weak learners.

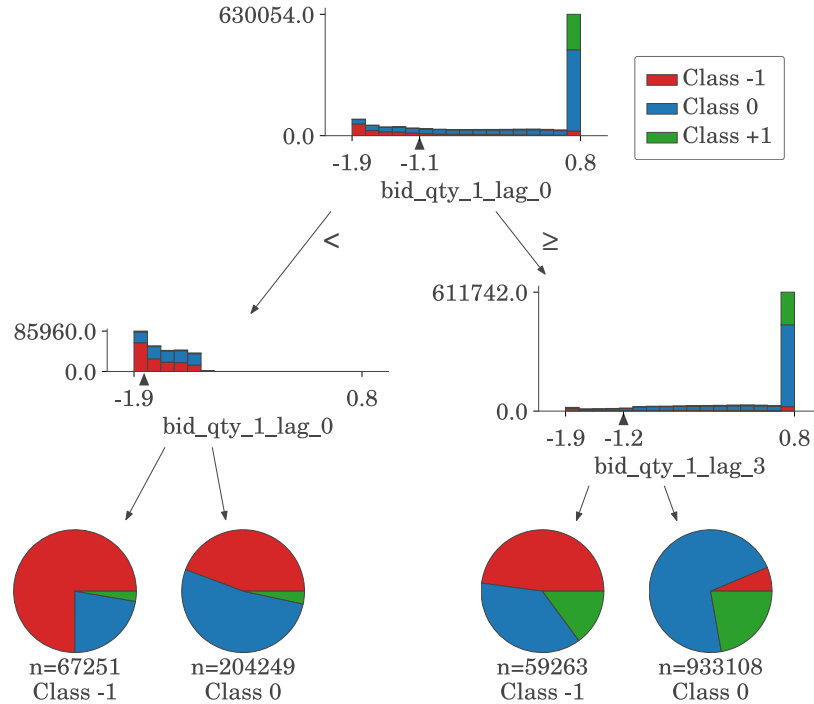


Figure 3.2 A visualization of a single decision tree weak learner with max depth set to 2.

3.2.3 Artificial Neural Networks

Artificial Neural Networks are a broad class of machine learning model that can efficiently approximate high dimensional non-linear functions. Perhaps the most famous example of an ANN (Artificial Neural Network) is that of the Multi-Layer Perceptron, first introduced in [16]. The basic idea is to take some input vector and successively project it onto new spaces with affine and then non-linear transformations. An MLP with N hidden layers can be defined mathematically as:

$$\begin{aligned} f_i(x; W_i, b_i) &= \sigma_i(W_i x + b_i) \\ f(x; W_1, W_2, \dots, W_N, b_1, b_2, \dots, b_N) &= f_N \circ f_{N-1} \circ \dots \circ f_2 \circ f_1(x) \end{aligned} \quad (3.10)$$

Where W_i are learnable weight matrices, b_i are learnable bias vectors, σ_i are fixed non-linear activation functions and \circ denotes function composition. MLPs are powerful because, as [17] shows, they are *universal function approximators*. This means that, with as few as one hidden layer and using arbitrary activation functions, they are capable of approximating any Borel measurable function from one finite dimensional space to another to any desired degree of accuracy, provided sufficiently many hidden units are available. The weight matrices and bias vectors are learnt by minimizing some loss function. If we denote our learnable parameters as θ , then our loss function is given by:

$$\mathcal{L}(\theta; x, y) := \frac{1}{n} \sum_{i=1}^n \ell(f(x_i; \theta), y_i) \quad (3.11)$$

Where ℓ is some observation-wise loss that measures how well our model predicts y_i given corresponding input x_i . For simple problems \mathcal{L} is commonly a convex function and so gradient descent methods can be used to perform the minimization. For example, for vanilla gradient descent, one might define the update rule as:

$$\theta^{(t+1)} \leftarrow \theta^{(t)} - \eta \nabla_{\theta} \mathcal{L}(\theta^{(t)}) \quad (3.12)$$

In practice the optimization problem is often not convex, with many local minima, and so alternative optimization methods are often used, such as *Stochastic Gradient Descent*, [35], or *ADAM*, [36]. Stochastic Gradient Descent is a stochastic approximation of the gradient descent method, that evaluates the gradient on a randomly sampled subset of the training data, instead of the entire training data. It can be shown, [35], that the stochastic approximation of the gradient converges in expectation to the gradient evaluated on the entire training dataset. This sub-sampling allows for fewer gradient evaluations and therefore faster training. Also the stochastic nature of the algorithm means it is less likely to get stuck in local minima. ADAM, first introduced in [36], is a more advanced type of Stochastic Gradient Descent that uses the concept of *Momentum*, [9]. Momentum accumulates the gradient from past updates to help guide the direction of the current step. It helps to reduce oscillations during descent and often leads to faster convergence.

The ADAM update step is given by:

$$\begin{aligned} m_{\theta}^{(t+1)} &\leftarrow \beta_1 m_{\theta}^{(t)} + (1 - \beta_1) \nabla_{\theta} \mathcal{L}(\theta^{(t)}) \\ v_{\theta}^{(t+1)} &\leftarrow \beta_2 v_{\theta}^{(t)} + (1 - \beta_2) \left(\nabla_{\theta} \mathcal{L}(\theta^{(t)}) \right)^2 \\ \hat{m}_{\theta} &= \frac{m_{\theta}^{(t+1)}}{1 - \beta_1^t} \\ \hat{v}_{\theta} &= \frac{v_{\theta}^{(t+1)}}{1 - \beta_2^t} \\ \theta^{(t+1)} &\leftarrow \theta^{(t)} - \eta \frac{\hat{m}_{\theta}}{\sqrt{\hat{v}_{\theta}} + \delta}. \end{aligned} \quad (3.13)$$

So we see that ADAM uses exponential moving averages with decay factors β_1 and β_2 to accumulate first and second gradient moments. Note that δ is some small constant, used to prevent zero division errors.

Using traditional differentiation methods, the $\nabla_{\theta} \mathcal{L}(\theta^{(t)})$ calculation would be very computationally expensive and training would be too slow to be practical. Instead, an algorithm called *backpropagation*, [9], can be used to efficiently differentiate the network with respect to the weights and biases. Backpropagation is an efficient implementation of the chain rule for differentiation that uses dynamic programming to avoid repeated calculations. The idea is to construct a *computational graph*, which is a graph datastructure, where nodes represent functions and the edges represent function compositions. So by doing a *forward pass* of the graph, we are essentially evaluating the network given some input. We then get an output, and do a *backward pass* to accumulate gradients in an efficient way using the chain rule. Backpropagation has computational complexity of the order of the number of edges in the computational graph, so for large networks it scales very well and can be made to run extremely efficiently.

3.2.4 Convolutional Neural Networks

Convolutional Neural Networks (CNNs) are a specialized class of artificial neural networks designed primarily for processing structured grid data, such as images. First introduced in [12], CNNs have become a cornerstone in the field of computer vision due to their ability to efficiently capture spatial hierarchies in data.

The fundamental building block of a CNN is the convolutional layer, which applies a series of learnable filters (or kernels) to the input data. Each filter *convolves* across the input. Mathematically, the output of a convolutional layer can be expressed as:

$$h_{ij} = \sigma((W * x)_{ij} + b) \quad (3.14)$$

where W are the learnable filters, b are the learnable biases, $*$ denotes the convolution operation, and σ is a non-linear activation function applied element-wise. Note that for a $k \times k$ filter, the discrete convolution operation is defined as:

$$(W * x)_{ij} := \sum_{m=-k}^k \sum_{n=-k}^k W_{mn} x_{i-m, j-n} \quad (3.15)$$

So essentially we're sliding a window/filter over our 2D data and taking the dot product at each position, resulting in a new 2D output for each filter. This means the number of 2D outputs (*channels*) is equal to the number of filters for that layer. The convolutional operation is a vector product and is differentiable with respect to the filters, so we can simply apply gradient descent, just the same as with ANNs, to learn our filters and biases.

In addition to convolutional layers, we also introduce *pooling layers* which down-sample the spatial dimensions of the input, reducing computational complexity and aiding in hierarchical feature extraction. The most common type of pooling is max-pooling, defined as:

$$h_{ij} = \max_{(m,n) \in P_{ij}} x_{mn} \quad (3.16)$$

where P_{ij} represents a pooling region around position (i, j) .

CNNs are powerful because they leverage three important ideas: local receptive fields, shared weights, and spatial subsampling. These ideas enable CNNs to only look at relevant information, be much more computationally efficient and also to be invariant to small translations, scale, and distortions, [37].

3.2.5 Long Short-Term Memory

First introduced in [11], a Long Short-Term Memory is a special type of Recurrent Neural Network. RNNs are neural networks that take in sequences of input iteratively. At each iteration, they take in the previous *hidden state* and the current input and then update the hidden state and give an output. This hidden state mechanism allows them to *remember* long-term dependencies between inputs and they are often used to learn temporal dependencies in timeseries data. One of the most famous simple RNNs is the Jordan network, introduced in [38], where the hidden state at each iteration, h_t and the output y_t are given by:

$$\begin{aligned} h_t &= \sigma_h(W_h x_t + U_h y_{t-1} + b_h) \\ y_t &= \sigma_y(W_y h_t + b_y) \end{aligned} \quad (3.17)$$

where x_t, h_t, y_t are the input, hidden state and output at iteration t respectively. W, U and b are all learnable parameter matrices/vectors and σ_h and σ_y are activation functions. Whilst in theory, simple RNNs should be able to remember any length dependency, in practice they suffer from the *vanishing gradients problem*, [39], where gradients converge to zero during training, and therefore learning stops. LSTMs were designed to address this problem, with special *forget gates* which learn to forget irrelevant information. The most common type of LSTMs are composed of an *input gate*, *output gate*, *forget gate* and a *cell*. The cell learns the information and the other gates regulate the flow of information from/to the cell. Mathematically this looks like:

$$\begin{aligned} f_t &= \sigma_g(W_f x_t + U_f h_{t-1} + b_f) \\ i_t &= \sigma_g(W_i x_t + U_i h_{t-1} + b_i) \\ o_t &= \sigma_g(W_o x_t + U_o h_{t-1} + b_o) \\ \tilde{c}_t &= \sigma_c(W_c x_t + U_c h_{t-1} + b_c) \\ c_t &= f_t \odot c_{t-1} + i_t \odot \tilde{c}_t \\ h_t &= o_t \odot \sigma_h(c_t) \end{aligned} \quad (3.18)$$

where \odot denotes the element-wise product, [40]. So essentially we are just expanding on the idea of the RNN with more hidden state for greater control over what information is learnt. Just like any other neural network, RNNs and LSTMs can be trained by gradient descent with backpropagation.

3.3 Model Architectures

In this section we introduce the specialized models we will be using for our classification problem.

3.3.1 Orderbook Features

Before we introduce our models, we first must introduce our features. We seek to define feature vectors $\mathbf{x}_t \in \mathbb{R}^d$ which capture the relevant orderbook information relating to future mid-price movement. We can then learn a model of the form:

$$\hat{y}(t) = \hat{f}(\mathbf{x}(t)) \quad (3.19)$$

that seeks to minimize some loss function w.r.t the true labels $y(t)$, i.e.

$$\hat{f} = \arg \min_f \mathcal{L}(\mathbf{y}, f(X)) \quad (3.20)$$

Raw Orderbook Features

[19] use the raw orderbook data for their model input i.e. $\mathbf{x}(t)$ takes the form:

$$\mathbf{x}(t) =: \mathbf{x}_t = [p_{t,\ell}^A, q_{t,\ell}^A, p_{t,\ell}^B, q_{t,\ell}^B]_{\ell=1}^L \in \mathbb{R}^{4L} \quad (3.21)$$

where L represents the maximum orderbook level in the data. For our data we have 10 orderbook levels, so $L = 10$. It is important to note that this is a non-stationary series. It also combines price and volume information, which have different units, which is not ideal for most models. Henceforth, we shall refer to this feature vector as the LOB (Limit OrderBook) feature vector.

Orderflow Features

[21] extend the idea of OFI, defined in (2.4), beyond the first level. Define ² the contribution of the n^{th} event at level ℓ on the (A)sk/(B)id side as:

$$e_{t,\ell}^A := I_{\{p_{n,\ell}^A \leq p_{n-1,\ell}^A\}} q_n^A - I_{\{p_{n,\ell}^A \geq p_{n-1,\ell}^A\}} q_{n-1,\ell}^A \quad (3.22)$$

$$e_{t,\ell}^B := I_{\{p_{n,\ell}^B \geq p_{n-1,\ell}^B\}} q_n^B - I_{\{p_{n,\ell}^B \leq p_{n-1,\ell}^B\}} q_{n-1,\ell}^B \quad (3.23)$$

Then we define the Orderflow feature vector as:

$$\mathbf{x}_t := [e_{t,\ell}^A, e_{t,\ell}^B]_{\ell=1}^L \in \mathbb{R}^{2L} \quad (3.24)$$

This feature vector is stationary and is given in units of volume, so is consistent across dimensions. It is also half the dimension of the LOB feature vector, a desirable property for the convergence of many models. Henceforth, we shall refer to this feature vector as the OF (OrderFlow) feature vector.

3.3.2 lrLOB & lrOF

For our use case, we will define two logistic regression models, one using the LOB feature vectors first introduced in 3.21 and the other using the OF features introduced in 3.24. Henceforth we will refer to these models as lrLOB and lrOF respectively. Of course, when dealing with timeseries modelling, it is also important to incorporate autoregressive features that allow the model to see previous observations for some lookback window. We define our lookback window to be the previous T observations. We incorporate these into our model by concatenating lagged versions of the feature vector, i.e. our model inputs will be:

$$\mathbf{x}_t^{AR} = [\mathbf{x}_t; \mathbf{x}_{t-1}; \mathbf{x}_{t-2}; \dots; \mathbf{x}_{t-T}] \in \mathbb{R}^{dT} \quad (3.25)$$

This will be the input to our logistic regression models. The output will be $\hat{y}_t \in \{-1, 0, 1\}$. Note that we choose $T = 10$, since larger values of T will hurt the convergence of the fitting algorithm and take too much memory and too long to fit. This is a major limitation of this model and in later sections we introduce models designed to handle much larger lookback windows.

²We interchangeably use the notation $p_t := p(t)$.

3.3.3 xgbLOB & xgbOF

XGBoost, first introduced in [27], is an extremely efficient implementation of Boosted Decision Trees. We choose XGBoost as one of our models for several reasons. Firstly XGBoost has been shown to be highly effective in a wide range of applications. It has great representational capacity, with the ability to capture high dimensional, non-linear relationships in the data, with tight control of overfitting. It handles high dimensional data well, with feature sub-sampling helping to reduce overfitting. It also has great explainability, with the ability to rank features by importance (which we will explore in a later section). As an added bonus, it can be run on a GPU, allowing for very fast training and inference. Interestingly there is little to no mention of its use for limit orderbook prediction in the literature, and we believe it has great potential for this purpose. XGBoost has many hyperparameters that one can tune. We fine-tune our models on validation data and present our fine-tuned hyperparameters along with their definitions here:

- **max depth** = 10. The max depth of each weak learner tree.
- **eta** = 0.1. Step size shrinkage used in update to prevent overfitting. After each boosting step, we can directly get the weights of new features, and eta shrinks the feature weights to make the boosting process more conservative.
- **data subsample ratio** = 0.8. The proportion of the training data that each weak learner can use.
- **column subsample ratio** = 0.8. The proportion of the features available when performing splits.
- **evaluation metric** = Multiclass classification error rate. The metric used during the boosting algorithm to determine weights.

Similar to our logistic regression models, we define two XGBoost models, one using the LOB feature vectors first introduced in 3.21 and the other using the OF features introduced in 3.24. Henceforth we will refer to these models as xgbLOB and xgbOF respectively. As before, we use the autoregressive feature concatenation introduced in 3.25. Through experimentation on the validation set, we find that setting $T := k$ gives best performance. However, as with the logistic regression models, we are limited by memory. This time we are limited by GPU memory. Specifically we find that $T := 20$ is the maximum feasible lookback for our setup and therefore we set $T := \min(k, 20)$.

3.3.4 DeepLOB

First introduced in [19], the DeepLOB model is a deep neural network that uses a combination of convolutional and LSTM layers to extract short and long term features from the raw order-book data. In this section we give a general overview of this model, but we refer the interested reader to [19] for a more in-depth exposition.

Firstly, it is important to understand the structure of the model input in order to understand the convolutional filter dimension choices. The model input is a vertical concatenation of our LOB feature vectors, denoted by $X_t \in \mathbb{R}^{T \times 4L}$, where $X_t :=$

$$\begin{bmatrix} p_{t-T,1}^A & q_{t-T,1}^A & p_{t-T,1}^B & q_{t-T,1}^B & \cdots & p_{t-T,L}^A & q_{t-T,L}^A & p_{t-T,L}^B & q_{t-T,L}^B \\ p_{t-(T-1),1}^A & q_{t-(T-1),1}^A & p_{t-(T-1),1}^B & q_{t-(T-1),1}^B & \cdots & p_{t-(T-1),L}^A & q_{t-(T-1),L}^A & p_{t-(T-1),L}^B & q_{t-(T-1),L}^B \\ \vdots & \vdots & \vdots & \vdots & \ddots & \vdots & \vdots & \vdots & \vdots \\ p_{t-1,1}^A & q_{t-1,1}^A & p_{t-1,1}^B & q_{t-1,1}^B & \cdots & p_{t-1,L}^A & q_{t-1,L}^A & p_{t-1,L}^B & q_{t-1,L}^B \\ p_{t,1}^A & q_{t,1}^A & p_{t,1}^B & q_{t,1}^B & \cdots & p_{t,L}^A & q_{t,L}^A & p_{t,L}^B & q_{t,L}^B \end{bmatrix}$$

Note that if we reshape and flatten this matrix, we recover our autoregressive LOB feature vector defined in (3.25), however in this case, we can use a much larger lookback without running out of memory, so we set $T = 100$.

The DeepLOB model is comprised of three main modules, a convolutional module, an inception module and an LSTM module. The output is then fed into a final linear layer before being passed through a softmax function to give probabilities of each class, where the function $\text{softmax} : \mathbb{R}^d \rightarrow \Delta^{d-1}$ is defined element-wise as:

$$\text{softmax}(x)_i = \frac{\exp(x_i)}{\sum_{j=1}^d \exp(x_j)} \quad (3.26)$$

$\text{LeakyReLU}(x) := \max(0, x) + 0.01 * \min(0, x)$, [41], activation functions are used between each layer to introduce non-linearity. Batch normalization is also used to ensure stable training. We use the ADAM optimizer, [36], with learning rate set to 0.0001 and the Cross Entropy Loss, [42], which is essentially a weighted log-softmax.

We present a schematic of the DeepLOB model in Figure 3.3 and give a more in-depth explanation of the three main modules below.

DeepLOB Main Modules

Convolutional Module:

- Conv 1 aggregates price and volume information for each level for each side;
- Conv 2 aggregates information across side for each level;
- Conv 3 aggregates information across the whole orderbook.

The convolutional blocks use horizontal filters of dimension 1×2 with stride 1×2 , in order to combine price and volume information. Then they use vertical 4×1 convolutional filters to combine information across time, 4 timesteps at a time. Then the final convolutional block uses a 1×10 convolutional filter to combine information across all 10 levels of the orderbook.

Inception Module: The inception module has three blocks. The 1×1 filters increase the dimensionality of the input and then the 3×1 and 5×1 simulate moving averages. The main idea is to simulate a *Network-In-Network*, [43]. A Network-In-Network essentially replaces the convolution operation with a small MLP that is shared among all convolutional windows. The output is obtained by sliding the MLP over the input in a similar manner as CNN. The outputs of each inception block are then concatenated and reshaped into a $\mathbb{R}^{T \times 192}$ timeseries which is then fed into the LSTM module.

LSTM Module: The LSTM module is comprised of an LSTM layer with 64 hidden units. The purpose of this layer is to capture long term dependencies from the inception output.

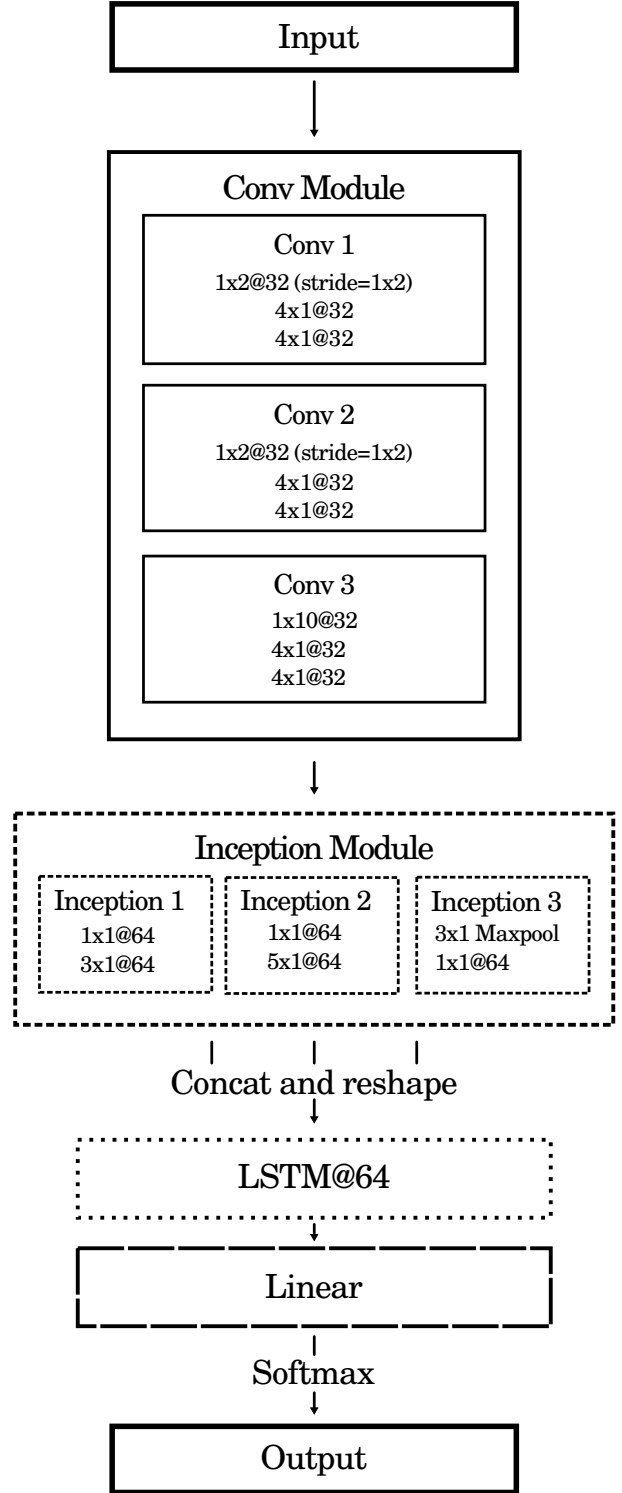


Figure 3.3 DeepLOB model architecture overview. Note: 1x2@32 denotes a convolutional layer with 32 filters and kernel size 1x2.

3.3.5 DeepOF

Introduced in [21], DeepOF is a modification of the DeepLOB architecture, using OF features, rather than LOB features. [21] show that using orderflow instead of the raw orderbook representation leads to better performance. The DeepOF input is given by:

$$X_t := \begin{bmatrix} e_{t-T,1}^A & e_{t-T,1}^B & \cdots & e_{t-T,L}^A & e_{t-T,L}^B \\ e_{t-(T-1),1}^A & e_{t-(T-1),1}^B & \cdots & e_{t-(T-1),L}^A & e_{t-(T-1),L}^B \\ \vdots & \vdots & \ddots & \vdots & \vdots \\ e_{t-1,1}^A & e_{t-1,1}^B & \cdots & e_{t-1,L}^A & e_{t-1,L}^B \\ e_{t,1}^A & e_{t,1}^B & \cdots & e_{t,L}^A & e_{t,L}^B \end{bmatrix} \in \mathbb{R}^{T \times 2L} \quad (3.27)$$

where we have extended the tick level orderflow definition from (2.4) to any arbitrary orderbook level, ℓ :

$$\begin{aligned} e_{t,\ell}^B &:= I_{\{p_{t,\ell}^B \geq p_{t-1,\ell}^B\}} q_{t,\ell}^B - I_{\{p_{t,\ell}^B \leq p_{t-1,\ell}^B\}} q_{t-1,\ell}^B \\ e_{t,\ell}^A &:= I_{\{p_{t,\ell}^A \leq p_{t-1,\ell}^A\}} q_{t,\ell}^A - I_{\{p_{t,\ell}^A \geq p_{t-1,\ell}^A\}} q_{t-1,\ell}^A \end{aligned} \quad (3.28)$$

In terms of model architecture, the DeepOF model is the same as the DeepLOB model, except without the first convolutional block, Conv 1. Recall that this block aggregates the price and volume information from the LOB input, so by using OF input, we have essentially aggregated the price and volume information manually using a predefined feature transform that has been shown to be predictive of mid-price movement. [20], [21].

3.4 Methodology

3.4.1 Sliding Window Setup

We use a sliding window evaluation method, with train, validation and testing splits. See Figure 3.4 for a visual representation of the splits.

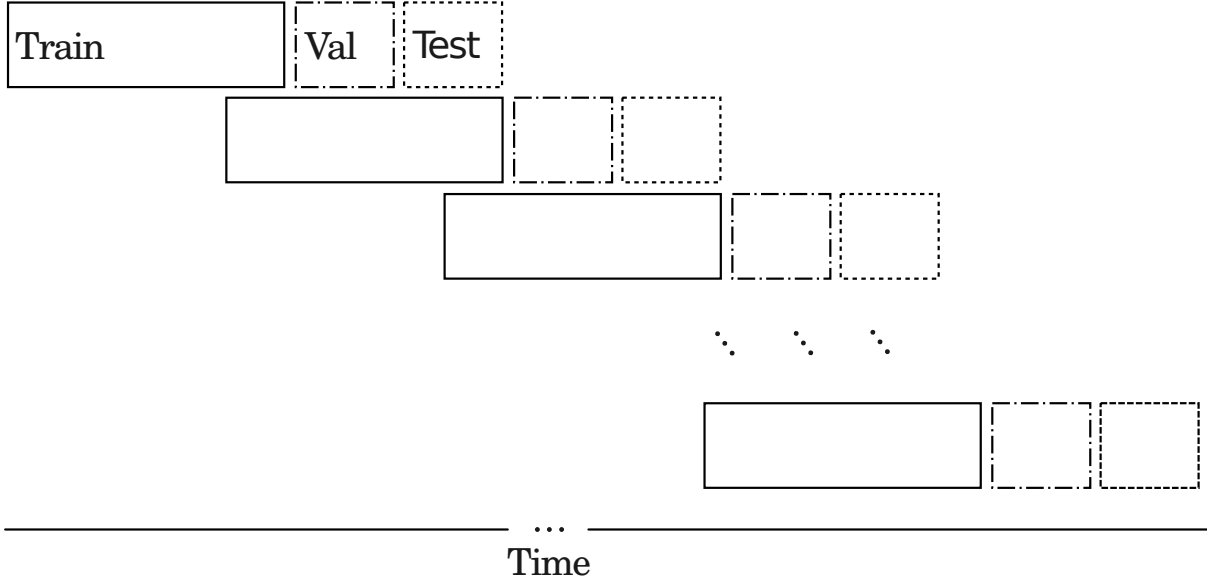


Figure 3.4 Sliding window visualization.

So using this method we are able to validate and test on almost the entire dataset, and only train on recent, relevant information. Note that we leave gaps between the train, val and test

blocks to avoid data leakage from features that look back in time. We fix the length of the initial training window to 48 hours and the validation and testing windows to 24 hours each.

The general testing procedure will be to train on the training set, then fine-tune our hyperparameters using the validation set, then once all of our hyperparameters have been chosen, we will test on the test set. Of course this means there will be a gap of 24 hours between our training and testing data. We could alternatively merge the training and validation data once hyperparameter tuning is complete and then re-train our models on the merged data before testing. However, leaving this gap will provide an extra guarantee of robustness and provide a better picture of the out of sample performance of our models.

3.4.2 Data Normalization

For several of our models, data normalization is important in order to ensure stable training and convergence. [22] and [19] use five day rolling window normalization whereas [21] use z -scores calculated using the training data. We find the rolling window normalization method to give worse performance, since it transforms our data in a non-linear way and so, for example, periods of no price change are no longer flat. So following [21], for each train-val-test window we calculate the sample mean and standard deviation of the training data, and use these to scale the training, validation and testing data via z -scores.

3.4.3 Choice of label discretization parameter

Following [22], we set our discretization parameter, ϵ , from (3.4) for each k and train-val-test window, w , so that the classes are roughly balanced. i.e.

$$\epsilon := \epsilon_{k,w} := \frac{|\hat{F}_{k,w}^{-1}(\frac{1}{3})| + \hat{F}_{k,w}^{-1}(\frac{2}{3})}{2} \quad (3.29)$$

Where $\hat{F}_{k,w}$ is the empirical distribution of the training set $\ell(t)$, (3.3), smoothed returns for prediction horizon k , and window w .

3.4.4 Model Training

Our DeepLOB and DeepOF models were trained with PyTorch, [44], on an Nvidia RTX 3060 12GB with 64GB memory and a 14-core 20-thread Intel i5 13600K. We use the ADAM optimizer, [36], with learning rate set to 0.0001. For our loss function we use the Cross Entropy Loss, [42]. We trained our models until the validation loss plateaued and then used the model from the epoch with highest validation loss.

3.5 Results

3.5.1 Classification Metrics

Recall that this is a multi-class classification problem, with our three classes, -1 , for negative smoothed mid-price change, 0 for insignificant smoothed mid-price change and $+1$ for positive mid-price change. This is an imbalanced problem, where we have up to $4\times$ more 0 labels for small k compared with -1 or $+1$ labels, since small time frames often mean no significant price change. For this reason, accuracy is perhaps not the only metric we should care about. In this case, *precision*, *recall* and *F1* scores are often more insightful, [34]. Precision for class c is defined as:

$$\text{Precision}_c := \frac{\text{TP}_c}{\text{TP}_c + \text{FP}_c} \quad (3.30)$$

where:

- TP_c is the number of true positives for class c .
- FP_c is the number of false positives for class c .

So essentially, precision says: “out of all the times that we guessed class c , how many times were we correct?”

Recall for class c is defined as:

$$\text{Recall}_c := \frac{\text{TP}_c}{\text{TP}_c + \text{FN}_c} \quad (3.31)$$

where:

- TP_c is the number of true positives for class c .
- FN_c is the number of false negatives for class c .

So essentially, recall says: “out of all the times the true class was c , how many times did we predict it correctly?”

F1-score for class c is the harmonic mean of precision and recall, defined as:

$$\text{F1-score}_c := 2 \cdot \frac{\text{Precision}_c \cdot \text{Recall}_c}{\text{Precision}_c + \text{Recall}_c} \quad (3.32)$$

To get the overall performance across all classes, we can compute the macro-averaged precision, recall, and F1-score:

$$\text{Macro-Precision} := \frac{1}{3} \sum_{c \in \{-1, 0, +1\}} \text{Precision}_c \quad (3.33)$$

$$\text{Macro-Recall} := \frac{1}{3} \sum_{c \in \{-1, 0, +1\}} \text{Recall}_c \quad (3.34)$$

$$\text{Macro-F1-score} := \frac{1}{3} \sum_{c \in \{-1, 0, +1\}} \text{F1-score}_c \quad (3.35)$$

i.e. the unweighted mean. We can also define the weighted-average which weights each classes’ score according to their support. (Support for class c is the number of instances of that class in the ground truth test labels).

3.5.2 Model Results

As previously stated, we train our models on the training windows, then validate and tune our hyperparameters on the validation windows and then test on the test windows. We present the results of the models on the test windows here.

We calculate the macro-averaged metrics on the test set for $k \in \{4, 10, 50, 200\}$ and present the results in tables 3.1 - 3.4. For brevity, we only present the results for BTCUSDT here. We will delve deeper into the comparative performance of each model for different trading pairs later on. See appendix for un-averaged model results for all trading pairs.

accuracy	precision	recall	f1-score	support	model
0.87 (0.03)	0.91 (0.03)	0.74 (0.01)	0.80 (0.01)	647295(30003)	xgbOF
0.79(0.04)	0.75(0.05)	0.68(0.02)	0.70(0.01)	647295(30003)	xgbLOB
0.84(0.04)	0.87(0.02)	0.70(0.01)	0.76(0.01)	647289(30003)	lrOF
0.69(0.07)	0.66(0.08)	0.60(0.07)	0.59(0.06)	647289(30003)	lrLOB
0.86(0.03)	0.88(0.03)	0.74 (0.01)	0.79(0.0)	647199(30003)	deepOF
0.75(0.2)	0.73(0.22)	0.70(0.04)	0.69(0.17)	647199(30003)	deepLOB

Table 3.1 Mean macro averaged BTCUSDT test set classification results across windows for $k = 4$. (Standard deviations are given in parenthesis).

accuracy	precision	recall	f1-score	support	model
0.80 (0.03)	0.84 (0.04)	0.75(0.01)	0.78 (0.02)	647289(30003)	xgbOF
0.72(0.02)	0.71(0.02)	0.71(0.01)	0.71(0.01)	647289(30003)	xgbLOB
0.76(0.04)	0.81(0.03)	0.72(0.01)	0.74(0.02)	647289(30003)	lrOF
0.58(0.07)	0.62(0.05)	0.62(0.04)	0.57(0.08)	647289(30003)	lrLOB
0.79(0.03)	0.81(0.02)	0.76 (0.01)	0.77(0.01)	647199(30003)	deepOF
0.74(0.06)	0.76(0.04)	0.71(0.05)	0.72(0.06)	647199(30003)	deepLOB

Table 3.2 Mean macro averaged BTCUSDT test set classification results across windows for $k = 10$.

accuracy	precision	recall	f1-score	support	model
0.64(0.04)	0.65 (0.03)	0.62(0.01)	0.63(0.02)	647279(30003)	xgbOF
0.56(0.04)	0.57(0.03)	0.58(0.04)	0.53(0.06)	647279(30003)	xgbLOB
0.57(0.05)	0.62(0.03)	0.55(0.0)	0.55(0.02)	647289(30003)	lrOF
0.51(0.06)	0.52(0.03)	0.54(0.03)	0.46(0.06)	647289(30003)	lrLOB
0.66 (0.03)	0.65 (0.02)	0.65 (0.02)	0.65 (0.02)	647199(30003)	deepOF
0.57(0.07)	0.58(0.04)	0.57(0.07)	0.55(0.09)	647199(30003)	deepLOB

Table 3.3 Mean macro averaged BTCUSDT test set classification results across windows for $k = 50$.

accuracy	precision	recall	f1-score	support	model
0.52(0.04)	0.53(0.03)	0.50(0.01)	0.51(0.01)	647279(30003)	xgbOF
0.46(0.04)	0.45(0.02)	0.48(0.02)	0.40(0.04)	647279(30003)	xgbLOB
0.48(0.05)	0.50(0.02)	0.46(0.01)	0.45(0.01)	647289(30003)	lrOF
0.44(0.05)	0.45(0.04)	0.47(0.03)	0.39(0.04)	647289(30003)	lrLOB
0.56(0.03)	0.56(0.02)	0.55(0.02)	0.55(0.02)	647199(30003)	deepOF
0.49(0.05)	0.48(0.04)	0.49(0.06)	0.47(0.05)	647199(30003)	deepLOB

Table 3.4 Mean macro averaged BTCUSDT test set classification results across windows for $k = 200$.

Overall we observe very decent performance with clear predictability. We see that for $k = 4$ and $k = 10$ xgbOF is the clear winner. We then see that deepOF takes over for $k = 50$ and $k = 200$. To give a clearer picture of comparative performance across windows, we plot the macro averaged precision, recall and F1 for each trading pair, for each window and for each k in Figures 3.5 - 3.8.

We see that for $k = 4$ and $k = 10$, generally, xgbOF has the best precision and deepLOB has the best recall, with very similar F1 scores. We also observe that, in general the models perform similarly for different trading pairs, with model rankings generally preserved, although we do see a slightly decreased performance for trading pairs with lower trade volume. It seems that the general performance of our models is an increasing function of trading pair liquidity when measured using macro F1. This is an interesting result, and suggests that perhaps higher volume trading pairs are more predictable.

As we increase k to 50 and then 200, we see that the deepOF model starts pulling away from the other models for all metrics. This is perhaps due to the fact that deepOF has a much larger, $T = 100$, lookback, whereas (due to memory constraints) our xgbOF model has lookback $T = \min(k, 20) = 20$ for $k = 50, 100$. We see that xgbOF and deepOF give the most stable results across windows in terms of variation. We see lrLOB has high variation and performs poorly. Interestingly lrOF performs very well, often beating out the much larger deepLOB and xgbLOB models. It is clear that the OF representation is far superior, since all OF based models generally exhibit superior performance (when not constrained by lookback).

Of course, whilst macro-averaging gives a good overall idea of comparative performance, it averages performance across classes, so therefore we don't yet have a clear picture of how our models perform comparatively for each class. In Figures 3.9 - 3.12 we present confusion matrices, with counts summed across windows.

Again we see that for smaller k values, this is a very imbalanced classification problem, with the majority of the labels being class 0, i.e. stationary mid-price change. We see that as we increase k the distribution of labels spreads out more equally across classes. We also observe that, all of our confusion matrices have most weight along their diagonals, which is good news and means our models all perform better than randomly guessing. We see that the distributions are symmetric for the $+1$ and -1 classes so henceforth, in our analysis we will group these classes together and refer to them as the non-zero classes.

Recall that precision is defined as the number of correctly predicted labels for a class divided by the number of predicted labels for that class, and recall is the number of correctly predicted labels for a class divided by the total number of labels for that class. Using a poker analogy, precision tells us, out of all the times that we played a hand, what proportion of times did we win. Recall tells us, out of all the times that we had a winning hand, how many times did

we play and win. So for a trading scenario, what we really care about is precision of the $+1$ and -1 classes, since for most applications, it would be much more harmful to play and lose, rather than not play and miss a winning hand. We see that the precision of the non-zero classes is much higher than the precision of the zero class, whereas the recall of the non-zero classes is much lower than the recall of the zero class. This is due to the imbalanced nature of our labels, and we see that, as we increase k , the precision and recall get closer. The precision of the non-zero classes is around 90% for our best models for small k , which is a great result for the reasons mentioned above.

We see that, as we move across trading pairs, we start seeing less weight on the zero labels and more predictions for the non-zero classes. This is perhaps due to the fact that, for our test data, MATICUSDT and SOLUSDT have more balanced support, compared with BTCUSDT and ETHUSDT. i.e. the distribution of the true labels is less imbalanced for MATICUSDT and SOLUSDT. This is perhaps due to MATICUSDT and SOLUSDT having higher volatility over our testing windows, so fewer non-zero price changes.

Window-wise Macro Average Test Set Classification Results for $k=4$

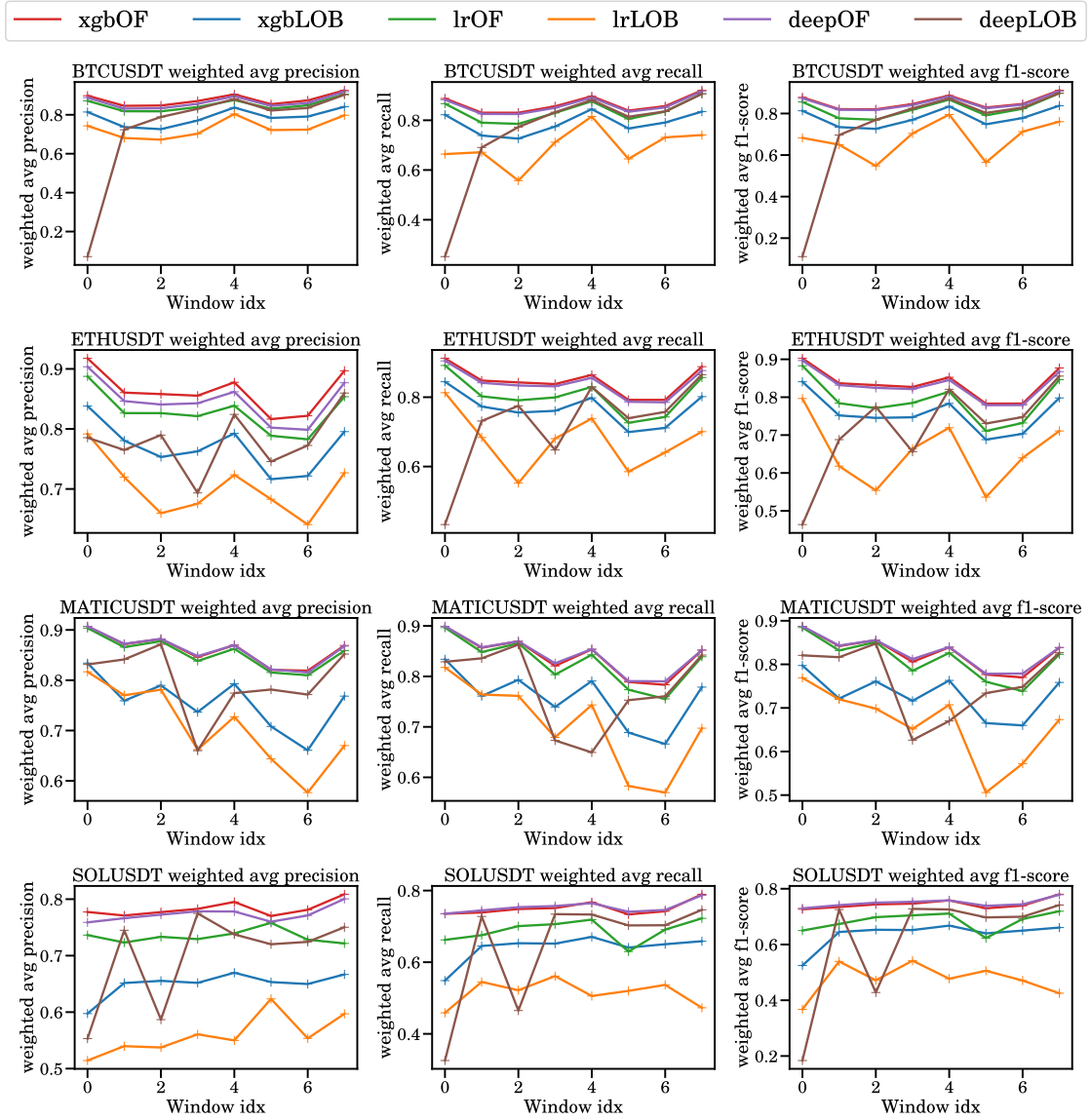


Figure 3.5 Comparing the macro averaged precision, recall and F1 score on the unseen test set for each window, for each trading pair, for $k = 4$.

Window-wise Macro Average Test Set Classification Results for $k=10$

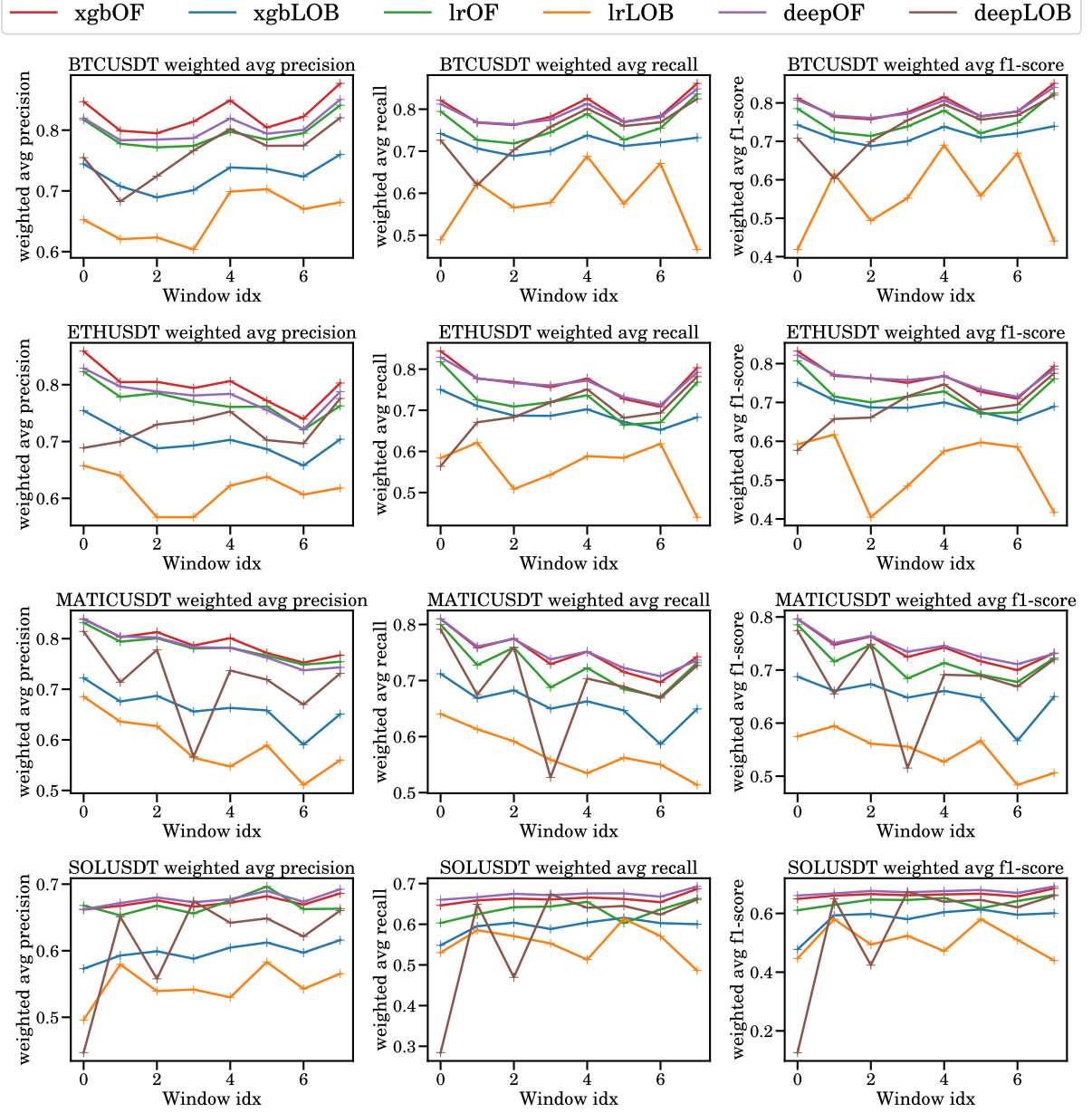


Figure 3.6 Comparing the macro averaged precision, recall and F1 score on the unseen test set for each window, for each trading pair, for $k = 10$.

Window-wise Macro Average Test Set Classification Results for $k=50$

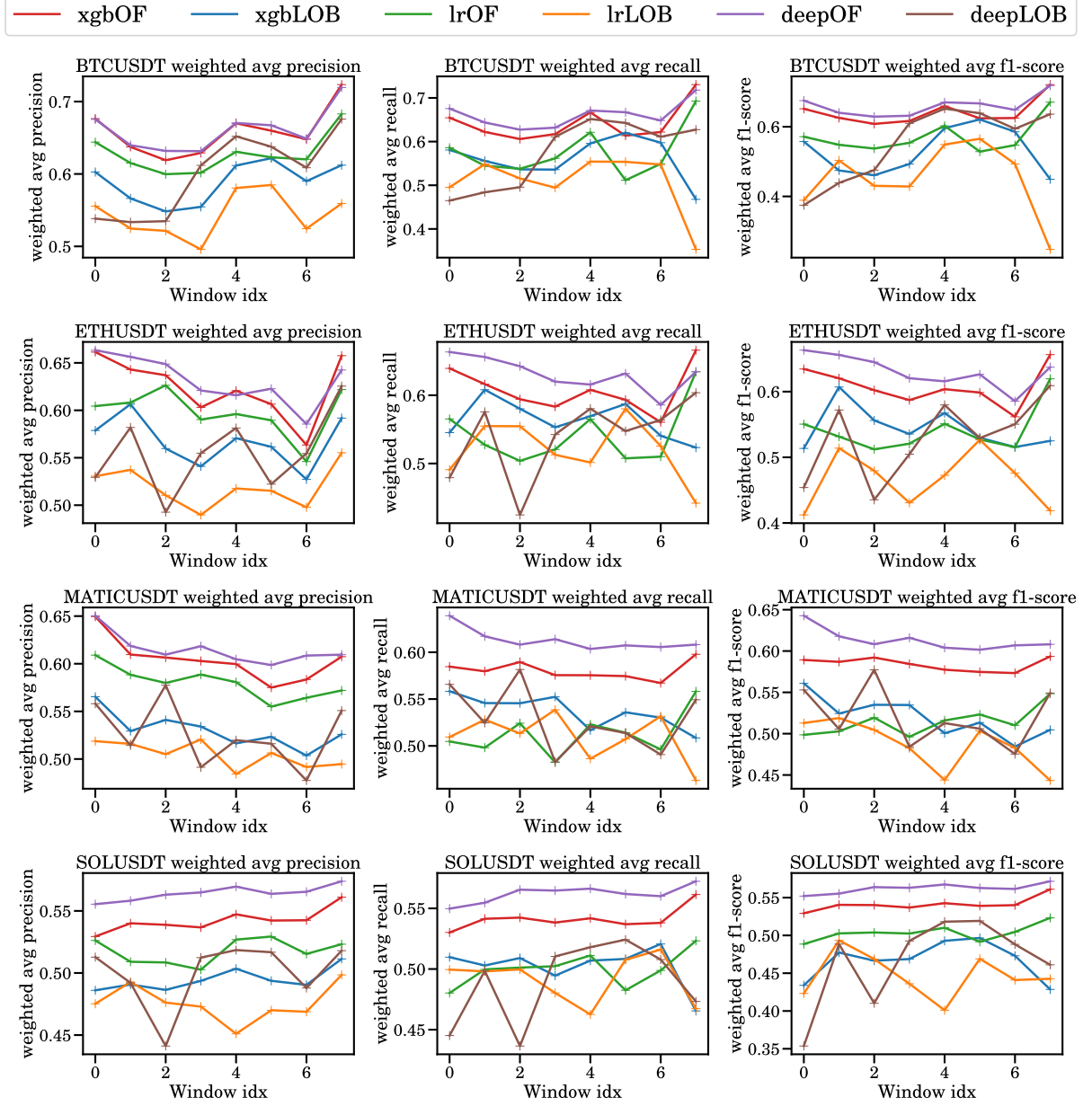


Figure 3.7 Comparing the macro averaged precision, recall and F1 score on the unseen test set for each window, for each trading pair, for $k = 50$.

Window-wise Macro Average Test Set Classification Results for $k=200$

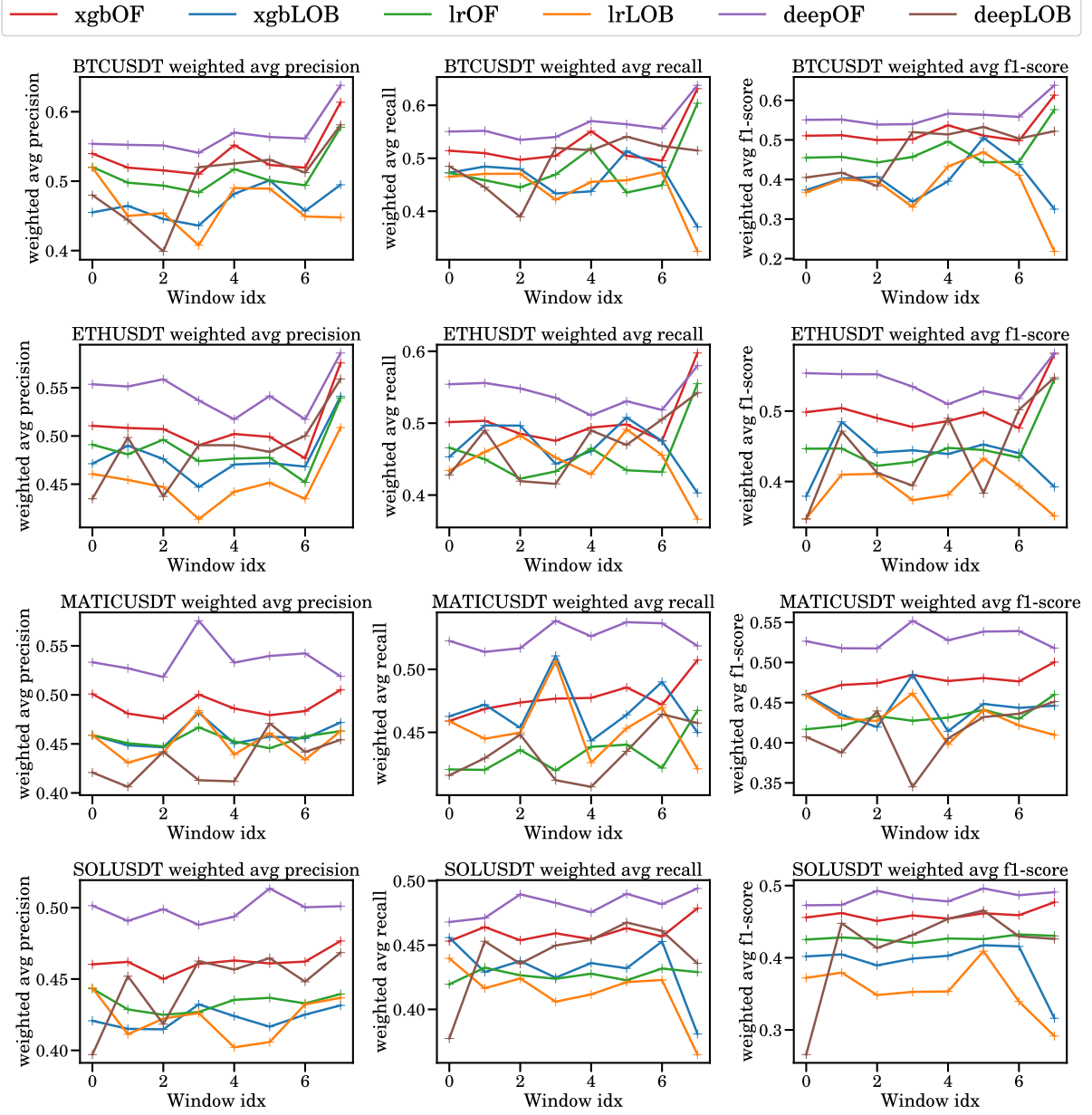


Figure 3.8 Comparing the macro averaged precision, recall and F1 score on the unseen test set for each window, for each trading pair, for $k = 200$.

BTCUSDT Confusion Matrices

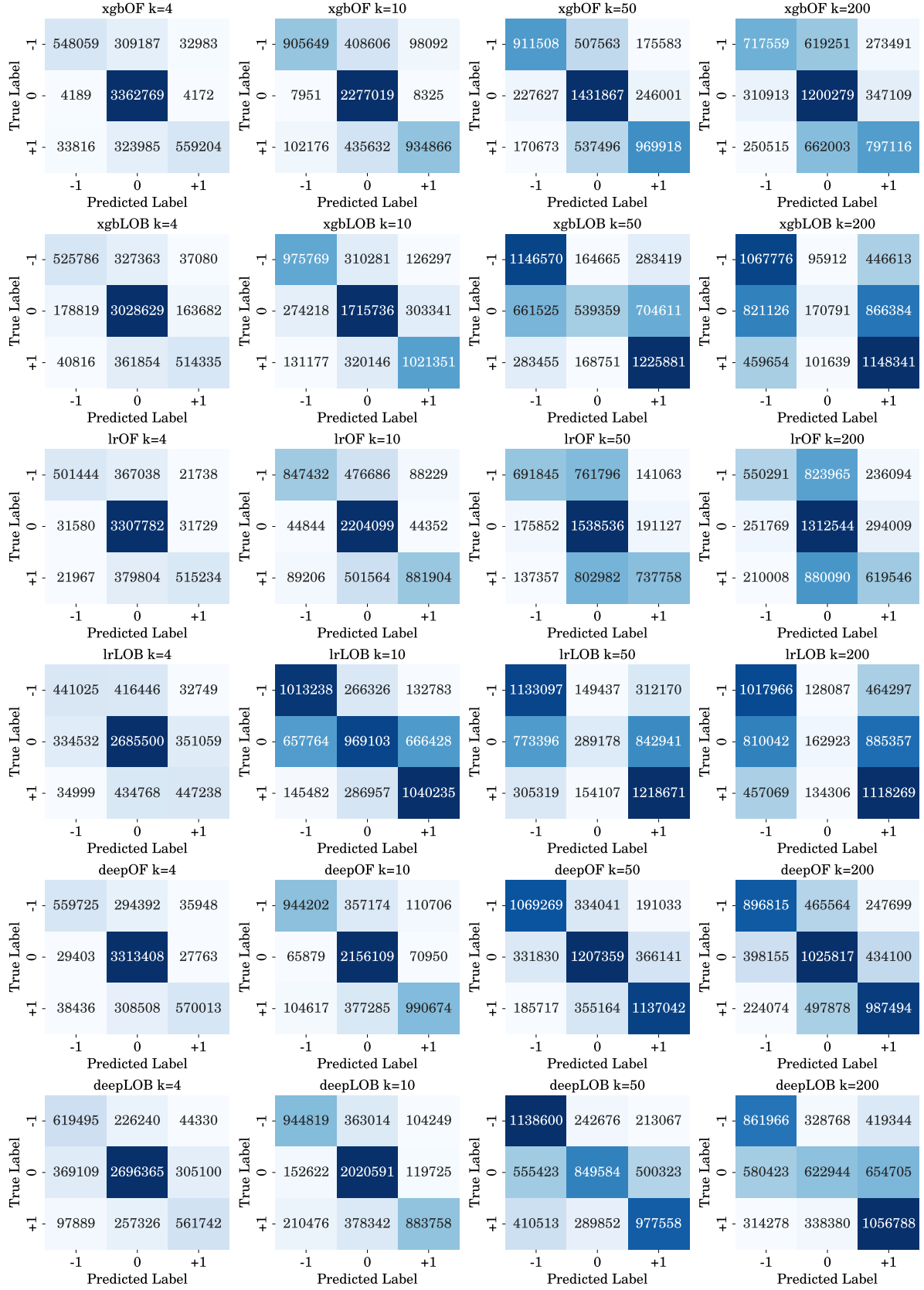


Figure 3.9 BTCUSDT confusion matrices. Note that counts are summed across windows.

ETHUSDT Confusion Matrices

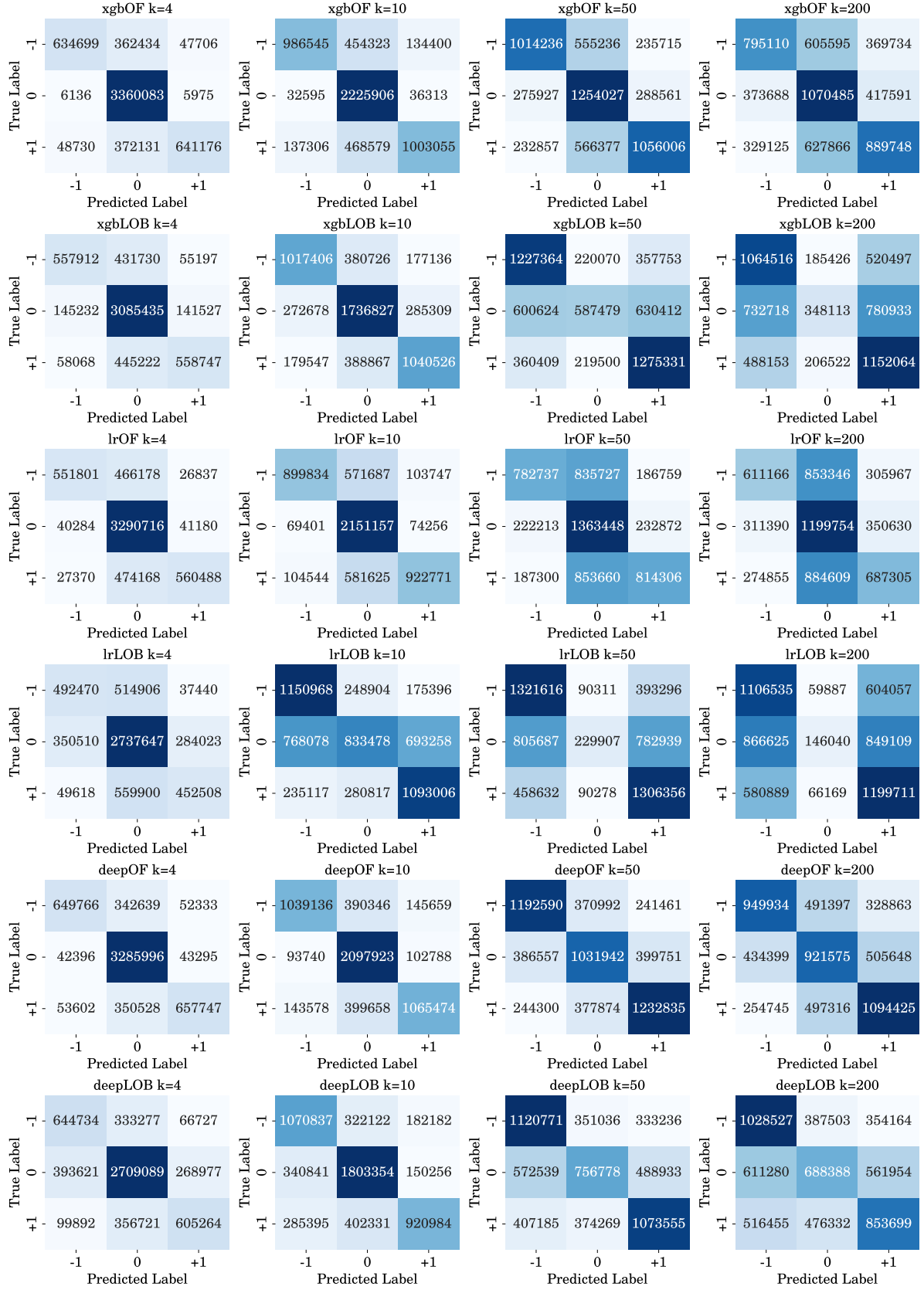


Figure 3.10 ETHUSDT confusion matrices. Note that counts are summed across windows.

MATICUSDT Confusion Matrices

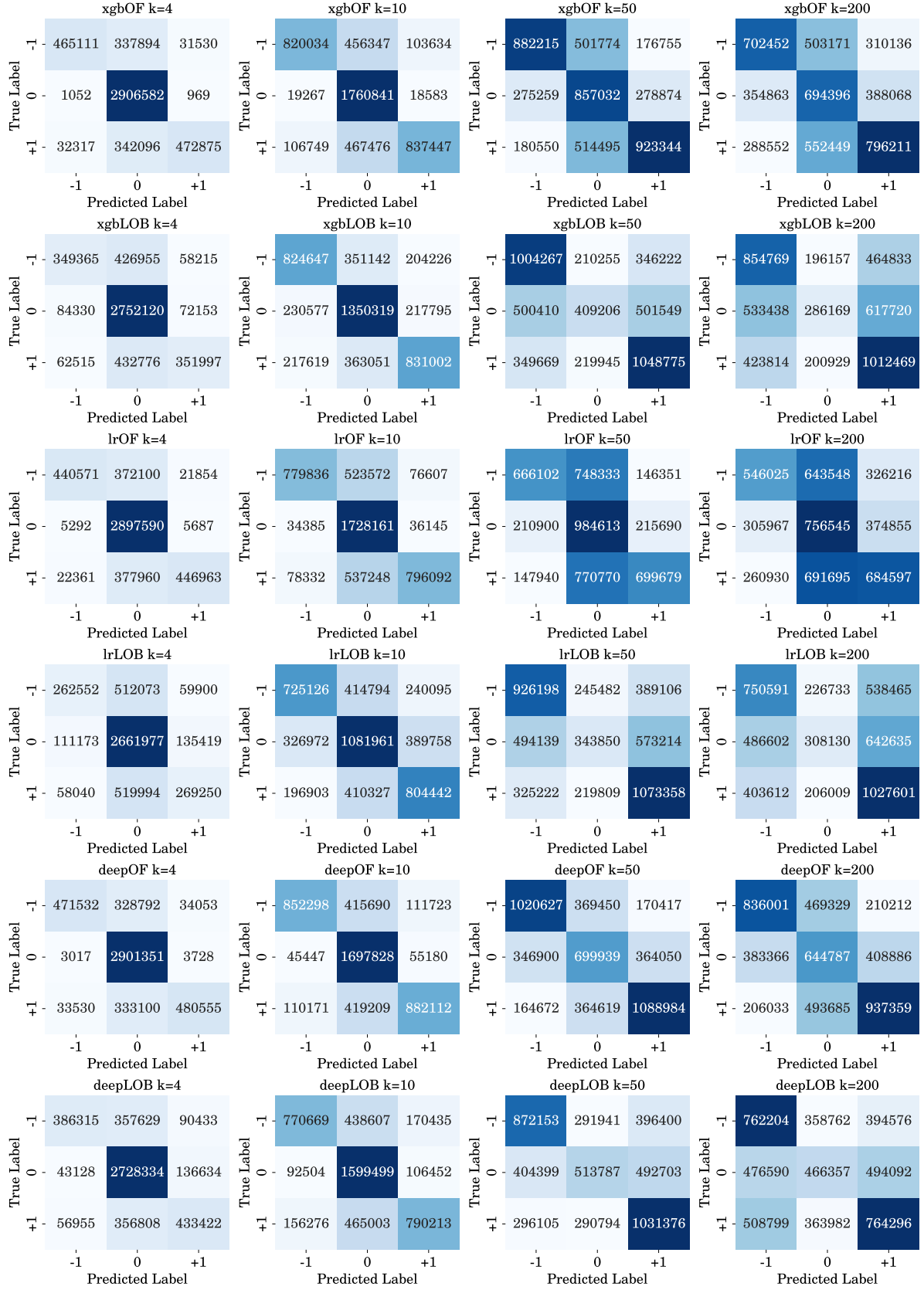


Figure 3.11 MATICUSDT confusion matrices. Note that counts are summed across windows.

SOLUSDT Confusion Matrices

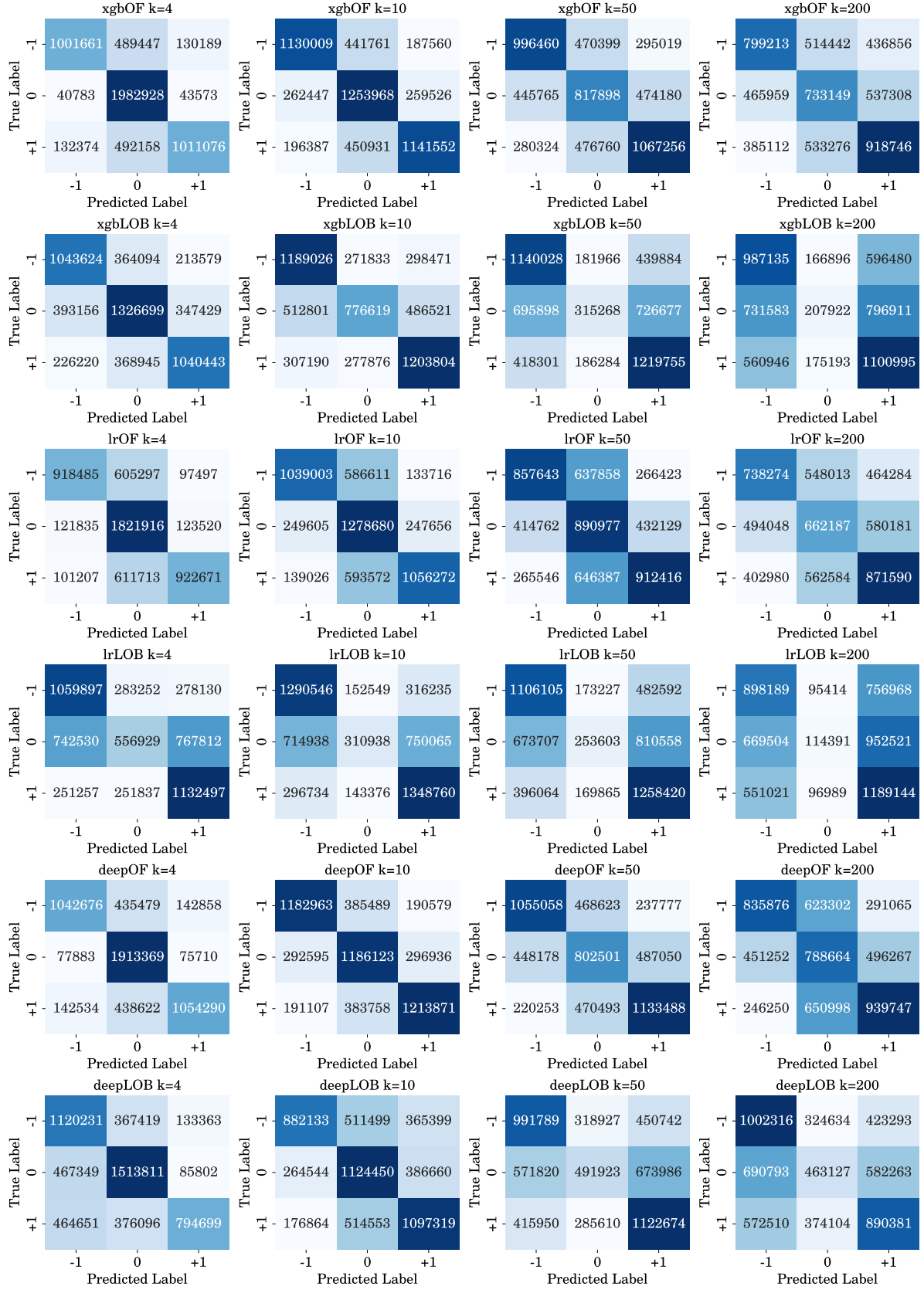


Figure 3.12 SOLUSDT confusion matrices. Note that counts are summed across windows.

3.5.3 Feature Importances

Another advantage of using a decision-tree-based model is that we get easily explainable feature importances. During training, we split the tree at each level, using the feature that gives us the best partition according to some metric. We can use this fact to rank features based on the number of times a feature was used to split the tree. We denote this count as the *weight* of the feature. More influential features will have a higher weight since they are the best discriminators of the data.

We plot the top 10 LOB features for xgbLOB BTCUSDT in Figure 3.13 for different k , prediction horizons. We see that for the LOB features, across all k , the highest weight features are the bid and ask quantities at the first level. This is very interesting, and tells us that for the LOB model the top levels of the orderbook are the most relevant. As we increase k , we start seeing larger lags being more important. Recall that due to memory constraints we set $T = \min(k, 20)$, so the maximum lag is 19. For $k > 20$ it seems we would certainly benefit from a larger lookback. Also a very important note; the majority of the top 10 features are quantity features. Recall that the LOB features are both quantity and price. Clearly this shows that the model is not using the price features effectively, and this demonstrates the need for a better representation, such as orderflow.

We also plot the top 10 OF features for xgbOF BTCUSDT in Figure 3.14. Again we see that the first level features are the most influential. This is good to see, since it confirms the commonly shared idea that the top of the orderbook has the most impact on price movement. Again we also see that, as we increase k , larger lag features start to appear.

Next we examine the distribution of weights over all non-zero weighted features in Figures 3.15 and 3.16. Instead of ordering the features by weight, we now order the features by their index. Recall the LOB features are:

$$[\text{ask_price}_{\ell_lag_p}, \text{ask_qty}_{\ell_lag_p}, \text{bid_price}_{\ell_lag_p}, \text{bid_qty}_{\ell_lag_p}]_{\ell=1,\dots,10,p=0,\dots,T}$$

And the OF features are:

$$[\text{ask_orderflow}_{\ell_lag_p}, \text{bid_orderflow}_{\ell_lag_p}]_{\ell=1,\dots,10,p=0,\dots,T}$$

Where ℓ indexes the orderbook level, and p indexes the lag. Note that in Figures 3.15 and 3.16 we distinguish different feature groups using different colors. Each color represent a unique (feature type, lag) pair, where feature type is either quantity or price for LOB and orderflow for OF. So for example, the first color represents all price features with lag 0. This allows us to compare feature weights for price vs. quantity features and also for different lags. Also since features are ordered by index, we can compare feature weights across levels, e.g. the first bar in a color group represents the first level for that feature type and lag.

Firstly we note that in 3.15 only every other bar has significant weight. These bars are quantity features and the price features have very small, often zero, weight for most levels and lags. This shows that the model is hardly using the price features, further confirming the inefficiency of the LOB representation. For both the OF representation and LOB representation we see that for each color the feature weights are decreasing as we increase the feature index. This shows that the features at the top levels have highest weight, and evidences the idea that deeper levels are less relevant for mid-price prediction. We also see that the first few levels all have similar weight across colors. This shows that the first few levels of the orderbook are roughly equally important across lags. For example, `ask_qty_1_lag_9` has similar importance to `ask_qty_1_lag_0`. So we see that using auto-regressive (lagged) features is important, but using deeper levels of the orderbook is less important.

Note that we do not distinguish between ask and bid features because we find them to be equally important.

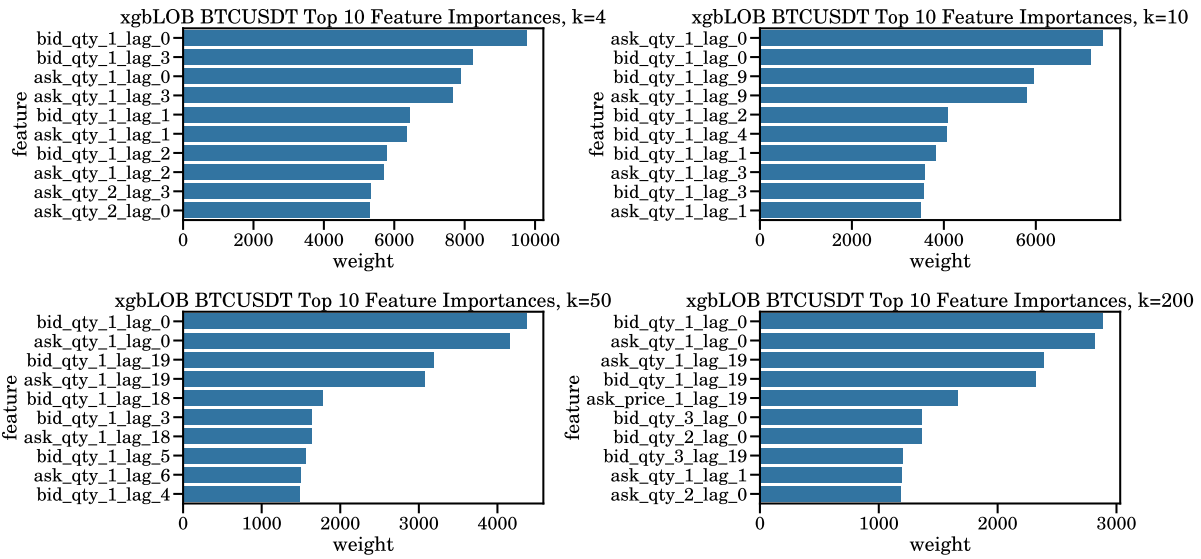


Figure 3.13 Top 10 XGBoost LOB Feature Importances for BTCUSDT, measured by weight = number of times a feature was split on.

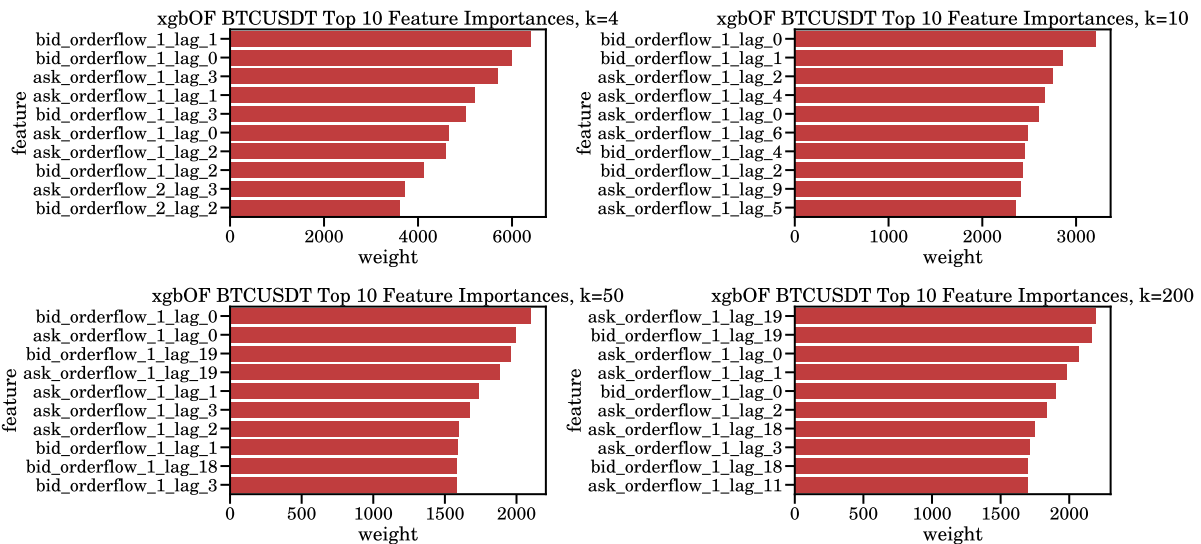


Figure 3.14 Top 10 XGBoost OF Feature Importances for BTCUSDT, measured by weight = number of times a feature was split on.

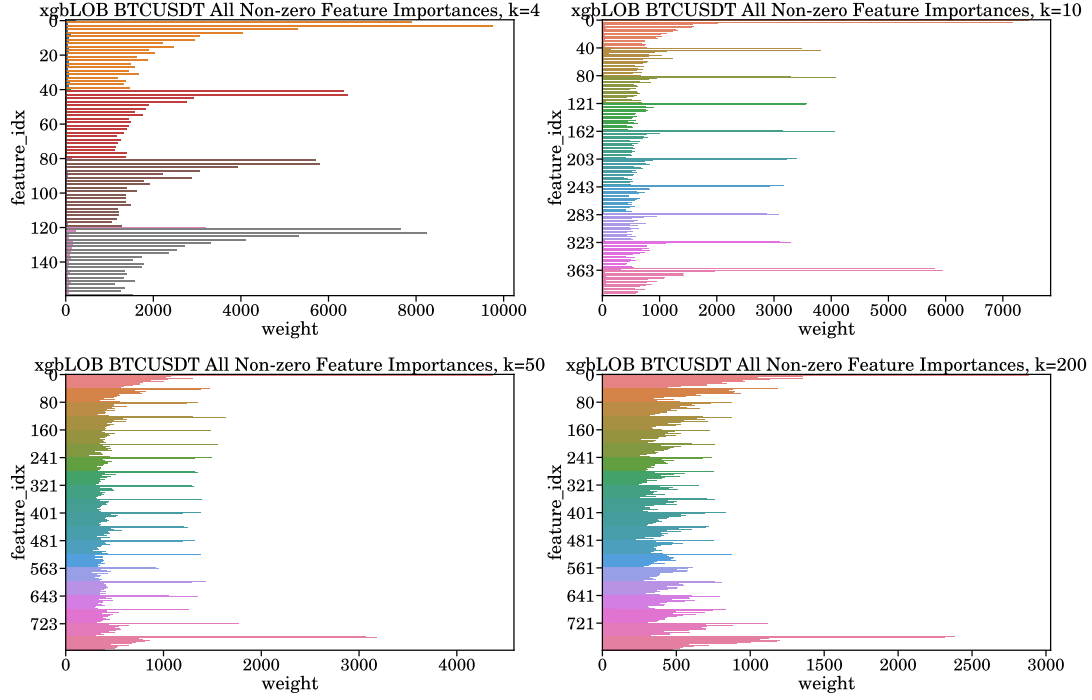


Figure 3.15 All non-zero LOB feature importances for BTCUSDT, measured by weight = number of times a feature was split on. Note that the colors represent unique (feature type, lag) pairs, where feature type is either quantity or price and lag $\in \{0, \dots, T\}$, e.g. the first color represents price features with lag 0.

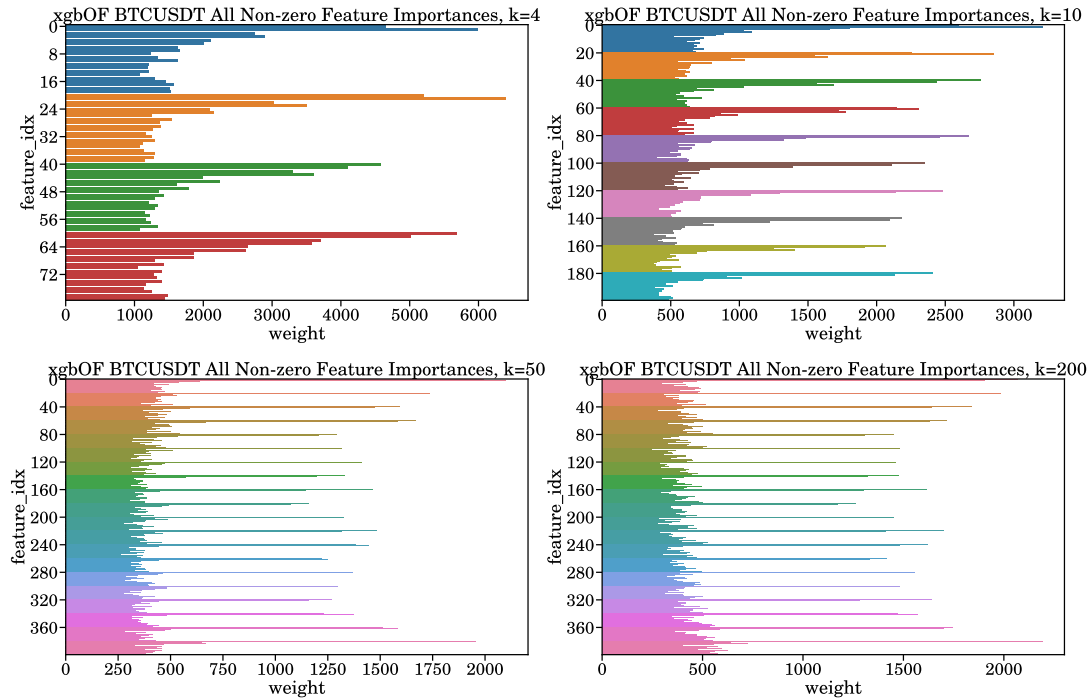


Figure 3.16 All non-zero OF feature importances for BTCUSDT, measured by weight = number of times a feature was split on. Note that the colors represent unique lags, where lag $\in \{0, \dots, T\}$. E.g. the first color represents all features with lag 0.

3.5.4 Modelling Recommendations

To conclude, we recommend the xgbOF model for shorter time horizons due its superior performance, ease of use, interpretability, scalability and lower training time. This is interesting since, to our knowledge, XGBoost is not mentioned in the literature for high frequency orderbook mid-price prediction. It would be interesting to see how the xgbOF model compares with the models presented in [19], [21] and [22] when trained on their data.

For longer time horizons deepOF was the clear winner. Whether this was due to superior ability to capture long term temporal dependencies or the fact that our xgbOF had a cap on lookback due to memory constraints remains to be seen and we recommend anyone looking to predict mid-prices at longer time horizons to try both models.

Chapter 4

Conclusion

4.1 Summary

In this paper we explored various machine learning models for predicting high frequency returns for four of the main cryptocurrency futures trading pairs, BTCUSDT, ETHUSDT, MATI-CUSDT and SOLUSDT. We constructed a novel data set from a live WebSocket stream from Binance, the worlds largest centralized cryptocurrency exchange. Following [20], we defined a stationary transformation of the raw orderbook data called orderflow, and motivated its definition by showing that under a stylized model of the orderbook, orderflow can be used to measure linear price impact of orderbook events. We then defined our modelling objective as a three-class classification problem, predicting the direction of the smoothed mid-price returns for several prediction horizons. For this task, we introduced several traditional machine learning and also deep learning models that use either the orderflow representation or the raw orderbook representation. Specifically, from traditional ML we introduced Logistic Regression and XGBoost models. For our deep learning models, we used the deepLOB model from [19] and the deepOF model from [21] which use the raw orderbook/orderflow representations respectively. We trained, validated and tested our models for each trading pair and multiple prediction horizons on 8 windows from 05-02-2024 to 25-02-2024. We presented the results on the test set and also evaluated the feature importances for each XGBoost model.

4.2 Conclusions

From our results section we showed that we can predict the direction of smoothed mid-price returns at multiple short term time horizons for our Binance WebSocket data with good performance. We also saw that the price features are not significantly used and we concluded that the orderflow representation is far superior to the raw orderbook data representation for this task. This agrees with the findings of [21]. We found that simpler traditional machine learning models have very competitive performance when compared with the much larger and more complex deep learning models. This is a significant result, since it challenges the idea that we need a large and complicated deep learning model to achieve state of the art performance for orderbook prediction. [19], [21], [22]. This is very good news for practical application, since simpler models are much more explainable, which is a very important quality for many quantitative applications.

4.3 Future Work

As previously mentioned, it would be interesting to see how our models compare with those found in [19], [21], [22] when applied to their data.

Also, in this paper we only explored 4 trading pairs, when in fact Binance has over two-hundred perpetual futures trading pairs available. It would be interesting to apply the same methodology presented in this paper to a larger group of trading pairs and explore the differences across pairs.

A major advantage of using the Binance WebSocket data is that it is freely available and live at any time. Our next steps would be to adapt the models presented here to be, *online*, i.e. continuously learning and adapting in real time. Then we could continuously test the models in real time for a longer period of time. This would show definitively whether this methodology is practical for real world trading applications.

Appendix A

Extended Classification Results

Here we present the results for each symbol, for each k , for each model, averaged across windows. We give standard deviations in parenthesis. For each metric we have an array of 3 values, where the first value represent the metric for class -1 , the second class 0 and the third class $+1$.

accuracy	precision	recall	f1-score	support	model
0.87(0.03)	[0.94 0.84 0.95]([0.03 0.04 0.03])	[0.61 1. 0.6]([0.01 0. 0.02])	[0.74 0.91 0.74]([0.01 0.03 0.01])	[111278 421391 114625]([32887 38390 34515])	xgbOF
0.79(0.04)	[0.71 0.81 0.72]([0.08 0.05 0.09])	[0.59 0.89 0.56]([0.06 0.06 0.05])	[0.64 0.85 0.62]([0.02 0.04 0.03])	[111278 421391 114625]([32887 38390 34515])	xgbLOB
0.84(0.04)	[0.9 0.82 0.9]([0.02 0.06 0.01])	[0.57 0.98 0.56]([0.02 0.01 0.01])	[0.69 0.89 0.69]([0.01 0.04 0.01])	[111277 421386 114625]([32887 38390 34515])	lrOF
0.69(0.07)	[0.61 0.78 0.6]([0.16 0.09 0.16])	[0.51 0.8 0.5]([0.18 0.19 0.18])	[0.5 0.76 0.5]([0.08 0.1 0.09])	[111277 421386 114625]([32887 38390 34515])	lrLOB
0.86(0.03)	[0.9 0.84 0.91]([0.03 0.04 0.02])	[0.62 0.98 0.62]([0.02 0.01 0.02])	[0.74 0.91 0.73]([0.01 0.02 0.01])	[111258 421321 114619]([32882 38387 34517])	deepOF
0.75(0.2)	[0.7 0.74 0.76]([0.2 0.28 0.21])	[0.69 0.8 0.62]([0.11 0.31 0.11])	[0.66 0.77 0.65]([0.09 0.3 0.11])	[111258 421321 114619]([32882 38387 34517])	deepLOB

Table A.1 Mean class-wise BTCUSDT test set classification results across windows for $k = 4$. (Standard deviations are given in parenthesis) Note that the class ordering is $[-1, 0, 1]$.

accuracy	precision	recall	f1-score	support	model
0.8(0.03)	[0.9 0.72 0.91]([0.03 0.06 0.03])	[0.64 0.99 0.63]([0.02 0. 0.02])	[0.75 0.84 0.74]([0.01 0.04 0.])	[176543 286661 184084]([41637 55324 43785])	xgbOF
0.72(0.02)	[0.7 0.73 0.7]([0.06 0.07 0.06])	[0.69 0.74 0.7]([0.04 0.07 0.03])	[0.7 0.73 0.7]([0.02 0.05 0.02])	[176543 286661 184084]([41637 55324 43785])	xgbLOB
0.76(0.04)	[0.86 0.69 0.87]([0.02 0.08 0.02])	[0.6 0.96 0.6]([0.01 0.01 0.01])	[0.71 0.8 0.71]([0.01 0.05 0.01])	[176543 286661 184084]([41637 55324 43785])	lrOF
0.58(0.07)	[0.59 0.7 0.59]([0.13 0.12 0.13])	[0.73 0.43 0.72]([0.14 0.26 0.14])	[0.62 0.46 0.62]([0.06 0.18 0.07])	[176543 286661 184084]([41637 55324 43785])	lrLOB
0.79(0.03)	[0.85 0.74 0.85]([0.01 0.06 0.02])	[0.67 0.94 0.67]([0.01 0.02 0.02])	[0.75 0.83 0.75]([0.01 0.04 0.01])	[176510 286617 184072]([41631 55319 43788])	deepOF
0.74(0.06)	[0.77 0.73 0.8]([0.1 0.06 0.02])	[0.66 0.87 0.61]([0.11 0.09 0.11])	[0.69 0.79 0.68]([0.05 0.06 0.08])	[176510 286617 184072]([41631 55319 43788])	deepLOB

Table A.2 Mean class-wise BTCUSDT test set classification results across windows for $k = 10$. (Standard deviations are given in parenthesis) Note that the class ordering is $[-1, 0, 1]$.

accuracy	precision	recall	f1-score	support	model
0.64(0.04)	[0.7 0.56 0.7]([0.02 0.1 0.03])	[0.57 0.73 0.57]([0.03 0.07 0.03])	[0.62 0.63 0.62]([0.02 0.09 0.03])	[199331 238186 209760]([46599 66246 48099])	xgbOF
0.56(0.04)	[0.55 0.6 0.55]([0.08 0.09 0.08])	[0.72 0.27 0.73]([0.05 0.17 0.03])	[0.62 0.34 0.62]([0.04 0.18 0.05])	[199331 238186 209760]([46599 66246 48099])	xgbLOB
0.57(0.05)	[0.68 0.49 0.69]([0.02 0.12 0.03])	[0.43 0.79 0.44]([0.02 0.05 0.03])	[0.53 0.6 0.53]([0.02 0.1 0.03])	[199338 238189 209762]([46601 66248 48098])	lrOF
0.51(0.06)	[0.51 0.53 0.52]([0.08 0.13 0.09])	[0.72 0.16 0.74]([0.08 0.15 0.07])	[0.59 0.2 0.6]([0.05 0.15 0.05])	[199338 238189 209762]([46601 66248 48098])	lrLOB
0.66(0.03)	[0.67 0.62 0.66]([0.02 0.09 0.03])	[0.66 0.61 0.67]([0.04 0.1 0.04])	[0.67 0.61 0.67]([0.03 0.09 0.03])	[199292 238166 209740]([46608 66246 48091])	deepOF
0.57(0.07)	[0.55 0.61 0.59]([0.08 0.1 0.08])	[0.71 0.42 0.6]([0.07 0.21 0.18])	[0.61 0.46 0.57]([0.04 0.19 0.11])	[199292 238166 209740]([46608 66246 48091])	deepLOB

Table A.3 Mean class-wise BTCUSDT test set classification results across windows for $k = 50$. (Standard deviations are given in parenthesis) Note that the class ordering is $[-1, 0, 1]$.

accuracy	precision	recall	f1-score	support	model
0.52(0.04)	[0.56 0.46 0.56]([0.02 0.1 0.02])	[0.44 0.62 0.45]([0.04 0.11 0.06])	[0.49 0.53 0.5]([0.03 0.1 0.04])	[201287 232287 213704]([42401 57709 43519])	xgbOF
0.46(0.04)	[0.45 0.44 0.46]([0.06 0.09 0.06])	[0.67 0.09 0.68]([0.04 0.09 0.03])	[0.53 0.13 0.55]([0.04 0.11 0.04])	[201287 232287 213704]([42401 57709 43519])	xgbLOB
0.48(0.05)	[0.54 0.42 0.53]([0.04 0.11 0.04])	[0.34 0.69 0.35]([0.03 0.07 0.04])	[0.41 0.52 0.43]([0.02 0.1 0.03])	[201293 232290 213705]([42398 57709 43520])	lrOF
0.44(0.05)	[0.45 0.44 0.45]([0.06 0.11 0.06])	[0.64 0.09 0.66]([0.08 0.13 0.07])	[0.52 0.11 0.53]([0.04 0.13 0.04])	[201293 232290 213705]([42398 57709 43520])	lrLOB
0.56(0.03)	[0.59 0.49 0.59]([0.03 0.1 0.04])	[0.55 0.53 0.57]([0.05 0.11 0.05])	[0.56 0.51 0.58]([0.03 0.11 0.04])	[201259 232259 213680]([42412 57703 43502])	deepOF
0.49(0.05)	[0.48 0.47 0.5]([0.05 0.13 0.06])	[0.54 0.32 0.62]([0.17 0.14 0.07])	[0.5 0.36 0.55]([0.09 0.14 0.04])	[201259 232259 213680]([42412 57703 43502])	deepLOB

Table A.4 Mean class-wise BTCUSDT test set classification results across windows for $k = 200$. (Standard deviations are given in parenthesis) Note that the class ordering is $[-1, 0, 1]$.

accuracy	precision	recall	f1-score	support	model
0.85(0.04)	[0.93 0.81 0.93]([0.03 0.05 0.02])	[0.6 1. 0.6]([0.02 0. 0.02])	[0.73 0.89 0.73]([0.01 0.04 0.01])	[130604 421524 132754]([40090 64487 41206])	xgbOF
0.77(0.04)	[0.72 0.77 0.73]([0.06 0.07 0.07])	[0.53 0.91 0.53]([0.03 0.02 0.03])	[0.61 0.84 0.61]([0.02 0.05 0.02])	[130604 421524 132754]([40090 64487 41206])	xgbLOB
0.8(0.05)	[0.88 0.78 0.89]([0.04 0.08 0.04])	[0.53 0.98 0.53]([0.03 0.01 0.03])	[0.66 0.86 0.66]([0.01 0.05 0.01])	[130602 421522 132753]([40089 64486 41206])	lrOF
0.67(0.08)	[0.61 0.73 0.64]([0.13 0.1 0.14])	[0.47 0.81 0.42]([0.17 0.17 0.16])	[0.49 0.75 0.47]([0.07 0.1 0.09])	[130602 421522 132753]([40089 64486 41206])	lrLOB
0.84(0.04)	[0.88 0.82 0.88]([0.02 0.06 0.02])	[0.62 0.97 0.61]([0.02 0.01 0.02])	[0.72 0.89 0.72]([0.01 0.04 0.01])	[130592 421460 132734]([40081 64471 41202])	deepOF
0.72(0.13)	[0.66 0.81 0.72]([0.02 0.08 0.19])	[0.63 0.82 0.58]([0.15 0.22 0.13])	[0.59 0.79 0.6]([0.12 0.13 0.11])	[130592 421460 132734]([40081 64471 41202])	deepLOB

Table A.5 Mean class-wise ETHUSDT test set classification results across windows for $k = 4$. (Standard deviations are given in parenthesis) Note that the class ordering is [-1, 0, 1].

accuracy	precision	recall	f1-score	support	model
0.77(0.04)	[0.86 0.69 0.86]([0.04 0.08 0.04])	[0.62 0.97 0.62]([0.02 0.04 0.02])	[0.72 0.81 0.72]([0.02 0.06 0.02])	[196908 286851 201117]([50710 82788 52165])	xgbOF
0.69(0.03)	[0.68 0.67 0.68]([0.06 0.09 0.07])	[0.64 0.75 0.64]([0.03 0.07 0.02])	[0.66 0.71 0.66]([0.03 0.07 0.04])	[196908 286851 201117]([50710 82788 52165])	xgbLOB
0.73(0.05)	[0.84 0.64 0.84]([0.05 0.11 0.06])	[0.57 0.94 0.57]([0.02 0.05 0.02])	[0.68 0.75 0.68]([0.02 0.08 0.02])	[196908 286851 201117]([50710 82788 52165])	lrOF
0.56(0.06)	[0.54 0.63 0.57]([0.11 0.13 0.12])	[0.74 0.36 0.69]([0.09 0.23 0.11])	[0.61 0.4 0.6]([0.06 0.19 0.06])	[196908 286851 201117]([50710 82788 52165])	lrLOB
0.77(0.03)	[0.81 0.71 0.81]([0.04 0.08 0.04])	[0.66 0.91 0.66]([0.02 0.06 0.03])	[0.73 0.79 0.72]([0.02 0.06 0.03])	[196892 286806 201088]([50704 82777 52162])	deepOF
0.69(0.06)	[0.67 0.7 0.76]([0.13 0.07 0.09])	[0.68 0.79 0.56]([0.14 0.11 0.14])	[0.65 0.74 0.62]([0.08 0.07 0.09])	[196892 286806 201088]([50704 82777 52162])	deepLOB

Table A.6 Mean class-wise ETHUSDT test set classification results across windows for $k = 10$. (Standard deviations are given in parenthesis) Note that the class ordering is [-1, 0, 1].

accuracy	precision	recall	f1-score	support	model
0.61(0.03)	[0.66 0.5 0.67]([0.04 0.1 0.04])	[0.55 0.66 0.56]([0.04 0.13 0.05])	[0.6 0.57 0.61]([0.03 0.11 0.04])	[225648 227314 231905]([45683 69573 47079])	xgbOF
0.56(0.03)	[0.55 0.54 0.56]([0.05 0.1 0.06])	[0.68 0.29 0.69]([0.04 0.15 0.04])	[0.61 0.36 0.62]([0.04 0.16 0.04])	[225648 227314 231905]([45683 69573 47079])	xgbLOB
0.54(0.04)	[0.66 0.44 0.66]([0.04 0.12 0.05])	[0.43 0.73 0.43]([0.03 0.09 0.04])	[0.52 0.54 0.52]([0.03 0.1 0.03])	[225652 227316 231908]([45685 69572 47077])	lrOF
0.52(0.04)	[0.5 0.47 0.52]([0.06 0.14 0.07])	[0.73 0.1 0.71]([0.03 0.09 0.03])	[0.59 0.16 0.6]([0.04 0.13 0.04])	[225652 227316 231908]([45685 69572 47077])	lrLOB
0.63(0.02)	[0.65 0.55 0.65]([0.04 0.1 0.05])	[0.65 0.54 0.66]([0.04 0.1 0.03])	[0.65 0.55 0.65]([0.04 0.1 0.04])	[225630 227281 231876]([45698 69573 47066])	deepOF
0.54(0.06)	[0.55 0.5 0.57]([0.06 0.15 0.05])	[0.62 0.38 0.58]([0.15 0.17 0.11])	[0.56 0.41 0.57]([0.06 0.15 0.06])	[225630 227281 231876]([45698 69573 47066])	deepLOB

Table A.7 Mean class-wise ETHUSDT test set classification results across windows for $k = 50$. (Standard deviations are given in parenthesis) Note that the class ordering is [-1, 0, 1].

accuracy	precision	recall	f1-score	support	model
0.5(0.04)	[0.52 0.44 0.52]([0.03 0.1 0.03])	[0.44 0.54 0.47]([0.06 0.13 0.07])	[0.48 0.48 0.49]([0.05 0.11 0.05])	[221304 232720 230842]([43833 66856 45862])	xgbOF
0.47(0.03)	[0.46 0.46 0.46]([0.06 0.1 0.06])	[0.6 0.17 0.62]([0.06 0.12 0.07])	[0.52 0.22 0.53]([0.04 0.13 0.05])	[221304 232720 230842]([43833 66856 45862])	xgbLOB
0.46(0.04)	[0.51 0.4 0.51]([0.05 0.11 0.05])	[0.34 0.63 0.37]([0.04 0.09 0.05])	[0.41 0.48 0.42]([0.03 0.1 0.04])	[221309 232721 230846]([43831 66855 45863])	lrOF
0.45(0.03)	[0.43 0.42 0.44]([0.06 0.11 0.05])	[0.63 0.06 0.64]([0.07 0.07 0.07])	[0.51 0.1 0.52]([0.04 0.1 0.05])	[221309 232721 230846]([43831 66855 45863])	lrLOB
0.54(0.02)	[0.57 0.46 0.56]([0.05 0.1 0.05])	[0.53 0.47 0.58]([0.05 0.1 0.08])	[0.55 0.46 0.57]([0.04 0.1 0.06])	[221274 232702 230810]([43849 66862 45856])	deepOF
0.47(0.04)	[0.48 0.43 0.5]([0.04 0.12 0.08])	[0.56 0.33 0.48]([0.16 0.22 0.2])	[0.51 0.33 0.45]([0.06 0.2 0.1])	[221274 232702 230810]([43849 66862 45856])	deepLOB

Table A.8 Mean class-wise ETHUSDT test set classification results across windows for $k = 200$. (Standard deviations are given in parenthesis) Note that the class ordering is [-1, 0, 1].

accuracy	precision	recall	f1-score	support	model
0.84(0.04)	[0.94 0.81 0.94]([0.02 0.05 0.02])	[0.55 1. 0.55]([0.01 0. 0.01])	[0.7 0.89 0.7]([0.01 0.03 0.01])	[104316 363575 105911]([35348 30026 35555])	xgbOF
0.76(0.05)	[0.74 0.76 0.76]([0.06 0.05 0.06])	[0.4 0.94 0.39]([0.08 0.06 0.08])	[0.5 0.84 0.51]([0.06 0.05 0.06])	[104316 363575 105911]([35348 30026 35555])	xgbLOB
0.83(0.05)	[0.94 0.8 0.94]([0.01 0.06 0.01])	[0.53 1. 0.53]([0.01 0. 0.02])	[0.68 0.88 0.68]([0.01 0.04 0.01])	[104315 363571 105910]([35346 30024 35555])	lrOF
0.7(0.08)	[0.68 0.72 0.68]([0.11 0.07 0.14])	[0.3 0.91 0.3]([0.1 0.12 0.12])	[0.4 0.8 0.38]([0.07 0.08 0.08])	[104315 363571 105910]([35346 30024 35555])	lrLOB
0.84(0.04)	[0.94 0.81 0.94]([0.02 0.05 0.02])	[0.56 1. 0.56]([0.02 0. 0.02])	[0.7 0.9 0.7]([0.01 0.03 0.01])	[104297 363512 105898]([35349 30020 35550])	deepOF
0.78(0.08)	[0.8 0.8 0.76]([0.15 0.07 0.19])	[0.46 0.94 0.51]([0.1 0.09 0.12])	[0.58 0.86 0.58]([0.11 0.05 0.11])	[104297 363512 105898]([35349 30020 35550])	deepLOB

Table A.9 Mean class-wise MATICUSDT test set classification results across windows for $k = 4$. (Standard deviations are given in parenthesis) Note that the class ordering is [-1, 0, 1].

accuracy	precision	recall	f1-score	support	model
0.75(0.03)	[0.87 0.65 0.88]([0.03 0.07 0.04])	[0.59 0.98 0.59]([0.02 0.03 0.02])	[0.7 0.78 0.7]([0.01 0.06 0.01])	[172501 224836 176459]([44068 43019 44986])	xgbOF
0.66(0.03)	[0.66 0.64 0.68]([0.06 0.05 0.05])	[0.58 0.73 0.57]([0.08 0.19 0.08])	[0.61 0.67 0.62]([0.03 0.12 0.03])	[172501 224836 176459]([44068 43019 44986])	xgbLOB
0.72(0.04)	[0.88 0.62 0.88]([0.04 0.09 0.03])	[0.56 0.96 0.56]([0.02 0.04 0.02])	[0.68 0.74 0.68]([0.01 0.07 0.01])	[172501 224836 176459]([44068 43019 44986])	lrOF
0.57(0.04)	[0.62 0.55 0.6]([0.09 0.09 0.11])	[0.5 0.57 0.54]([0.16 0.3 0.18])	[0.52 0.52 0.53]([0.08 0.2 0.09])	[172501 224836 176459]([44068 43019 44986])	lrLOB
0.75(0.03)	[0.86 0.66 0.85]([0.05 0.07 0.05])	[0.61 0.94 0.62]([0.03 0.06 0.03])	[0.71 0.78 0.71]([0.01 0.06 0.01])	[172463 224806 176436]([44070 43012 44979])	deepOF
0.69(0.07)	[0.77 0.63 0.77]([0.06 0.09 0.1])	[0.56 0.88 0.55]([0.09 0.12 0.09])	[0.64 0.73 0.63]([0.07 0.09 0.07])	[172463 224806 176436]([44070 43012 44979])	deepLOB

Table A.10 Mean class-wise MATICUSDT test set classification results across windows for $k = 10$. (Standard deviations are given in parenthesis) Note that the class ordering is [-1, 0, 1].

accuracy	precision	recall	f1-score	support	model
0.58(0.01)	[0.66 0.45 0.68]([0.03 0.06 0.03])	[0.56 0.6 0.56]([0.04 0.11 0.05])	[0.6 0.51 0.61]([0.02 0.08 0.02])	[195093 176395 202298]([30848 30669 32032])	xgbOF
0.54(0.02)	[0.54 0.47 0.56]([0.04 0.06 0.04])	[0.64 0.28 0.64]([0.03 0.12 0.05])	[0.59 0.34 0.59]([0.02 0.11 0.03])	[195093 176395 202298]([30848 30669 32032])	xgbLOB
0.51(0.02)	[0.65 0.39 0.66]([0.03 0.07 0.03])	[0.42 0.7 0.43]([0.04 0.08 0.04])	[0.51 0.5 0.52]([0.02 0.07 0.02])	[195098 176400 202298]([30848 30671 32032])	lrOF
0.51(0.02)	[0.53 0.43 0.53]([0.05 0.07 0.05])	[0.59 0.24 0.66]([0.07 0.13 0.07])	[0.56 0.28 0.58]([0.03 0.12 0.03])	[195098 176400 202298]([30848 30671 32032])	lrLOB
0.61(0.01)	[0.67 0.48 0.67]([0.04 0.06 0.02])	[0.65 0.49 0.67]([0.02 0.08 0.03])	[0.66 0.48 0.67]([0.02 0.07 0.02])	[195061 176361 202284]([30844 30654 32028])	deepOF
0.53(0.03)	[0.56 0.46 0.54]([0.03 0.08 0.04])	[0.57 0.35 0.64]([0.08 0.1 0.04])	[0.56 0.39 0.58]([0.04 0.09 0.03])	[195061 176361 202284]([30844 30654 32028])	deepLOB

Table A.11 Mean class-wise MATICUSDT test set classification results across windows for $k = 50$. (Standard deviations are given in parenthesis) Note that the class ordering is [-1, 0, 1].

accuracy	precision	recall	f1-score	support	model
0.48(0.01)	[0.52 0.39 0.53]([0.03 0.07 0.02])	[0.46 0.47 0.48]([0.05 0.11 0.06])	[0.49 0.42 0.5]([0.03 0.08 0.04])	[189469 179665 204651]([32165 33834 33109])	xgbOF
0.47(0.02)	[0.47 0.4 0.48]([0.04 0.07 0.03])	[0.56 0.19 0.61]([0.05 0.1 0.06])	[0.51 0.25 0.54]([0.03 0.09 0.03])	[189469 179665 204651]([32165 33834 33109])	xgbLOB
0.43(0.02)	[0.49 0.36 0.49]([0.04 0.07 0.02])	[0.36 0.52 0.41]([0.04 0.08 0.06])	[0.41 0.42 0.44]([0.02 0.07 0.04])	[189473 179670 204652]([32162 33833 33110])	lrOF
0.45(0.03)	[0.46 0.41 0.46]([0.05 0.07 0.04])	[0.5 0.21 0.62]([0.08 0.11 0.07])	[0.47 0.26 0.53]([0.04 0.1 0.04])	[189473 179670 204652]([32162 33833 33110])	lrLOB
0.53(0.01)	[0.58 0.39 0.6]([0.04 0.07 0.04])	[0.55 0.44 0.57]([0.05 0.06 0.03])	[0.56 0.41 0.58]([0.04 0.06 0.03])	[189442 179629 204634]([32186 33839 33094])	deepOF
0.43(0.02)	[0.45 0.37 0.46]([0.05 0.06 0.03])	[0.5 0.3 0.46]([0.16 0.19 0.16])	[0.45 0.31 0.45]([0.06 0.13 0.09])	[189442 179629 204634]([32186 33839 33094])	deepLOB

Table A.12 Mean class-wise MATICUSDT test set classification results across windows for $k = 200$. (Standard deviations are given in parenthesis) Note that the class ordering is [-1, 0, 1].

accuracy	precision	recall	f1-score	support	model
0.75(0.02)	[0.86 0.67 0.86]([0.02 0.04 0.01])	[0.62 0.96 0.62]([0.02 0.01 0.02])	[0.71 0.79 0.72]([0.01 0.03 0.01])	[202662 258410 204451]([25577 31919 27918])	xgbOF
0.64(0.03)	[0.64 0.65 0.65]([0.06 0.06 0.05])	[0.64 0.64 0.64]([0.06 0.15 0.04])	[0.64 0.63 0.64]([0.02 0.09 0.02])	[202662 258410 204451]([25577 31919 27918])	xgbLOB
0.69(0.03)	[0.81 0.6 0.81]([0.05 0.07 0.05])	[0.57 0.88 0.56]([0.06 0.05 0.06])	[0.66 0.71 0.66]([0.03 0.04 0.03])	[202659 258408 204448]([25577 31918 27918])	lrOF
0.52(0.03)	[0.54 0.57 0.53]([0.1 0.1 0.08])	[0.66 0.28 0.7]([0.15 0.22 0.1])	[0.57 0.31 0.59]([0.07 0.14 0.03])	[202659 258408 204448]([25577 31918 27918])	lrLOB
0.75(0.02)	[0.82 0.68 0.83]([0.01 0.03 0.02])	[0.64 0.93 0.64]([0.02 0.01 0.02])	[0.72 0.79 0.72]([0.01 0.03 0.01])	[202626 258370 204430]([25573 31914 27919])	deepOF
0.64(0.15)	[0.66 0.67 0.76]([0.19 0.05 0.07])	[0.69 0.73 0.48]([0.14 0.31 0.22])	[0.64 0.64 0.56]([0.08 0.26 0.22])	[202626 258370 204430]([25573 31914 27919])	deepLOB

Table A.13 Mean class-wise SOLUSDT test set classification results across windows for $k = 4$. (Standard deviations are given in parenthesis) Note that the class ordering is [-1, 0, 1].

accuracy	precision	recall	f1-score	support	model
0.66(0.01)	[0.71 0.58 0.72]([0.02 0.06 0.02])	[0.64 0.7 0.64]([0.02 0.03 0.02])	[0.67 0.63 0.67]([0.02 0.05 0.02])	[219916 221992 223608]([29850 45009 31685])	xgbOF
0.6(0.02)	[0.59 0.58 0.6]([0.03 0.06 0.03])	[0.67 0.42 0.67]([0.05 0.15 0.03])	[0.63 0.46 0.64]([0.02 0.15 0.02])	[219916 221992 223608]([29850 45009 31685])	xgbLOB
0.63(0.02)	[0.73 0.52 0.73]([0.04 0.08 0.04])	[0.59 0.72 0.59]([0.03 0.05 0.04])	[0.65 0.6 0.65]([0.02 0.05 0.02])	[219916 221992 223608]([29850 45009 31685])	lrOF
0.55(0.04)	[0.56 0.49 0.56]([0.06 0.09 0.06])	[0.73 0.17 0.75]([0.06 0.11 0.03])	[0.63 0.23 0.64]([0.03 0.13 0.04])	[219916 221992 223608]([29850 45009 31685])	lrLOB
0.67(0.01)	[0.71 0.6 0.71]([0.02 0.05 0.02])	[0.67 0.66 0.68]([0.02 0.04 0.02])	[0.69 0.63 0.69]([0.01 0.05 0.02])	[219878 221956 223592]([29848 45001 31686])	deepOF
0.58(0.13)	[0.7 0.57 0.55]([0.11 0.12 0.22])	[0.51 0.63 0.6]([0.24 0.18 0.24])	[0.53 0.57 0.57]([0.23 0.1 0.22])	[219878 221956 223592]([29848 45001 31686])	deepLOB

Table A.14 Mean class-wise SOLUSDT test set classification results across windows for $k = 10$. (Standard deviations are given in parenthesis) Note that the class ordering is [-1, 0, 1].

accuracy	precision	recall	f1-score	support	model
0.54(0.01)	[0.58 0.45 0.58]([0.02 0.06 0.02])	[0.56 0.46 0.58]([0.03 0.07 0.03])	[0.57 0.46 0.58]([0.02 0.06 0.02])	[220234 217230 228042]([24357 36028 26024])	xgbOF
0.5(0.01)	[0.51 0.45 0.51]([0.03 0.07 0.03])	[0.65 0.17 0.67]([0.04 0.09 0.02])	[0.57 0.24 0.58]([0.02 0.1 0.02])	[220234 217230 228042]([24357 36028 26024])	xgbLOB
0.5(0.01)	[0.56 0.41 0.57]([0.03 0.07 0.03])	[0.49 0.51 0.5]([0.03 0.06 0.03])	[0.52 0.45 0.53]([0.02 0.05 0.02])	[220240 217233 228043]([24357 36026 26024])	lrOF
0.49(0.02)	[0.51 0.41 0.49]([0.04 0.07 0.03])	[0.63 0.14 0.69]([0.06 0.1 0.04])	[0.56 0.18 0.58]([0.02 0.12 0.02])	[220240 217233 228043]([24357 36026 26024])	lrLOB
0.56(0.01)	[0.61 0.45 0.61]([0.02 0.07 0.03])	[0.6 0.46 0.62]([0.03 0.05 0.03])	[0.6 0.46 0.61]([0.02 0.06 0.02])	[220182 217216 228029]([24360 36026 26021])	deepOF
0.49(0.03)	[0.51 0.46 0.51]([0.04 0.09 0.05])	[0.56 0.27 0.62]([0.17 0.13 0.13])	[0.52 0.32 0.54]([0.07 0.13 0.06])	[220182 217216 228029]([24360 36026 26021])	deepLOB

Table A.15 Mean class-wise SOLUSDT test set classification results across windows for $k = 50$. (Standard deviations are given in parenthesis) Note that the class ordering is [-1, 0, 1].

accuracy	precision	recall	f1-score	support	model
0.46(0.01)	[0.48 0.4 0.48]([0.03 0.06 0.02])	[0.45 0.41 0.5]([0.04 0.07 0.05])	[0.47 0.4 0.49]([0.03 0.06 0.03])	[218813 217052 229641]([24225 37077 23982])	xgbOF
0.43(0.02)	[0.43 0.37 0.44]([0.03 0.06 0.03])	[0.57 0.12 0.6]([0.05 0.05 0.04])	[0.49 0.17 0.51]([0.02 0.06 0.02])	[218813 217052 229641]([24225 37077 23982])	xgbLOB
0.43(0.0)	[0.45 0.37 0.45]([0.04 0.06 0.03])	[0.42 0.38 0.47]([0.04 0.06 0.04])	[0.44 0.37 0.46]([0.02 0.04 0.02])	[218821 217052 229644]([24224 37077 23982])	lrOF
0.41(0.02)	[0.43 0.41 0.42]([0.04 0.06 0.04])	[0.52 0.06 0.65]([0.12 0.06 0.12])	[0.46 0.1 0.5]([0.04 0.07 0.03])	[218821 217052 229644]([24224 37077 23982])	lrLOB
0.48(0.01)	[0.55 0.38 0.54]([0.05 0.07 0.02])	[0.48 0.45 0.51]([0.08 0.04 0.05])	[0.51 0.41 0.52]([0.03 0.05 0.03])	[218780 217022 229624]([24236 37085 23972])	deepOF
0.44(0.03)	[0.45 0.39 0.47]([0.05 0.08 0.03])	[0.57 0.26 0.48]([0.14 0.09 0.2])	[0.49 0.31 0.44]([0.03 0.07 0.17])	[218780 217022 229624]([24236 37085 23972])	deepLOB

Table A.16 Mean class-wise SOLUSDT test set classification results across windows for $k = 200$. (Standard deviations are given in parenthesis) Note that the class ordering is [-1, 0, 1].

Appendix B

Extended PanelOLS Results

Here we display the OFI price impact PanelOLS results for all trading pairs.

BTCUSDT PanelOLS Results for $h = 1000\text{ms}$

Dep. Variable:	Δp_δ	R-squared:	0.3590
Estimator:	PanelOLS	R-squared (Between):	-0.3865
No. Observations:	12891080	R-squared (Within):	0.3590
Date:	Tue, Mar 26 2024	R-squared (Overall):	0.3585
Time:	16:15:04	Log-likelihood	-6.11e+07
Cov. Estimator:	Clustered		
		F-statistic:	7.218e+06
Entities:	956	P-value	0.0000
Avg Obs:	1.348e+04	Distribution:	F(1,12890123)
Min Obs:	953.00		
Max Obs:	1.676e+04	F-statistic (robust):	4743.2
		P-value	0.0000
Time periods:	16761	Distribution:	F(1,12890123)
Avg Obs:	769.11		
Min Obs:	1.0000		
Max Obs:	956.00		

	Parameter	Std. Err.	T-stat	P-value	Lower CI	Upper CI
OFI	1.1829	0.0172	68.871	0.0000	1.1492	1.2166

F-test for Poolability: 19.309,
Distribution: F(955,12890123),
Included effects: Entity.

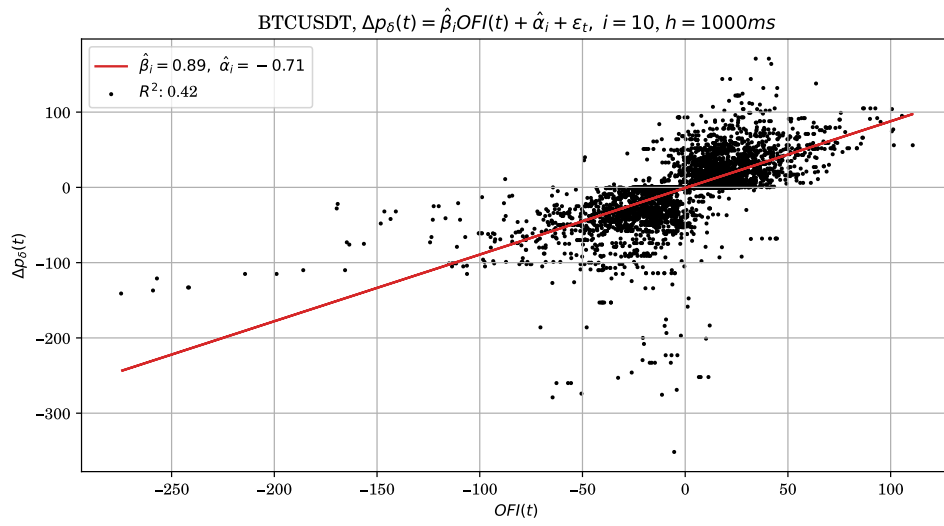


Figure B.1 OFI contemporaneous regression for an example half-hour window for BTCUSDT.

ETHUSDT PanelOLS Results for h = 1000ms

Dep. Variable:	Δp_δ	R-squared:	0.3407
Estimator:	PanelOLS	R-squared (Between):	-0.5821
No. Observations:	13612890	R-squared (Within):	0.3407
Date:	Tue, Mar 26 2024	R-squared (Overall):	0.3401
Time:	16:18:43	Log-likelihood	-5.922e+07
Cov. Estimator:	Clustered		
		F-statistic:	7.034e+06
Entities:	956	P-value	0.0000
Avg Obs:	1.424e+04	Distribution:	F(1,13611933)
Min Obs:	1.058e+04		
Max Obs:	1.654e+04	F-statistic (robust):	4554.0
		P-value	0.0000
Time periods:	16538	Distribution:	F(1,13611933)
Avg Obs:	823.13		
Min Obs:	1.0000		
Max Obs:	956.00		

	Parameter	Std. Err.	T-stat	P-value	Lower CI	Upper CI
OFI	0.0891	0.0013	67.483	0.0000	0.0866	0.0917

F-test for Poolability: 21.726,
Distribution: F(955,13611933),
Included effects: Entity.

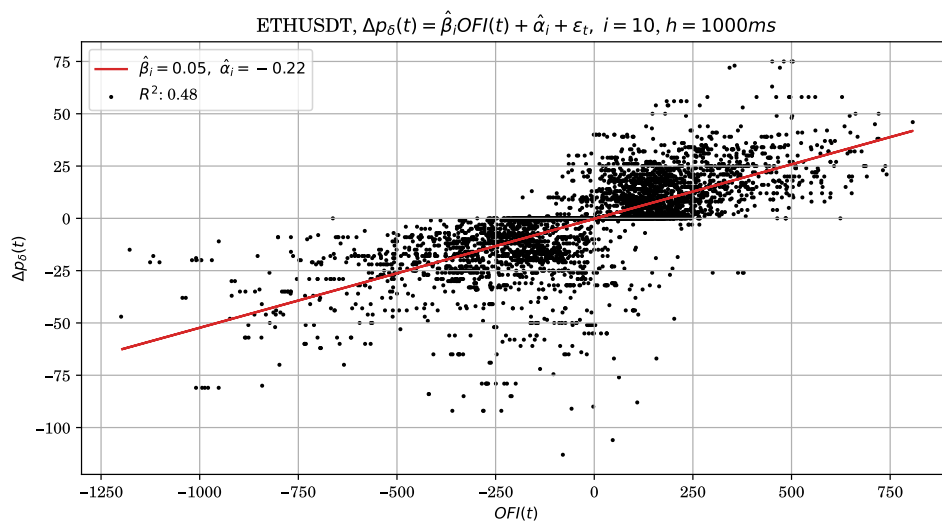


Figure B.2 OFI contemporaneous regression for an example half-hour window for ETHUSDT.

SOLUSDT PanelOLS Results for h = 1000ms

Dep. Variable:	Δp_δ	R-squared:	0.2828
Estimator:	PanelOLS	R-squared (Between):	-0.3992
No. Observations:	13334051	R-squared (Within):	0.2828
Date:	Tue, Mar 26 2024	R-squared (Overall):	0.2824
Time:	16:21:12	Log-likelihood	-5.176e+07
Cov. Estimator:	Clustered		
		F-statistic:	5.258e+06
Entities:	957	P-value	0.0000
Avg Obs:	1.393e+04	Distribution:	F(1,13333093)
Min Obs:	7478.0		
Max Obs:	1.647e+04	F-statistic (robust):	428.29
		P-value	0.0000
Time periods:	16473	Distribution:	F(1,13333093)
Avg Obs:	809.45		
Min Obs:	1.0000		
Max Obs:	957.00		

	Parameter	Std. Err.	T-stat	P-value	Lower CI	Upper CI
OFI	0.0128	0.0006	20.695	0.0000	0.0116	0.0140

F-test for Poolability: 15.871,
Distribution: F(956,13333093),
Included effects: Entity.

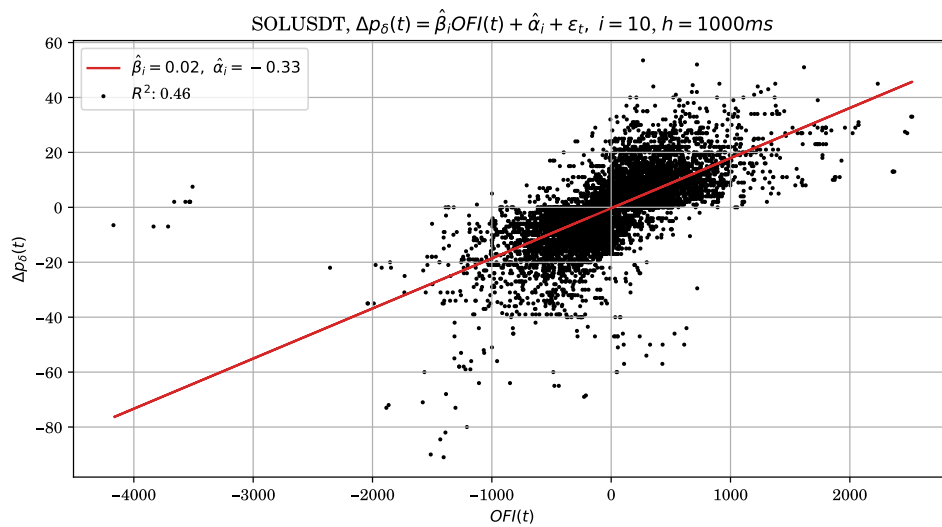


Figure B.3 OFI contemporaneous regression for an example half-hour window for SOLUSDT.

MATICUSDT PanelOLS Results for h = 1000ms

Dep. Variable:	Δp_δ	R-squared:	0.4133
Estimator:	PanelOLS	R-squared (Between):	-0.0188
No. Observations:	11294487	R-squared (Within):	0.4133
Date:	Tue, Mar 26 2024	R-squared (Overall):	0.4130
Time:	16:23:26	Log-likelihood	-1.58e+07
Cov. Estimator:	Clustered		
		F-statistic:	7.955e+06
Entities:	956	P-value	0.0000
Avg Obs:	1.181e+04	Distribution:	F(1,11293530)
Min Obs:	5754.0		
Max Obs:	1.639e+04	F-statistic (robust):	2882.6
		P-value	0.0000
Time periods:	16388	Distribution:	F(1,11293530)
Avg Obs:	689.19		
Min Obs:	1.0000		
Max Obs:	956.00		

	Parameter	Std. Err.	T-stat	P-value	Lower CI	Upper CI
OFI	3.108e-05	5.789e-07	53.690	0.0000	2.995e-05	3.222e-05

F-test for Poolability: 15.992,
Distribution: F(955,11293530),
Included effects: Entity.

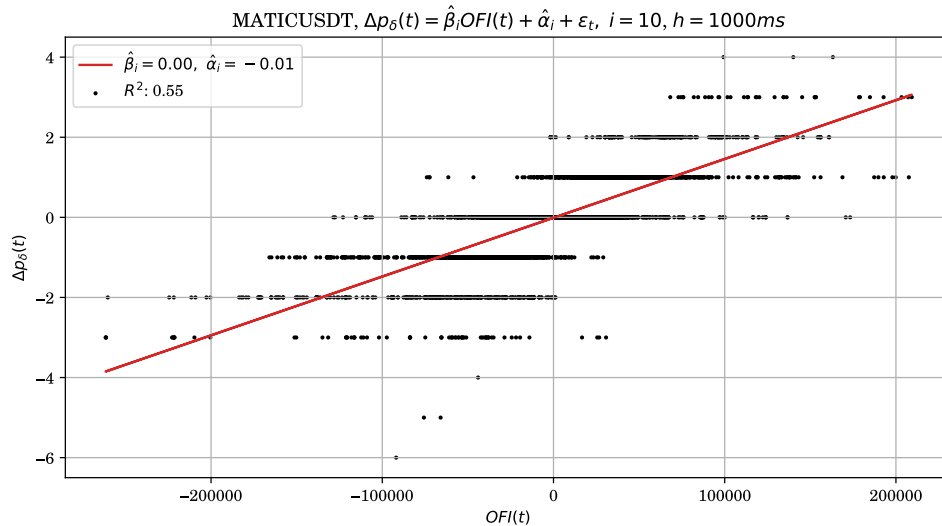


Figure B.4 OFI contemporaneous regression for an example half-hour window for MATICUSDT.

Appendix C

Websocket Data Summary Statistics

We present the summary statistics for the entire dataset for each trading pair here. For each trading pair we have approximately 13 million observations ranging from 2024-02-05 13:07:53.664 to 2024-02-25 11:18:50.866.

	ask_qty_1	ask_qty_2	ask_qty_3	ask_qty_4	ask_qty_5	ask_qty_6	ask_qty_7	ask_qty_8	ask_qty_9	ask_qty_10
count	12891081.00	12891081.00	12891081.00	12891081.00	12891081.00	12891081.00	12891081.00	12891081.00	12891081.00	12891081.00
mean	6.20	0.34	0.31	0.33	0.34	0.33	0.32	0.32	0.32	0.31
std	8.37	2.04	1.57	1.81	2.24	2.23	2.38	2.25	2.61	2.38
min	0.00	0.00	0.00	0.00	0.00	0.00	0.00	0.00	0.00	0.00
25%	1.93	0.00	0.01	0.01	0.01	0.01	0.01	0.01	0.01	0.01
50%	4.66	0.01	0.05	0.05	0.05	0.05	0.05	0.05	0.05	0.05
75%	8.41	0.18	0.21	0.24	0.24	0.24	0.24	0.24	0.24	0.24
max	859.16	559.55	802.35	796.21	499.30	989.40	558.80	584.51	680.40	584.51

	bid_qty_1	bid_qty_2	bid_qty_3	bid_qty_4	bid_qty_5	bid_qty_6	bid_qty_7	bid_qty_8	bid_qty_9	bid_qty_10
count	12891081.00	12891081.00	12891081.00	12891081.00	12891081.00	12891081.00	12891081.00	12891081.00	12891081.00	12891081.00
mean	6.23	0.38	0.31	0.34	0.34	0.32	0.32	0.31	0.31	0.30
std	10.27	2.63	1.77	2.66	2.53	2.01	2.25	2.21	2.37	2.19
min	0.00	0.00	0.00	0.00	0.00	0.00	0.00	0.00	0.00	0.00
25%	1.98	0.00	0.01	0.01	0.01	0.01	0.01	0.01	0.01	0.01
50%	4.63	0.02	0.05	0.05	0.05	0.05	0.05	0.05	0.05	0.05
75%	8.40	0.21	0.22	0.24	0.24	0.24	0.23	0.23	0.23	0.23
max	1008.05	861.61	777.20	781.40	781.40	781.40	997.10	997.10	997.41	767.82

	ask_price_1	ask_price_2	ask_price_3	ask_price_4	ask_price_5	ask_price_6	ask_price_7	ask_price_8	ask_price_9	ask_price_10
count	12891081.00	12891081.00	12891081.00	12891081.00	12891081.00	12891081.00	12891081.00	12891081.00	12891081.00	12891081.00
mean	49385.06	49385.19	49385.45	49385.68	49385.90	49386.10	49386.30	49386.48	49386.66	49386.83
std	3107.13	3107.13	3107.15	3107.16	3107.17	3107.18	3107.19	3107.19	3107.20	3107.21
min	42311.30	42311.40	42312.00	42312.10	42312.60	42313.10	42313.40	42313.60	42313.80	42313.90
25%	47454.30	47454.40	47454.60	47454.90	47455.20	47455.50	47455.70	47455.90	47456.00	47456.20
50%	51086.00	51086.20	51086.30	51086.50	51086.80	51087.00	51087.20	51087.40	51087.60	51087.80
75%	51790.00	51790.10	51790.40	51790.60	51790.80	51791.00	51791.20	51791.50	51791.80	51791.90
max	53087.70	53087.90	53088.70	53089.80	53090.00	53090.20	53090.50	53090.80	53090.90	53091.00

	bid_price_1	bid_price_2	bid_price_3	bid_price_4	bid_price_5	bid_price_6	bid_price_7	bid_price_8	bid_price_9	bid_price_10
count	12891081.00	12891081.00	12891081.00	12891081.00	12891081.00	12891081.00	12891081.00	12891081.00	12891081.00	12891081.00
mean	49384.96	49384.83	49384.57	49384.34	49384.12	49383.92	49383.72	49383.54	49383.36	49383.19
std	3107.13	3107.13	3107.12	3107.10	3107.09	3107.08	3107.08	3107.07	3107.06	3107.06
min	42311.20	42311.10	42311.00	42310.90	42310.80	42310.70	42310.60	42310.50	42310.40	42310.30
25%	47454.20	47454.10	47453.80	47453.60	47453.40	47453.20	47453.00	47452.90	47452.60	47452.50
50%	51085.90	51085.70	51085.40	51085.20	51085.00	51084.90	51084.70	51084.50	51084.40	51084.20
75%	51789.90	51789.80	51789.50	51789.30	51789.00	51788.80	51788.50	51788.40	51788.20	51788.00
max	53087.30	53086.80	53086.70	53085.90	53084.30	53081.90	53080.00	53079.00	53078.70	53078.10

Table C.1 Summary statistics for BTCUSDT websocket data.

	ask_qty_1	ask_qty_2	ask_qty_3	ask_qty_4	ask_qty_5	ask_qty_6	ask_qty_7	ask_qty_8	ask_qty_9	ask_qty_10
count	13612891.00	13612891.00	13612891.00	13612891.00	13612891.00	13612891.00	13612891.00	13612891.00	13612891.00	13612891.00
mean	55.23	3.62	3.09	3.56	3.63	4.02	4.26	4.50	4.79	4.97
std	99.00	32.41	26.30	26.81	25.79	30.65	28.90	25.88	28.91	26.91
min	0.00	0.00	0.00	0.00	0.00	0.00	0.00	0.00	0.00	0.00
25%	14.98	0.01	0.07	0.07	0.08	0.08	0.10	0.13	0.16	0.18
50%	35.91	0.15	0.43	0.50	0.57	0.69	0.95	1.08	1.23	1.43
75%	71.94	2.15	2.92	3.06	3.29	3.58	3.90	4.15	4.53	5.00
max	7612.08	7357.27	5443.50	5926.07	7315.07	5873.18	7974.45	5696.58	6124.07	6123.37
	bid_qty_1	bid_qty_2	bid_qty_3	bid_qty_4	bid_qty_5	bid_qty_6	bid_qty_7	bid_qty_8	bid_qty_9	bid_qty_10
count	13612891.00	13612891.00	13612891.00	13612891.00	13612891.00	13612891.00	13612891.00	13612891.00	13612891.00	13612891.00
mean	53.26	3.63	3.10	3.53	3.67	3.82	4.29	4.38	4.66	4.85
std	89.38	31.08	21.56	27.54	25.38	25.80	30.64	25.90	25.48	22.62
min	0.00	0.00	0.00	0.00	0.00	0.00	0.00	0.00	0.00	0.00
25%	14.85	0.01	0.08	0.08	0.08	0.08	0.11	0.14	0.17	0.20
50%	35.25	0.20	0.44	0.52	0.60	0.71	1.00	1.12	1.28	1.48
75%	71.20	2.40	2.97	3.05	3.28	3.55	3.86	4.10	4.48	4.98
max	10228.23	10221.75	10221.74	10221.74	9607.48	1.02	9829.58	10224.01	7143.02	9817.49
	ask_price_1	ask_price_2	ask_price_3	ask_price_4	ask_price_5	ask_price_6	ask_price_7	ask_price_8	ask_price_9	ask_price_10
count	13612891.00	13612891.00	13612891.00	13612891.00	13612891.00	13612891.00	13612891.00	13612891.00	13612891.00	13612891.00
mean	2704.80	2704.81	2704.83	2704.85	2704.87	2704.88	2704.90	2704.91	2704.93	2704.94
std	223.88	223.88	223.88	223.88	223.89	223.89	223.89	223.89	223.89	223.89
min	2282.36	2282.38	2282.40	2282.41	2282.42	2282.44	2282.46	2282.47	2282.48	2282.49
25%	2494.37	2494.38	2494.40	2494.41	2494.43	2494.44	2494.46	2494.47	2494.48	2494.50
50%	2776.17	2776.18	2776.20	2776.21	2776.23	2776.25	2776.26	2776.28	2776.29	2776.31
75%	2920.21	2920.23	2920.24	2920.26	2920.28	2920.30	2920.32	2920.33	2920.35	2920.36
max	3053.11	3053.12	3053.32	3053.51	3053.54	3053.59	3053.69	3053.70	3053.71	3053.72
	bid_price_1	bid_price_2	bid_price_3	bid_price_4	bid_price_5	bid_price_6	bid_price_7	bid_price_8	bid_price_9	bid_price_10
count	13612891.00	13612891.00	13612891.00	13612891.00	13612891.00	13612891.00	13612891.00	13612891.00	13612891.00	13612891.00
mean	2704.79	2704.78	2704.76	2704.74	2704.72	2704.71	2704.69	2704.67	2704.66	2704.65
std	223.88	223.88	223.88	223.88	223.87	223.87	223.87	223.87	223.87	223.87
min	2282.35	2282.32	2282.31	2282.28	2282.27	2282.23	2282.21	2282.20	2282.17	2282.16
25%	2494.36	2494.35	2494.33	2494.32	2494.30	2494.28	2494.27	2494.26	2494.24	2494.23
50%	2776.16	2776.15	2776.12	2776.10	2776.08	2776.06	2776.05	2776.03	2776.02	2776.00
75%	2920.20	2920.19	2920.17	2920.15	2920.13	2920.12	2920.10	2920.08	2920.07	2920.05
max	3053.10	3053.09	3053.07	3053.06	3053.03	3053.02	3052.99	3052.96	3052.95	3052.89

Table C.2 Summary statistics for ETHUSDT websocket data.

	ask_qty_1	ask_qty_2	ask_qty_3	ask_qty_4	ask_qty_5	ask_qty_6	ask_qty_7	ask_qty_8	ask_qty_9	ask_qty_10
count	11294488.00	11294488.00	11294488.00	11294488.00	11294488.00	11294488.00	11294488.00	11294488.00	11294488.00	11294488.00
mean	12716.18	23685.36	38829.90	49438.51	58123.57	62507.59	60930.95	55367.95	49777.05	45230.33
std	19985.48	21545.45	33115.61	33501.64	36397.22	36074.49	34204.86	31431.88	29423.23	27729.75
min	1.00	1.00	2.00	5.00	5.00	5.00	5.00	5.00	5.00	5.00
25%	5269.00	13057.00	18610.00	27384.00	33447.00	38708.00	39230.00	36148.00	31811.00	28155.00
50%	10097.00	19536.00	29812.00	42883.00	52081.00	57505.00	56367.00	51253.00	45577.00	41255.00
75%	16399.00	28774.00	50104.00	64126.00	75982.00	80202.00	76991.00	69533.00	62500.00	57491.00
max	2921095.00	2431682.00	2917345.00	2436953.00	2436953.00	2150536.00	2150151.00	2172650.00	2166177.00	2110610.00
	bid_qty_1	bid_qty_2	bid_qty_3	bid_qty_4	bid_qty_5	bid_qty_6	bid_qty_7	bid_qty_8	bid_qty_9	bid_qty_10
count	11294488.00	11294488.00	11294488.00	11294488.00	11294488.00	11294488.00	11294488.00	11294488.00	11294488.00	11294488.00
mean	12779.39	23928.98	38887.18	46815.71	54853.76	59332.21	58452.96	54253.30	49710.25	45841.90
std	20186.24	30727.91	43285.03	40321.36	44909.71	43983.18	41601.12	42093.02	39812.07	38648.16
min	1.00	1.00	1.00	1.00	1.00	6.00	5.00	6.00	6.00	6.00
25%	5178.00	13061.00	17648.00	24198.00	28938.00	33737.00	35554.00	34653.00	31671.00	28502.00
50%	10013.00	19524.00	28130.00	39084.00	46815.00	52633.00	52927.00	49867.00	45679.00	41671.00
75%	16379.00	28632.00	49179.00	60990.00	72526.00	77182.00	74448.00	67999.00	62337.00	57838.00
max	3795122.00	3817190.00	3817875.00	3827721.00	3849124.00	3850149.00	3860481.00	3881703.00	3890275.00	3885535.00
	ask_price_1	ask_price_2	ask_price_3	ask_price_4	ask_price_5	ask_price_6	ask_price_7	ask_price_8	ask_price_9	ask_price_10
count	11294488.00	11294488.00	11294488.00	11294488.00	11294488.00	11294488.00	11294488.00	11294488.00	11294488.00	11294488.00
mean	0.91	0.91	0.91	0.91	0.91	0.91	0.91	0.91	0.91	0.91
std	0.07	0.07	0.07	0.07	0.07	0.07	0.07	0.07	0.07	0.07
min	0.77	0.77	0.77	0.77	0.77	0.77	0.77	0.77	0.77	0.77
25%	0.85	0.85	0.85	0.85	0.85	0.85	0.85	0.85	0.85	0.85
50%	0.90	0.90	0.90	0.90	0.90	0.90	0.90	0.90	0.90	0.90
75%	0.98	0.98	0.98	0.98	0.98	0.98	0.98	0.98	0.98	0.98
max	1.07	1.07	1.07	1.07	1.07	1.07	1.07	1.07	1.07	1.07
	bid_price_1	bid_price_2	bid_price_3	bid_price_4	bid_price_5	bid_price_6	bid_price_7	bid_price_8	bid_price_9	bid_price_10
count	11294488.00	11294488.00	11294488.00	11294488.00	11294488.00	11294488.00	11294488.00	11294488.00	11294488.00	11294488.00
mean	0.91	0.91	0.91	0.91	0.91	0.91	0.91	0.91	0.90	0.90
std	0.07	0.07	0.07	0.07	0.07	0.07	0.07	0.07	0.07	0.07
min	0.77	0.77	0.77	0.77	0.77	0.77	0.77	0.77	0.77	0.77
25%	0.85	0.85	0.85	0.85	0.85	0.84	0.84	0.84	0.84	0.84
50%	0.90	0.90	0.90	0.90	0.90	0.90	0.90	0.90	0.90	0.90
75%	0.98	0.97	0.97	0.97	0.97	0.97	0.97	0.97	0.97	0.97
max	1.06	1.06	1.06	1.06	1.06	1.06	1.06	1.06	1.06	1.06

Table C.3 Summary statistics for MATICUSDT websocket data.

	ask_qty_1	ask_qty_2	ask_qty_3	ask_qty_4	ask_qty_5	ask_qty_6	ask_qty_7	ask_qty_8	ask_qty_9	ask_qty_10
count	13334052.00	13334052.00	13334052.00	13334052.00	13334052.00	13334052.00	13334052.00	13334052.00	13334052.00	13334052.00
mean	145.89	39.46	39.46	42.48	45.36	49.41	49.24	51.38	53.52	53.52
std	612.39	329.36	307.82	313.65	338.84	343.93	340.86	351.44	404.63	374.13
min	1.00	1.00	1.00	1.00	1.00	1.00	1.00	1.00	1.00	1.00
25%	30.00	3.00	5.00	6.00	7.00	8.00	8.00	9.00	10.00	10.00
50%	82.00	13.00	17.00	20.00	20.00	22.00	23.00	25.00	26.00	26.00
75%	165.00	43.00	44.00	47.00	48.00	53.00	53.00	56.00	57.00	57.00
max	100015.00	96598.00	92722.00	96614.00	96654.00	96655.00	96615.00	66776.00	96596.00	96654.00
	bid_qty_1	bid_qty_2	bid_qty_3	bid_qty_4	bid_qty_5	bid_qty_6	bid_qty_7	bid_qty_8	bid_qty_9	bid_qty_10
count	13334052.00	13334052.00	13334052.00	13334052.00	13334052.00	13334052.00	13334052.00	13334052.00	13334052.00	13334052.00
mean	149.28	41.87	42.54	43.52	46.18	50.08	50.02	52.05	53.16	54.65
std	863.95	560.08	587.61	506.86	534.82	561.51	571.15	567.41	563.31	632.98
min	1.00	1.00	1.00	1.00	1.00	1.00	1.00	1.00	1.00	1.00
25%	28.00	3.00	5.00	6.00	6.00	7.00	8.00	9.00	9.00	10.00
50%	80.00	13.00	17.00	19.00	20.00	21.00	22.00	24.00	25.00	26.00
75%	163.00	43.00	44.00	47.00	47.00	51.00	51.00	54.00	55.00	55.00
max	119226.00	119696.00	112113.00	100918.00	102320.00	100934.00	100916.00	100916.00	100916.00	100913.00
	ask_price_1	ask_price_2	ask_price_3	ask_price_4	ask_price_5	ask_price_6	ask_price_7	ask_price_8	ask_price_9	ask_price_10
count	13334052.00	13334052.00	13334052.00	13334052.00	13334052.00	13334052.00	13334052.00	13334052.00	13334052.00	13334052.00
mean	106.70	106.70	106.70	106.70	106.71	106.71	106.71	106.71	106.71	106.71
std	5.83	5.83	5.83	5.83	5.83	5.83	5.83	5.83	5.83	5.83
min	93.13	93.13	93.14	93.14	93.14	93.14	93.14	93.14	93.14	93.14
25%	102.61	102.61	102.61	102.61	102.61	102.62	102.62	102.62	102.62	102.62
50%	107.52	107.52	107.53	107.53	107.53	107.53	107.53	107.53	107.53	107.54
75%	111.36	111.37	111.37	111.37	111.37	111.37	111.37	111.37	111.38	111.38
max	118.83	118.83	118.83	118.83	118.84	118.84	118.84	118.84	118.84	118.84
	bid_price_1	bid_price_2	bid_price_3	bid_price_4	bid_price_5	bid_price_6	bid_price_7	bid_price_8	bid_price_9	bid_price_10
count	13334052.00	13334052.00	13334052.00	13334052.00	13334052.00	13334052.00	13334052.00	13334052.00	13334052.00	13334052.00
mean	106.70	106.70	106.70	106.69	106.69	106.69	106.69	106.69	106.69	106.69
std	5.83	5.83	5.83	5.83	5.83	5.83	5.83	5.83	5.83	5.83
min	93.13	93.13	93.13	93.13	93.13	93.12	93.12	93.12	93.12	93.12
25%	102.61	102.61	102.60	102.60	102.60	102.60	102.60	102.60	102.60	102.60
50%	107.52	107.52	107.52	107.52	107.52	107.52	107.51	107.51	107.51	107.51
75%	111.36	111.36	111.36	111.36	111.36	111.36	111.36	111.36	111.36	111.35
max	118.83	118.82	118.82	118.82	118.82	118.82	118.82	118.82	118.82	118.82

Table C.4 Summary statistics for SOLUSDT websocket data.

Appendix D

Alternative Data Source

D.1 Introduction

Initially we were not using the Websocket endpoint to gather our data. Instead we used the Binance historical tick-level orderbook API endpoint. This returns compressed L2 representations of the orderbook going back multiple years and for all available trading pairs. This proved an interesting challenge to parse, so we present our journey here. This is a cautionary tale, since in the end, we were unable to use this data, so this chapter also serves as a warning for anyone looking to use this data for a similar application.

TL;DR: This data source has a large amount of missing data.

The data is organized into compressed directories, one for each day. In each directory there is a snapshot file and an updates file. The snapshot file contains all levels of the orderbook at the start of the day. See Table D.1 ¹ for an example of a snapshot DataFrame.

Row	timestamp	first_update_id	last_update_id	side	price	qty
1	1689033589005	3046269468672	3046269468672	0	30395.5	5.174
2	1689033589005	3046269468672	3046269468672	0	30395.6	0.002
3	1689033589005	3046269468672	3046269468672	0	30395.7	0.001
4	1689033589005	3046269468672	3046269468672	0	30395.8	0.001
⋮	⋮	⋮	⋮	⋮	⋮	⋮
100343	1689033589005	3046269468672	3046269468672	1	30395.0	0.002
100344	1689033589005	3046269468672	3046269468672	1	30395.1	0.002
100345	1689033589005	3046269468672	3046269468672	1	30395.2	0.329
100346	1689033589005	3046269468672	3046269468672	1	30395.3	0.002

Table D.1 Example snapshot data for BTCUSDT.

The updates file contains all of the updates for the day. Each row of the updates file represents a change to a price level or a new price level. So the idea is to start with the snapshot, then iteratively apply the updates, row by row, to update the state of the orderbook. For example,

¹Originally the raw data was using "b" for bids and "a" for asks in the side column, but we encode bids with 1s and asks with 0s so that our data is entirely numerical.

if a row of the updates table has quantity 0.0, this means at that time, the corresponding price level cleared and we delete that row from our reconstructed orderbook. So in this way we can reconstruct the orderbook at any time by taking our snapshot and applying the updates that happened up to that time. See Table D.2 for an example of an updates DataFrame.

Row	timestamp	first_update_id	last_update_id	side	price	qty
1	1689033589005	3046269468673	3046269468673	1	30379.8	0.24
2	1689033589005	3046269468685	3046269468685	1	5000.0	0.648
3	1689033589005	3046269468690	3046269468690	0	30401.4	1.101
4	1689033589005	3046269468692	3046269468692	1	30379.9	0.0
⋮	⋮	⋮	⋮	⋮	⋮	⋮
146793483	1689119989003	3049606768393	3049606768393	1	5000.0	0.534
146793484	1689119989003	3049606768394	3049606768396	1	5000.0	0.528
146793485	1689119989004	3049606768405	3049606768405	0	30618.1	3.906
146793486	1689119989004	3049606768408	3049606768408	1	5000.0	0.53

Table D.2 Example updates data for BTCUSDT.

D.2 On Efficient Parsing

For our purposes, we want the top L best bids and asks at regular intervals, so we have to apply the updates to the snapshots for each day and parse this data. This is non-trivial and took some effort, so we take a small detour here to present our parsing algorithm and analyze its efficiency.

This task is harder than one might think on first consideration, due to the fact that we can't just keep track of the top L levels, since the updates need to be applied iteratively. For example, if the last price level is cleared and then the $L + 1^{\text{th}}$ level becomes the L^{th} level, but we were only applying updates to the top L levels, then this level will not have been correctly updated. For this reason, we must keep track of the state of the entire orderbook at all times.

Our algorithm initialises the reconstructed orderbook using the snapshot, then iteratively applies the updates to the reconstructed orderbook. At regular intervals (every Δt updates) we then record the top L best bids and asks from our reconstructed orderbook.

When applying an update, we have three cases that we have to handle:

1. A new price level is instantiated.
2. An existing price level is cleared/deleted.
3. An existing price level is updated (quantity updated).

For each of these cases, we determine the index in our reconstructed orderbook where the change needs to happen, then we apply the change. In order to efficiently do this, we split our orderbook into bids and asks and maintain a sorted ascending order. This means we can use binary search to find the index which runs in $O(\log_2(S))$ where S is the length of the orderbook. Also since most of the updates happen at the top of the orderbook, if we order the bids/asks so the smallest values are first (ascending order), then we have a very good average case runtime. Also for consistency we want the best bid/ask to be first. Since smaller asks are better, this just means we have to sort our asks in ascending order. For bids we have the issue that higher bids are better, so we could use branching if statements here but this is inefficient for a large number of iterations, so instead we use a trick. We sort the bids in descending order, so that the best bid

is first, and then we multiply the prices by -1, so that the smallest values are first. This leads to very fast runtimes in practice.

Once we have found this index, we either insert the update, delete the row or update an existing row.

Every Δt updates, we store the top L best bids and asks from our reconstructed orderbook in a DataFrame, which is then returned once all the updates have been applied. Since we know the number of updates and also Δt , we can pre-allocated this DataFrame with $\lceil \text{length}(\text{updates}) / \Delta t \rceil + 1$ rows², so that adding a record is only $O(1)$.

D.3 The Parsing Algorithm

See Algorithm 1.

D.4 Complexity Analysis

If we denote U to be the number of updates and S to be the size of the initial snapshot/number of levels in our reconstructed orderbook (on average this should be roughly constant). Then we see that Algorithm 1 has $O(US)$ worst case runtime complexity, since for each of the U updates, we searchsorted through our reconstructed orderbook, which runs in $O(\log_2(S))$ worst case, and then either delete, insert or update a price level. Inserting and deleting are both $O(S)$ worst case, but updating is only $O(1)$, so worst case we have $O(\log_2(S) + S) = O(S)$ time complexity per iteration. So in total we have $O(US)$ worst case time complexity. Then we also have $O(U + S)$ memory complexity since we store the updates and reconstructed orderbook in memory at all times. In practice we can use a RecordCursor object to efficiently read the updates line by line, instead of having to load them into memory all at once. This reduces the memory complexity down to $O(S)$.

Note that $U \gg S$ and so for efficiency we mostly care about the complexities in terms of U . For our data we observe $U \approx 1.5 \times 10^3 S$.

So we see that we achieve linear worst case time complexity in U and, due to the sequential nature of the updates, this is clearly the best possible time complexity for this problem. We verify the linear time complexity experimentally in Figure D.1

D.5 Data Issues

We can apply our algorithm to each day of data and then combine the results. In order to check our data, we parse the data for several months in 2023 of BTCUSDT data and then compare to a reference. For our reference, we have access to hourly BTCUSDT mid-prices from an undisclosed source, going back 1 year. We resample our parsed data to an hourly resolution and then calculate hourly mid-prices. We plot our parsed data against the reference data in Figure D.2.

Unfortunately we find that there is a lot of missing data and we verify that this is from the underlying raw data and not an issue with our parsing. Due to this, we are unable to use this historical data for our purposes.

²+1 is for the initial snapshot, $t=0$ case.

Algorithm 1 reconstruct_orderbook

```
1: function RECONSTRUCT_ORDERBOOK(Int  $L$ , Int  $\Delta t$ , DataFrame snap, DataFrame updates)
2:   asks  $\leftarrow$  snap[side == 0, :]
3:   bids  $\leftarrow$  snap[side == 1, :]
4:   sort!(bids, by=price, ascending=false)  $\triangleright$  Best bid/ask in first row
5:   bids[:, price] *= -1.0  $\triangleright$  Trick so we have ascending order
6:    $N \leftarrow \lceil \text{length}(\text{updates}) / \Delta t \rceil + 1$   $\triangleright$  + 1 for initial snapshot row
7:   top_bids  $\leftarrow$  bids[1:L, :]  $\triangleright$  Initial case
8:   top_asks  $\leftarrow$  asks[1:L, :]
9:   levels  $\leftarrow$  zeros( $N$ ,  $1 + 4L$ )  $\triangleright$  Pre-allocate our parsed levels
10:  levels[1, :]  $\leftarrow$  concat([  $\triangleright$  Initial edge case
11:    snap[1, timestamp],
12:    top_bids[:, price] * -1.0,
13:    top_asks[:, price],
14:    top_bids[:, qty],
15:    top_asks[:, qty]
16:  ])
17:  levels_idx  $\leftarrow$  2
18:  for (t, update) in enumerate(updates) do  $\triangleright$  Iterate over each row of updates
19:    if update.side == 1 then
20:      orderbook  $\leftarrow$  bids  $\triangleright$  orderbook is a reference not a copy
21:      update.price *= -1  $\triangleright$  Trick so we have descending order
22:    else
23:      orderbook  $\leftarrow$  asks
24:    end if
25:    insert_idx  $\leftarrow$  searchsortedfirst(orderbook[:, price], update.price)
26:    if insert_idx > nrow(orderbook) or orderbook[insert_idx, price]  $\neq$  update.price then
27:      insert!(orderbook, insert_idx, update)  $\triangleright$  Case 1: New price
28:    else if update.qty == 0.0 then  $\triangleright$  Case 2: Deleting a price
29:      deleteat!(orderbook, insert_idx)
30:    else  $\triangleright$  Case 3: Updating the quantity for a price
31:      orderbook[insert_idx, :]  $\leftarrow$  update
32:    end if
33:
34:    if t %  $\Delta t$  == 0 then  $\triangleright$  Record the state of the top  $L$  levels every  $\Delta t$  updates.
35:      top_bids  $\leftarrow$  bids[1:L, :]
36:      top_asks  $\leftarrow$  asks[1:L, :]
37:      levels[levels_idx, :]  $\leftarrow$  concat([
38:        update.timestamp,
39:        top_bids[:, price] * -1.0,
40:        top_asks[:, price],
41:        top_bids[:, qty],
42:        top_asks[:, qty]
43:      ])
44:      levels_idx += 1
45:    end if
46:  end for
47:  return levels
48: end function
```

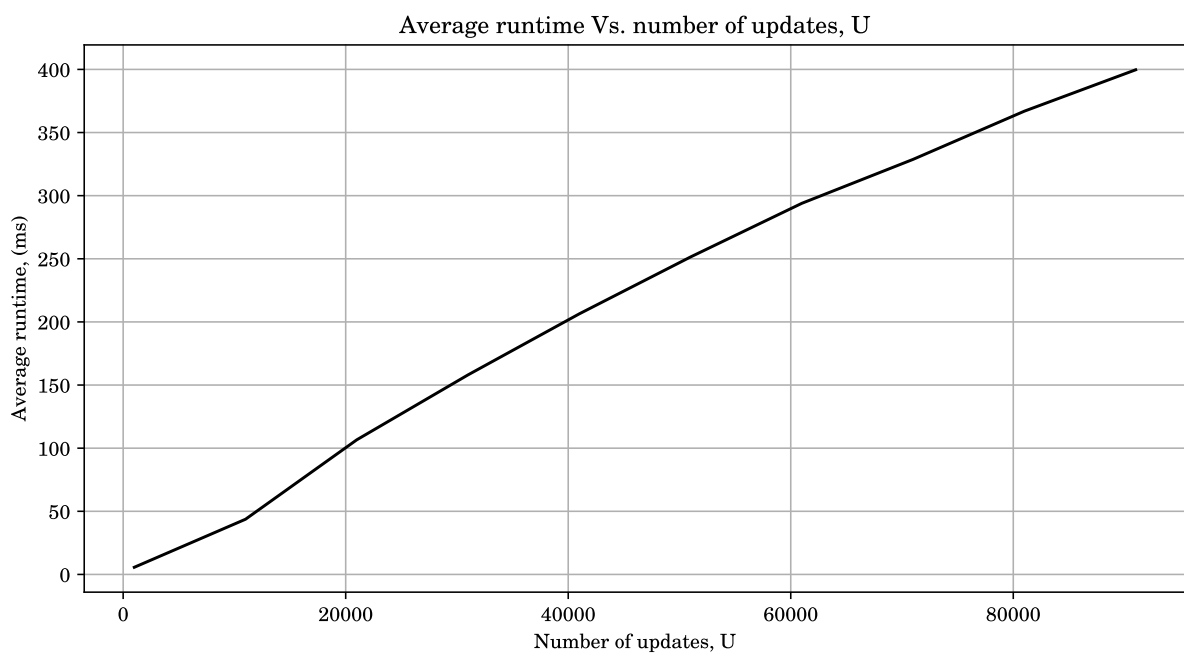


Figure D.1 `reconstruct_orderbook` runtime as a function of the number of updates, U . Note that the runtimes are recorded 100 times and then averaged.

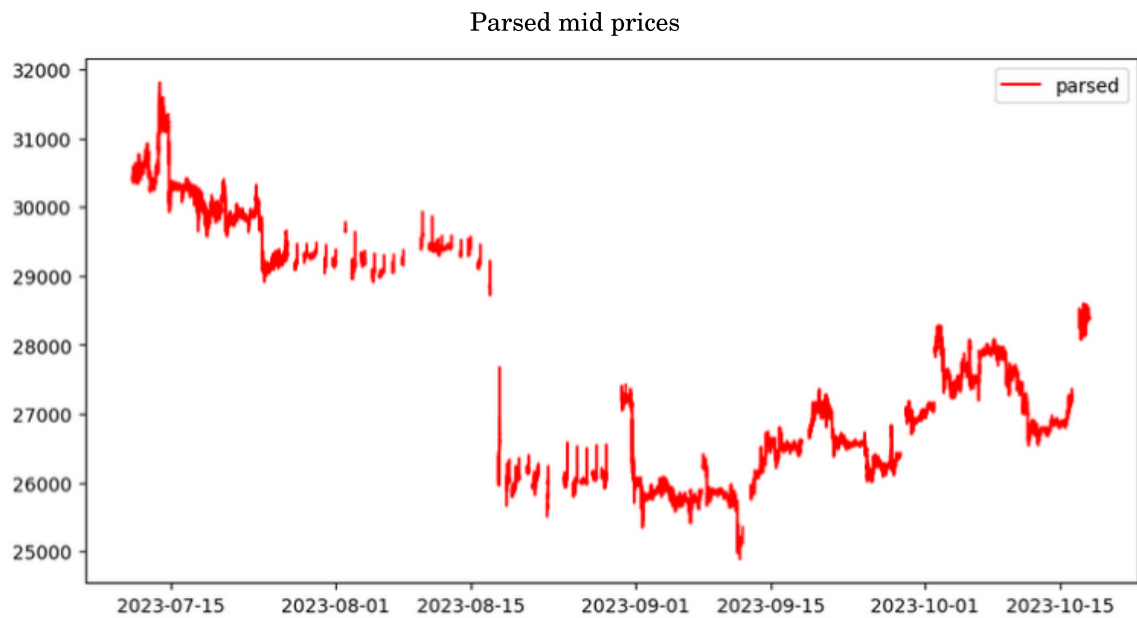
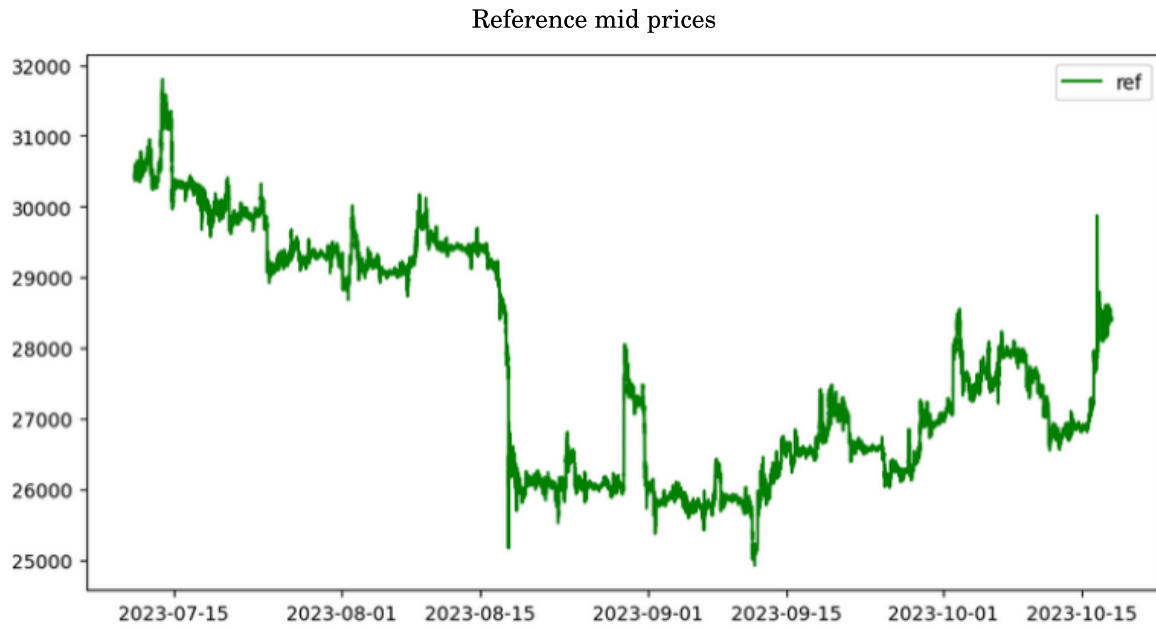


Figure D.2 Reference hourly mid-prices (top) Vs. parsed mid-prices (bottom). Observe the general shape is correct, however there are large irregular gaps due to missing data.

Appendix E

DeepLOB Detailed Model Architecture

Layer Type	Parameters	Details
Conv 1 Conv2d LeakyReLU BatchNorm2d Conv2d LeakyReLU BatchNorm2d Conv2d LeakyReLU BatchNorm2d	1×2 , 32 filters, stride 1×2 negative slope = 0.01 32 features 4×1 , 32 filters negative slope = 0.01 32 features 4×1 , 32 filters negative slope = 0.01 32 features	Spatial aggregation of price and volume for each level and side. Activation function. Normalization. Temporal aggregation of price and volume for each level and side. Temporal aggregation of price and volume for each level and side.
Conv 2 Conv2d Tanh BatchNorm2d Conv2d Tanh BatchNorm2d Conv2d Tanh BatchNorm2d	1×2 , 32 filters, stride 1×2 32 features 4×1 , 32 filters 32 features 4×1 , 32 filters 32 features	Spatial aggregation of imbalance information across sides for each level. Activation function. Temporal aggregation of imbalance information across time for each side and level. Temporal aggregation of imbalance information across time for each side and level.
Conv 3 Conv2d LeakyReLU BatchNorm2d Conv2d LeakyReLU BatchNorm2d Conv2d LeakyReLU BatchNorm2d	1×10 , 32 filters negative slope = 0.01 32 features 4×1 , 32 filters negative slope = 0.01 32 features 4×1 , 32 filters negative slope = 0.01 32 features	Spatial aggregation of imbalance information across all levels. Temporal aggregation of imbalance information across all levels. Temporal aggregation of imbalance information across all levels.
Inception 1 Conv2d LeakyReLU BatchNorm2d Conv2d LeakyReLU BatchNorm2d	1×1 , 64 filters, padding negative slope = 0.01 64 features 3×1 , 64 filters, padding negative slope = 0.01 64 features	Increasing dimensionality. Temporal aggregation simulating a moving average with window size 3.
Inception 2 Conv2d LeakyReLU BatchNorm2d Conv2d LeakyReLU BatchNorm2d	1×1 , 64 filters, padding negative slope = 0.01 64 features 5×1 , 64 filters, padding negative slope = 0.01 64 features	Increasing dimensionality. Temporal aggregation, simulating a moving average with window size 5.
Inception 3 MaxPool2d Conv2d LeakyReLU BatchNorm2d	3×1 , stride 1×1 , padding (1, 0) 1×1 , 64 filters, padding negative slope = 0.01 64 features	Temporal maximum. Increasing dimensionality.
LSTM Layer	input size = 192, hidden size = 64, num layers = 1	Learn long term temporal features.
Fully Connected	input size = 64, output size = 3	Output.

Table E.1 DeepLOB model architecture.

Bibliography

- [1] S. Nakamoto. Bitcoin: A peer-to-peer electronic cash system. <https://bitcoin.org/bitcoin.pdf>, 2008.
- [2] G. Angeris and T. Chitra. Improved price oracles: Constant function market makers. *arXiv preprint arXiv:2003.10001*, 2020.
- [3] N. Reiff, E. Rasure, and V. Velasquez. The collapse of ftx: What went wrong with the crypto exchange? <https://www.investopedia.com/what-went-wrong-with-ftx-6828447>, June 2024.
- [4] I. Salami. Challenges and approaches to regulating decentralized finance. *AJIL Unbound*, 115:425–429, 2021.
- [5] N. G. Mankiw. *Principles of Economics*. Cengage Learning, 7th edition, 2014. Chapter 4: The Market Forces of Supply and Demand.
- [6] C. Cao, O. Hansch, and X. Wang. The information content of an open limit-order book. *Journal of Futures Markets*, 29(1):16–41, 2009.
- [7] E. Bacry and J. F. Muzy. Hawkes model for price and trades high-frequency dynamics. *Quantitative Finance*, 14, 2013.
- [8] D. T. Tran, A. Iosifidis, J. Kannianen, and M. Gabbouj. Temporal attention augmented bilinear network for financial time-series data analysis. *CoRR*, abs/1712.00975, 2017.
- [9] D. E. Rumelhart., G. E. Hinton, and R. J. Williams. Learning representations by back-propagating errors. *Nature*, 323(6088):533–536, 1986.
- [10] Y. LeCun, B. Boser, J. Denker, D. Henderson, R. Howard, W. Hubbard, and L. Jackel. Handwritten digit recognition with a back-propagation network. In D. Touretzky, editor, *Advances in Neural Information Processing Systems*, volume 2. Morgan-Kaufmann, 1989.
- [11] S. Hochreiter and J. Schmidhuber. Long short-term memory. *Neural computation*, 9:1735–80, 12 1997.
- [12] Y. LeCun, L. Bottou, Y. Bengio, and P. Haffner. Gradient-based learning applied to document recognition. *Proceedings of the IEEE*, 86(11):2278–2324, 1998.
- [13] A. Krizhevsky, I. Sutskever, and G. E. Hinton. Imagenet classification with deep convolutional neural networks. In F. Pereira, C. Burges, L. Bottou, and K. Weinberger, editors, *Advances in Neural Information Processing Systems*, volume 25. Curran Associates, Inc., 2012.
- [14] A. Vaswani, N. Shazeer, N. Parmar, J. Uszkoreit, L. Jones, A. N. Gomez, L. u. Kaiser, and I. Polosukhin. Attention is all you need. In I. Guyon, U. V. Luxburg, S. Bengio, H. Wallach, R. Fergus, S. Vishwanathan, and R. Garnett, editors, *Advances in Neural Information Processing Systems*, volume 30. Curran Associates, Inc., 2017.

- [15] M. Dixon, D. Klabjan, and J. H. Bang. Classification-based financial markets prediction using deep neural networks. *Pre-print*, 2017.
- [16] F. Rosenblatt. The perceptron: a probabilistic model for information storage and organization in the brain. *Psychological review*, 65 6:386–408, 1958.
- [17] K. Hornik, M. Stinchcombe, and H. White. Multilayer feedforward networks are universal approximators. *Neural Networks*, 2(5):359–366, 1989.
- [18] N. Passalis, A. Tefas, J. Kannianen, M. Gabbouj, and A. Iosifidis. Temporal bag-of-features learning for predicting mid price movements using high frequency limit order book data. *IEEE Transactions on Emerging Topics in Computational Intelligence*, 4(6):774–785, 2018.
- [19] Z. Zhang, S. Zohren, and S. Roberts. Deeplob: Deep convolutional neural networks for limit order books. *IEEE Transactions on Signal Processing*, 67(11):3001–3012, June 2019.
- [20] R. Cont, A. Kukanov, and S. Stoikov. The price impact of order book events. *Journal of Financial Econometrics*, 12(1):47–88, June 2013.
- [21] P. N. Kolm, J. Turiel, and N. Westray. Deep order flow imbalance: Extracting alpha at multiple horizons from the limit order book. *Mathematical Finance*, 33(4):1044–1081, 2023.
- [22] L. Lucchese, M. S. Pakkanen, and A. E. Veraart. The short-term predictability of returns in order book markets: A deep learning perspective. *International Journal of Forecasting*, 2024.
- [23] R. Huang and T. Polak. Lobster: Limit order book reconstruction system. *Information Systems & Economics eJournal*, 2011.
- [24] E. Akyildirim, O. Cepni, S. Corbet, and G. S. Uddin. Forecasting mid-price movement of bitcoin futures using machine learning. *Annals of Operations Research*, 330(1):553–584, 2023.
- [25] M. Shin, D. Mohaisen, and J. Kim. Bitcoin price forecasting via ensemble-based lstm deep learning networks. In *2021 International Conference on Information Networking (ICOIN)*, pages 603–608, 2021.
- [26] I. Fette and A. Melnikov. The websocket protocol. <https://www.rfc-editor.org/rfc/rfc6455>, December 2011.
- [27] T. Chen and C. Guestrin. Xgboost: A scalable tree boosting system. *Proceedings of the 22nd ACM SIGKDD International Conference on Knowledge Discovery and Data Mining*, page 785–794, 2016.
- [28] A. Pan and A. K. Misra. A comprehensive study on bid-ask spread and its determinants in india. *Cogent Economics & Finance*, 9(1):1898735, 2021.
- [29] M. D. Gould, M. A. Porter, S. Williams, M. McDonald, D. J. Fenn, and S. D. Howison. Limit order books. *Quantitative Finance*, 13(11):1709–1742, 2013.
- [30] S. Tully. How binance really operates: The world’s largest crypto exchange boasts vast profits, hefty influencer payouts, and a ticking time bomb on its balance sheet. *Fortune*, March 28 2023. Archived from the original on April 9, 2023.
- [31] R. Fielding, J. Gettys, J. Mogul, H. Frystyk, L. Masinter, P. Leach, and T. Berners-Lee. Hypertext transfer protocol – http/1.1. <https://www.rfc-editor.org/rfc/rfc2616>, June 1999. Obsoleted by RFCs 7230-7235.

- [32] A. Tsantekidis, N. Passalis, A. Tefas, J. Kannianen, M. Gabbouj, and A. Iosifidis. Forecasting stock prices from the limit order book using convolutional neural networks. *2017 IEEE 19th Conference on Business Informatics (CBI)*, 01:7–12, 2017.
- [33] D. R. Cox. The regression analysis of binary sequences. *Journal of the Royal Statistical Society: Series B (Methodological)*, 20(2):215–232, 1958.
- [34] T. Hastie, R. Tibshirani, and J. Friedman. *The Elements of Statistical Learning*. Springer Series in Statistics. Springer New York Inc., New York, NY, USA, 2001.
- [35] H. E. Robbins. A stochastic approximation method. *Annals of Mathematical Statistics*, 22: 400–407, 1951.
- [36] D. P. Kingma and J. Ba. Adam: A method for stochastic optimization. In *Proceedings of the 3rd International Conference for Learning Representations, San Diego, 2015*, 2017.
- [37] E. Kauderer-Abrams. Quantifying translation-invariance in convolutional neural networks. *Pre-print*, 2017.
- [38] M. I. Jordan. Chapter 25 - serial order: A parallel distributed processing approach. In J. W. Donahoe and V. Packard Dorsel, editors, *Neural-Network Models of Cognition*, volume 121 of *Advances in Psychology*, pages 471–495. North-Holland, 1997.
- [39] R. Pascanu, T. Mikolov, and Y. Bengio. On the difficulty of training recurrent neural networks. *Pre-print*, 2013.
- [40] F. Gers., J. Schmidhuber, and F. Cummins. Learning to forget: continual prediction with lstm. In *1999 Ninth International Conference on Artificial Neural Networks ICANN 99. (Conf. Publ. No. 470)*, volume 2, pages 850–855 vol.2, 1999.
- [41] A. L. Maas. Rectifier nonlinearities improve neural network acoustic models. In *Rectifier Nonlinearities Improve Neural Network Acoustic Models*, 2013.
- [42] A. Paszke and S. Chintala. Pytorch cross entropy loss. <https://pytorch.org/docs/stable/generated/torch.nn.CrossEntropyLoss.html>, 2017.
- [43] M. Lin, Q. Chen, and S. Yan. Network in network. In *Proceedings of iclr2014*, 2014.
- [44] A. Paszke, S. Gross, S. Chintala, G. Chanan, E. Yang, Z. DeVito, Z. Lin, A. Desmaison, L. Antiga, and A. Lerer. Automatic differentiation in pytorch. *Pre-print*, 2017.